DRAFT

THE EISCAT POLAR CAP RADAR

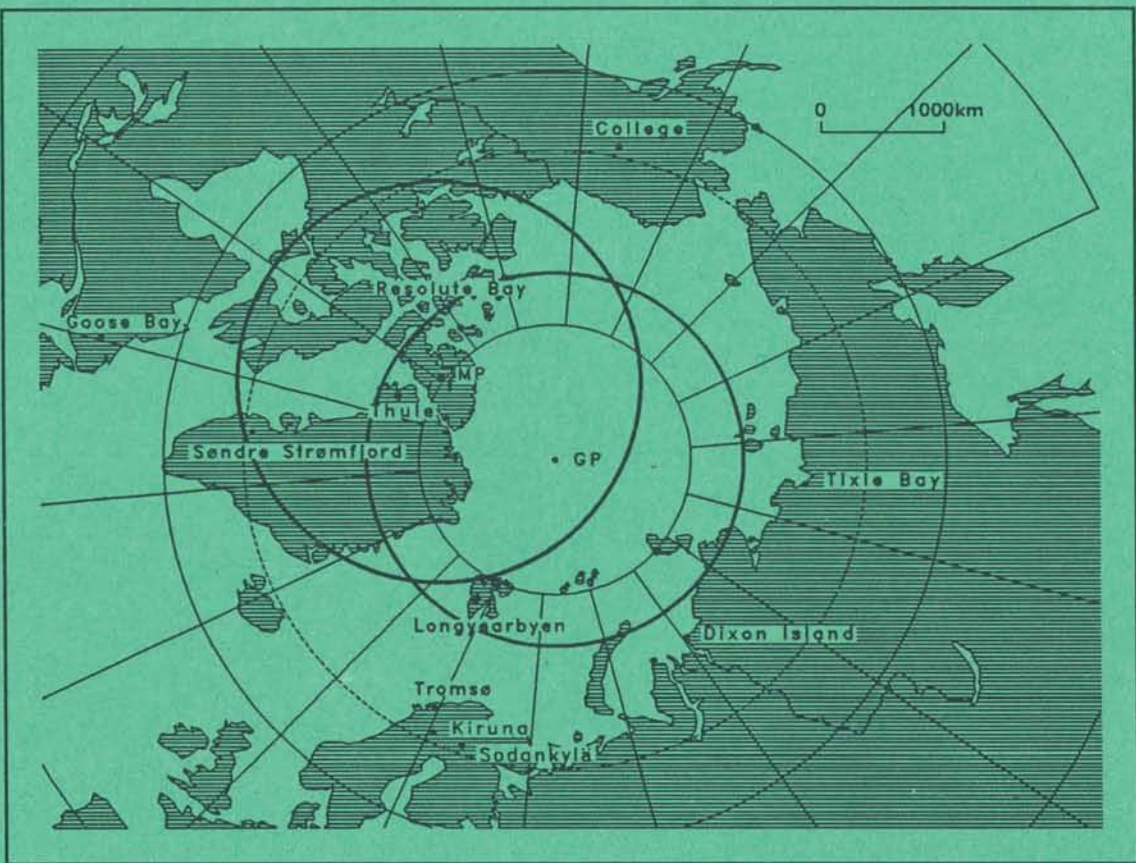

Report on the design specification for an incoherent scatter radar facility based on the archipelago of Svalbard

Prepared by the POLAR CAP RADAR WORKING GROUP established by EISCAT Council on 11 May 1990

Science and Engineering Research Council
Rutherford Appleton Laboratory

SERC TWENTY FIFTH ANNIVERSARY 1965-1990

Chilton DIDCOT Oxon
OX11 0QX
Tel Abingdon (0235) 821900 ext 6529
Direct Line (0235) 44 6529
Telex 83159 RUTHLB G
Fax (0235) 44 5848
Direct Fax (0235)

21 November 1990

Dr A.P. van Eyken,

Dear Tony,

I am sending you a personal copy of the Report prepared by the Polar Cap Radar Working Group, which was submitted to EISCAT Council on 8/9 November 1990.

The Report was endorsed by EISCAT Council and a decision was made to appoint a Project Manager and a Project Engineer (both for one year in the first instance) to continue the work started by the Polar Cap Radar Working Group. The Working Group itself has some further work to undertake, particularly with regard to recurrent expenditure, and a revised report has to be prepared for the next EISCAT Council meeting in May 1991.

It was agreed by EISCAT Council that the present version of the report could be released for distribution provided it was clearly marked "DRAFT".

On behalf of the Polar Cap Radar Working Group, I would like to thank you for your contribution towards the preparation of this report. It is obvious that a report of this type could not have been completed without the assistance of many people and I hope you will regard the report itself and its endorsement by EISCAT Council as a fitting testimonial to the collective efforts of the entire "EISCAT community".

I should welcome any comments you may have on the contents and presentation of the report. I know that a few typographical errors could not be corrected at the very last moment because of the need to adhere to a very strict timetable for copying and compilation. Nevertheless, I should welcome your suggestions for improvements to the revised version of the report.

With many thanks once again for your help.

Yours sincerely

David

D M Willis

Enc:

THE EISCAT POLAR CAP RADAR

Report on the design specification for an incoherent scatter radar facility based on the archipelago of Svalbard

Prepared by the POLAR CAP RADAR WORKING GROUP established by EISCAT Council on 11 May 1990

Submitted to EISCAT Council on 8/9 November 1990

November 1990

Polar Cap Radar Working Group

Professor N. Bjørnå (Chairman)

Auroral Observatory, University of Tromsø, N-9000 Tromsø, Norway

Professor B. Hultqvist

Swedish Institute of Space Physics,
Box 812, S-981 28 Kiruna, Sweden

Dr W. Kofman

CEPHAG/ENSIEG, CNRS URA346, BP 46,
38402 St Martin d'Hères Cédex, France

Dr J. Röttger

EISCAT Scientific Association, Box 812, S-981 28 Kiruna, Sweden

Dr K. Schlegel

MPI für Aeronomie, Postfach 20, D-3411 Katlenburg-Lindau 3, Germany

Dr T. Turunen

Geophysical Observatory, SF-99600 Sodankylä, Finland

Dr D.M. Willis (Secretary)

Rutherford Appleton Laboratory, Chilton, Didcot, OX11 0QX, UK

The Polar Cap Radar Working Group wishes to express its sincere thanks to all those who have contributed to the preparation of this Report. The names of the scientific consultants who have played a key role in helping to prepare this design specification for an incoherent scatter radar on Svalbard are given in Appendix C. Many others have provided indispensable scientific advice, important written contributions, authoritative information on Svalbard, and invaluable help with the preparation of this Report: their names are listed in Appendix D. The Working Group also acknowledges financial contributions from the Institutions listed in Appendix E.

The possible technical designs for the Polar Cap Radar have been investigated in detail by a Technical Panel comprising: Dr W. Kofman, Dr J. Röttger (Convener), Dr. G.N. Taylor and Dr G. Wannberg. The drafting of this Report has been delegated by the Polar Cap Radar Working Group to an Editorial Panel comprising: Professor N. Bjørnå (Chairman), Dr W. Kofman, Dr P.J.S. Williams and Dr D.M. Willis.

Frontispiece

Auroral arcs over Adventdalen, Svalbard, as seen from the Auroral Observing Huts in the bottom of the valley. The lights from Mine No. 7 and the proposed site for the Polar Cap Radar can be seen to the left of the picture (photograph courtesy of K. Henriksen, University of Tromsø).

RAL

photoservices

Number. 90FC6765

RUTHERFORD APPLETON LABORATORY
CHILTON, DIDCOT, OXON. OX11 0QX
Telephone: 0235 21900
ACKNOWLEDGEMENT REQUIRED

I. EXECUTIVE SUMMARY

I.A. Introduction

In 1989 the Science and Engineering Research Council of the UK published a plan for future research in astronomy and planetary science using ground-based research. The four key projects in this plan included a major ionospheric and atmospheric radar to be built in the polar cap, possibly on Svalbard.
A small panel refined the scientific case for such a radar and drew up a technical specification which was published in September 1989. The new radar was envisaged as an extension of EISCAT, operating as an international facility. The proposal was therefore presented to the EISCAT Scientific Advisory Committee, which fully endorsed the scientific case and recommended the project to EISCAT Council. The Council set up an international Working Group to examine the proposal and this is its report.

I.B. Scientific Case

The scientific case has been developed under 8 headings in each of which the new radar will make a significant contribution. The proposed site at Longyearbyen is ideal for studies of the cusp and the ionospheric image of the solar-wind/magnetosphere coupling processes. This will be especially important in conjunction with the Cluster satellite project. A powerful incoherent-scatter radar scanning northwards from this site will be able to monitor the polar-cap convection pattern up to invariant latitude 85°, while pointing southwards it will combine with EISCAT in an unique study of the boundary between the polar cap and auroral zone. Looking upwards along the magnetic field, the new radar will measure field-aligned plasma velocities at high altitudes, including the cleft ion fountain, the light-ion polar wind and the large upward fluxes that occur in the night sector, which provide a substantial flow of ionisation into the magnetosphere. In addition to geophysical studies of the polar-cap ionosphere, a major part of the scientific programme of the new radar will be directed towards high-latitude plasma physics. The study of particle acceleration along the field-line is, perhaps, the most important topic in this field but, in addition, the polar cap radar will collaborate with EISCAT in recording the spectra of signals scattered from non-Maxwellian plasmas at different aspect angles, and it will also measure plasma irregularities generated by large electric fields or by sharp gradients in plasma density.

Finally, the new radar will fill a vital gap in studying the neutral atmosphere at high latitudes. The ion drag imposed by ionospheric convection is a crucial factor in determining the dynamics of the thermosphere, while the dynamics of the stratosphere and troposphere in the region of the polar vortex are of major general interest, especially in connection with the 'ozone hole'.

I.C. Technical Specification

It is essential that the technical specifications of the new radar match the importance of the scientific programme. The polar cap is an extremely dynamic region and in order to make valid measurements of plasma velocity it is necessary to determine three components of the velocity at the same time. In EISCAT this is achieved by receiving the scattered signal from three separate sites. This will be more difficult to achieve on Svalbard, so an alternative proposal is to employ three or more quasi-simultaneous beams from a single site.

Three ways of achieving this have been explored : a phased-array mounted on a platform that could be mechanically steered, a large dish with a feed system that could provide three well-spaced beams, or three smaller dishes that could either operate as three separate radars pointing in three different directions, or transmit and receive coherently in the same direction to operate as a single antenna.

The phased-array is the most expensive option. The multi-beam dish is also expensive and would require a totally new design. The three-dish option is the cheapest and safest, and it allows the project to be developed in phases as funds become available.

The choice of operating frequency has been carefully considered. At 224 MHz (the EISCAT VHF frequency) the sky noise is very high and limits sensitivity; moreover, the long correlation time for ionacoustic waves at lower frequency makes it difficult to measure spectra in the E region. Also, a radar operating at Longyearbyen at such a low frequency is vulnerable to coherent echoes. At 931 MHz (the EISCAT UHF frequency) the wide bandwidth of the scattered signal limits sensitivity and the Debye cut-off excludes measurements in the topside and hence eliminates studies of the upward acceleration of plasma. The optimum frequency is therefore in the range 400-500 MHz.

It has been agreed that the ideal system should consist of three 32-m parabolic dishes with prime-focus feeds and a 3 MW distributed transmitter operating at about 450 MHz. The transmitter should supply the antennas through a switchyard which allows the three antennas to act as three independent radars, with power switched from one antenna to another between pulses, or to transmit the same signal simultaneously in the same direction and so achieve maximum sensitivity.

I.D. Modes of Operation

Four modes of operation of the system have been outlined.

Single-beam observations along the field line will be used for measurements of plasma-flow in the topside. Multi-beam observations will be made across the northern horizon to monitor the convection flow in the polar cap, while measurements to the south will be made in conjunction with EISCAT. Finally, multi-beam observations centred on the field line will be important for studies of the distribution of electric fields and currents in the cusp region, at the polar-cap boundary and in the vicinity of auroral structures. A similar mode will also be ideal for MST studies.

I.E. Recommendations

In order that initial measurements can be made in conjunction with the Cluster satellite mission, it is urged that the first phase of the project, with a 1.5 MW transmitter and one or two antennas, should proceed immediately. It is estimated that this would be possible with a budget ranging from 100 MSEK to 145 MSEK, depending on the price of antennas following competitive tender and the number of antennas subsequently purchased. A careful analysis of the scientific return from different systems has confirmed that valuable scalar measurements can be made with a single antenna, although the great scientific potential of the new radar will only be realised when at least two antennas are in operation. It is anticipated, therefore, that excellent and worthwhile science will emerge from measurements made during the first phase of the project, even if only one antenna is available. However, in view of the really major scientific advances that would result from the provision of two (or preferably three) antennas, it is strongly recommended that the goal should be to enhance the initial system as further funds become available.

II. SCIENCE

II.A. Major Scientific Goals in Solar-Terrestrial Physics

Solar-terrestrial physics (STP) may be defined as the study of the generation, flow and dissipation of energy and the transfer of mass within the solar-terrestrial system, which comprises the sun, the solar wind, the magnetosphere, the ionosphere-thermosphere sub-system, and the middle atmosphere. By virtue of its nature, solar-terrestrial physics is linked to astrophysics at the solar end of the system, to atmospheric physics and chemistry at the terrestrial end, and to space plasma physics in the intervening regions. The range of observational techniques used to investigate the STP system includes: i) in situ measurements of the Earth's upper atmosphere and outer space using satellites, rockets and balloons : ii) in situ measurements using a variety of ground based equipment : and iii) remote sensing from the ground upwards and from space downwards. Theoretical investigations involve analytical studies in hydromagnetics, plasma physics and wave propagation, non-linear dynamics, and numerical modelling and simulation (computer experiments). Therefore, solar-terrestrial physics embraces the disciplines of astrophysics, space physics and atmospheric science.

Solar-terrestrial research has now reached the stage when it is necessary to put greater emphasis on a comprehensive study of the natural linkages between the various regions of space from the sun to the earth; this is a natural extension to the traditional study of the individual regions themselves. Accordingly, a major international programme of research in solar-terrestrial physics has been planned for the next decade by the Scientific Committee on Solar-Terrestrial Physics (SCOSTEP). This cooperative enterprise is called the Solar-Terrestrial Energy Programme, or 'STEP' for short. It will focus on the solar-terrestrial environment as a complex interactive system where overall behaviour often departs drastically from that expected from the simple superposition of its component parts.

The main goal of STEP will be to advance quantitative understanding of the coupling mechanisms that are responsible for the transfer of energy and mass from one region of the solar-terrestrial system to another. The STEP research programme will involve ground-based, aircraft, balloon and satellite experiments; theory and simulation studies; and dedicated data and information systems. An important element of STEP will be the set of solar-terrestrial spacecraft missions approved by the Inter-Agency Consultative Group as the next cooperative project of NASA, ESA ISAS and INTERCOSMOS. The STEP research programme will also take advantage of results obtained by other relevant spacecraft missions. The programme is intended to begin in 1990 and terminate in 1995; however, it seems likely that the STEP interval will be extended, particularly if some key spacecraft missions are delayed.

The basic framework of STEP will comprise five 'Priority Areas', each one of which has specific scientific goals designed to elucidate understanding of the interaction mechanisms controlling energy and mass transfer between the different regions of the solar-terrestrial system. The goals of the five priority areas may be summarised succinctly as follows (text taken from the Executive Summary of the booklet entitled 'Solar-Terrestrial Energy Program 1990-1995: A Framework for Action', prepared by the Scientific Committee on Solar-Terrestrial Physics (SCOSTEP), November 1988) :

1) *The Sun as a Source of Energy and Disturbance*

   To achieve an understanding of the principal source mechanisms for electromagnetic and corpuscular emissions on the sun and in the solar environment, and to formulate physical models for improving the predictability of short-term perturbations (minutes to days) and long-term variability (years to decades).

2) *Energy and Mass Transfer Through the Interplanetary Medium and the Magnetosphere-Ionosphere System*

   To achieve an understanding of the energy, momentum and mass transfer mechanisms across shocks and the boundaries that separate the distinct plasma regions of the solar-terrestrial system, and to study the acceleration, diffusion and convection processes and large-scale instabilities that distribute and modify the complex corpuscular flows and fields in that system.

3) *Ionosphere-Thermosphere Coupling and Response to Energy and Momentum Inputs*

To achieve an understanding of the global processes which determine the coupling and interactions among the neutral and ionised species in the ionosphere-thermosphere system, and to study the response of the system to changes in solar input, and to energy and momentum transfer by particles, fields and waves from adjacent regions.

4) *Middle Atmosphere Response to Forcing from Above and Below*

To achieve an understanding of the response of the middle atmosphere to changes in solar and near-space inputs and to volcanic, tectonic, meteorological, biospheric and anthropogenic activity, and to study the extent to which this response feeds back to the regions of the geosphere below and above.

5) *Solar Variability Effects in Regions Adjacent to the Earth's Surface*

To determine the influences of solar variability on the physical and chemical properties and the large-scale behaviour of the lower atmosphere, on man-made technological systems, on earth currents and on biota and to formulate, test and study mechanisms responsible for these effects.

It seems inevitable that existing SCOSTEP programmes (eg MAC, PAD, SIV and WITS) will eventually be fully incorporated into STEP. Moreover, the International Council of Scientific Unions (ICSU) is planning a very ambitious enterprise of international scientific cooperation during the next decade, called the International Geosphere-Biosphere Programme, or IGBP. The purpose of this programme is to advance understanding of the Earth as a coupled system and to provide the body of knowledge needed to assess trends and anticipate natural and anthropogenic changes (eg the 'greenhouse effect' and the 'ozone hole') in the next 50-100 years. It is clear that STEP will act as an important complement to IGBP.

Within the framework of this immensely challenging and exciting future international research programme in solar-terrestrial physics, the Polar Cap Radar Working Group has considered the scientific and technical requirements for an advanced incoherent scatter radar on the archipelago of Svalbard. As a useful preliminary, however, the historical background to the compelling reasons for making incoherent scatter radar measurements at high latitudes is summarised in Section II B. The detailed scientific case for a polar cap radar is presented in Section II C, which includes a careful assessment of the main scientific problems that could be investigated by such a radar.

II.B. Background to Research in Solar-Terrestrial Physics

Studies of the solar-terrestrial system are of direct relevance to society. For example, the reliability of world-wide communication and navigation systems depends on accurate forecasts of the prevailing conditions in the Earth's atmosphere and the interplanetary medium. Large magnetic storms induce damaging voltage surges in power lines and corrosive currents in pipelines; they also produce increased drag on low-altitude satellites, causing premature re-entry into the Earth's atmosphere. Enhanced fluxes of charged particles in the magnetosphere can damage the electronic systems of satellites. The concentration of stratospheric ozone, which provides protection from the harmful effects of solar ultraviolet radiation, is known to be affected by energetic solar protons. Therefore there are compelling reasons for studying the physical properties of the solar-terrestrial system and thus attempting to improve forecasts of the 'weather' in space.

Quite apart from these important practical applications, studies of the solar-terrestrial system also provide fundamental information on basic plasma processes that occur elsewhere in the universe. For example, magnetic reconnection and particle acceleration are important phenomena that are not yet fully understood, but which appear to occur also in solar flares, supernovae, pulsars, quasars and radio galaxies. However, reconnection at the dayside magnetopause and acceleration in the cusp have the unique advantage that they can be studied at close range, using the powerful combination of incoherent scatter radar and satellite-borne instrumentation.

The outstanding successes of the research programmes of the European Incoherent Scatter (EISCAT) Scientific Association have confirmed beyond doubt that incoherent scatter radar is the most powerful and comprehensive ground-based technique for studying the upper atmosphere. The theory of the scattering process is well understood and under normal conditions, when the velocity of the plasma with respect to the neutral atmosphere is less than the neutral thermal speed, an analysis of the frequency spectrum of the scattered signals allows the following parameters to be measured directly :-

1) electron concentration, 2) electron temperature, 3) ion temperature, 4) ion composition, 5) ion-neutral collision frequency, 6) line-of-sight plasma velocity and 7) electric current density along the magnetic field line.

In addition, recent experiments using EISCAT as a coherent scatter radar have measured 8) the backscatter cross-section for echoes from irregularities in the auroral E-region and 9) the correlation time of these echoes.

From these direct measurements other parameters can often be derived reliably, including :-

10) electric field strength, 11) Hall and Pedersen conductivity, 12) Hall and Pedersen currents, 13) Joule heating, 14) Lorentz forces, 15) neutral air temperature, 16) changes in neutral composition, 17) neutral wind speed, 18) spectrum of suprathermal precipitating electrons, 19) particle heating, 20) flux of conducted heat along the magnetic field line, 21) frequency and wavelength of wave-like structures, and 22) the ratio of negative ion to electron density.

Very good precision, with errors of a few percent in most cases, can generally be achieved. The technique does not significantly perturb the medium and thus the results are not affected by systematic errors arising from such perturberations, which often affect measurements using other techniques. Moreover, incoherent scatter gives continuous measurements with a time resolution of a minute or less over an altitude range from 70 km to 2000 km or above (though not all parameters can be measured over the whole range) and when an incoherent scatter facility is complete it will continue to operate successfully for many years, typically two or more solar cycles (in excess of twenty years).

Until the 1970s all incoherent scatter systems had been constructed near the equator or at mid-latitudes and when EISCAT was first proposed many of the major scientific questions relating to the low- and mid-latitude ionosphere had been answered. However, the most interesting phenomena - such as the penetration of magnetospheric electric fields to lower latitudes, the generation and propagation of large-scale atmospheric gravity waves, and the world-wide effects in the thermosphere accompanying magnetic disturbances - clearly had their origin in the auroral zone, where the ionosphere is connected by magnetic field lines to the magnetosphere and hence serves as a sensitive detector for magnetospheric processes.

In 1975, therefore, significant progress in the field demanded an advanced incoherent scatter radar in the auroral zone, and EISCAT (the European Incoherent Scatter Radar) was established by agreement between six European countries.

EISCAT has since proved to be one of the major success stories in ionospheric and magnetospheric physics. This is confirmed when we compare the list of pertinent scientific topics in the original proposal for EISCAT with the list of new results actually achieved (see Appendix A). For every topic on the original list EISCAT can claim a major advance, and these results have fully justified the support EISCAT has enjoyed. Nevertheless, amongst the most important results are those which were totally unforeseen and it is important to stress that this list of novel results is increasing steadily.

As a result, the situation today has significant parallels to 1975. EISCAT has solved many of the long-established problems of the auroral zone, but the most exciting work leads us even further north, to the cusp and the polar cap where the ionosphere is linked to the interplanetary medium along open magnetic field lines. This region is the most crucial in the transfer of energy and momentum from the solar wind into the magnetosphere and hence into the ionosphere, and yet it is a region barely explored. However, the indications given by EISCAT, operating at the very limit of its range, point emphatically to an advanced incoherent scatter radar on Svalbard. Such a facility will transform our understanding of magnetic reconnection and the role of flux transfer events in coupling the solar wind with the magnetosphere. It will also add new information about the polar wind, ion outflow and how the magnetosphere is populated by ionospheric ions.

European countries have a major investment in both the EISCAT incoherent scatter radars and ESA's four-spacecraft CLUSTER mission, due for launch in December 1995. One of the main aims of CLUSTER is to study the boundary between interplanetary space and the terrestrial magnetosphere and the important interactions which occur across this boundary. The magnetic field lines which lie close to this boundary intersect the Earth at high latitudes on the dayside and Svalbard is an ideal location from which the entire dayside boundary can be studied. This is especially significant in mid-winter when the sun is always at zenith angles greater than 100° so that complementary optical studies of the dayside aurora are possible (see Figure 1). In fact, Svalbard is the only available landmass in the northern hemisphere where simultaneous radar and optical studies of the dayside cusp can be made. Hence a radar with a field of view over and around the Svalbard islands will provide vital complementary observations for CLUSTER. Of particular interest is the transfer of magnetic flux (and hence matter, energy and momentum) across the boundary in isolated events (Flux Transfer Events or FTE's). Detailed studies of FTE's with CLUSTER will be possible for 2-3 hour periods, and simultaneous radar observations of the corresponding effects in the ionosphere will be possible at all local times and will permit an investigation of the evolution, geometry and importance of FTE's as a mechanism for driving flows in the coupled ionosphere-magnetosphere system.

Furthermore, CLUSTER will make detailed observations of the explosive release during substorms of energy stored in the geomagnetic tail, and the combination of EISCAT and a Svalbard radar would give sufficient resolution and geographic coverage to allow the corresponding sequence of events in the ionosphere to be monitored continuously. Lastly, CLUSTER will provide near-Earth solar-wind data, both just outside the subsolar bow shock and within the shocked magnetosheath plasma. The proposed radar would enable the excitation and decay of flows in the ionosphere, in response to changes in the solar wind and interplanetary magnetic field (IMF), to be studied on both the dayside and the nightside. Such observations have been carried out with great success using EISCAT and AMPTE but only for the dayside during southward IMF. These measurements are of great importance to our understanding of how energy is coupled into the ionosphere, both directly and via storage in the geomagnetic tail.

The establishment of a major incoherent scatter facility on Svalbard, to operate in co-operation with EISCAT, would therefore support major advances both in the understanding of the whole chain of solar-terrestrial relationships and in the study of plasma physics. The full range of scientific problems are discussed below. Together they offer a programme of new research that will both match and complement the achievements of EISCAT.

II.C. Scientific Case for a Polar Cap Radar

The scientific case is very strong, and, in this report, seven separate topics which call for a radar on Svalbard have been identified and discussed extensively by the scientific community. There are, of course, other study areas which also provide strong support for such a radar and which could have been selected for this purpose, and some of these are listed briefly in Section 8.

1. IONOSPHERIC SIGNATURE OF MAGNETOSPHERE CUSP/CLEFT PROCESSES
    - a) Dayside Auroral and Plasma-Flow Transients
    - b) Birkeland Currents
    - c) The Cusp/Cleft Ion Fountain
2. POLAR CAP POTENTIAL AND CONVECTION PATTERN
    - a) Polar Cap Convection
    - b) Polar Cap Precipitation
    - c) Coupling between Auroral and Polar Zones

3. IONOSPHERE-MAGNETOSPHERE PLASMA EXCHANGE
   a) Large Upward Flows in the Midnight Sector
   b) Polar Wind
4. POLAR IONOSPHERE
   a) Ionization, Composition and Thermal Structure of the Ionosphere
   b) Patches, Blobs and Irregularities
5. THERMOSPHERIC STUDIES
   a) Thermospheric Response to IMF
6. HIGH-LATITUDE PLASMA PHYSICS
   a) Extraction of Ionospheric Plasma by Magnetospheric Processes
   b) Non-Thermal Plasmas
7. MST STUDIES IN THE POLAR CAP
   a) Coupling Processes between the Lower Thermosphere and the Mesosphere
   b) The Polar Stratosphere and Troposphere investigated by the Polar Cap Radar in ST Mode
8. OTHER SUBJECTS OF STUDY

1. Ionospheric Signature of Magnetosphere Cusp/Cleft Processes

1.(a) Dayside Auroral and Plasma-Flow Transients

The convective flow of plasma and magnetic flux, which occurs in the magnetosphere, together with its corresponding image in the high-latitude ionosphere, has its origin in two related sets of processes. First, coupling occurs at the magnetopause, on the dayside and on the flanks, between the fast-flowing magnetosheath plasma and terrestrial magnetic flux tubes, resulting in the latter being carried anti-sunward, over the pole, and stretched out into a long magnetotail. Second, the stress imposed on the tail flux tubes by the inflow of magnetosheath momentum is at some time relaxed and the flux tubes collapse earthward. These flows are of dominant importance in governing the structure and dynamics of the magnetosphere, and also a major factor in determining the properties and behaviour of the high-latitude ionosphere.

Several types of process have been suggested as significant in causing coupling across the magnetopause and these would lead to different ionospheric signatures. Spacecraft data obtained in situ suggest that magnetic reconnection is, under most circumstances, the dominant coupling process, especially when IMF B_z is small or southward. However, observations also show that the process can be quasi-steady or can occur in bursts of a few minutes termed 'flux transfer events' or FTE's. In such cases, impulsive, bursty, poleward plasma flows are anticipated.

The spatial scale of these bursts is a matter of controversy. The original interpretation suggested a spatial scale of a few thousand kilometres, both along and transverse to the magnetopause. This would map to scales of about 100 km in the ionosphere; impulsively-accelerated ionospheric filaments of this size would then be expected and they would generate localised, mini-twin-vortex flow systems. However, several authors have recently argued that the observations may also be explained by impulsive reconnection occurring over a much wider region of the magnetopause, in which case flow surges would occur over a much broader front in the cusp. Other authors have suggested that impulsive plasma flows in the dayside ionosphere could be generated by the penetration of filaments of magnetosheath plasma into the magnetosphere. In principle, flows generated in this way can be distinguished from bursty reconnection as, in this case, the initial motion of the flux tubes in the centre of the burst would be equatorward, and the disturbance as a whole would also move equatorward - both being opposite to the bursty, FTE scenario. Recent STARE and magnetometer observations have shown relatively large twin-vortex flow patterns in which the central flows are directed poleward but the disturbances as a whole propagate in the east-west direction; this is inconsistent with both 'impulsive reconnection' and 'impulsive penetration', but might be due to either large amplitude Kelvin-Helmholtz waves propagating at the magnetopause or large dynamic pressure changes in the solar wind.

EISCAT has revealed tantalising glimpses of the dynamic phenomena associated with coupling at the dayside magnetopause, but cannot make reliable measurements of their velocity components. Because the radar is usually sub-auroral at noon, when the flux tubes from the dayside magnetopause map into the polar cusp ionosphere far to the north, it can only study dayside coupling by operating in the 'POLA' mode, setting the UHF radar at the lowest possible elevation and using 'beam-swinging' to measure the plasma-drift vector velocity. While operating in this mode, some of the most important events observed by EISCAT have been short-lived, rapid, poleward bursts observed to the far north (see Figure 2). These can be interpreted as the ground signatures of pulses of enhanced solar-wind dynamic pressure (top panel, Figure 2) impinging upon the dayside magnetopause.

Other recent EISCAT observations, in conjunction with optical observations made at Ny-Ålesund, Spitsbergen, and the ISEE spacecraft at the magnetopause, have found the first clear evidence for the ionospheric signatures of FTE's and found that their associated electrostatic potential can be surprisingly large (see Figure 3). However, localised events occurring on a time-scale of a few minutes are totally unsuitable for measurement by the 'beam-swinging' technique. For example, the optical data show the transient reconnection events last between 2 and 15 minutes; however, EISCAT, because of its reliance on beam swinging at the northern extreme of its range, can only study those few, long-lived, events which occur at exceptionally low latitudes (like the second example shown in Figure 3). The spatial scales implied by these observations are very interesting in that the north-south dimension of the flow bursts are typically 200 km but the east-west extents can be as great as 2000-3000 km. However, these results are derived using the beam swinging technique and are open to some question because the optical images reveal some structure down to 10 km scale lengths, which is an order of magnitude smaller than the separation of the beams. Indeed, in some other cases huge transient ion temperature rises have been observed in one azimuth of the beam swing, but not in the other. In such cases the spatial structure in the flow burst responsible is smaller than the beam separation and errors in the derived vectors undoubtably occur when beam swinging is used.

Moreover, the recent EISCAT/optical observations have generated much debate concerning how stable the cusp particle precipitation really is. Data from polar-orbiting spacecraft have traditionally been interpreted in terms of a relatively steady spatial structure. However, these satellites only pass through the cusp of a given hemisphere roughly once every hour and can give no information on the variability on minute time scales. Hence ground-based observations of the cusp are vital in determining how steady cusp precipitation really is.

The investigation of the occurrence of flow surges, their spatial scale, flow patterns and the local time zone over which they are observed is therefore a prime research topic. It is essential to study the nature of the processes that result in coupling at the magnetopause, the consequent transfer of flux to the tail and the related processes that result in its subsequent return. The aim is to investigate the flows that occur in the ionosphere in the vicinity of the dayside cusp at noon in order to study the coupling between the solar wind and the magnetosphere.

Observations must be extended towards the pole, especially on the dayside. It is important to measure the extent of reconnection-driven flow interactions because recent EISCAT observations suggests that such high-latitude convection is driven through only a very narrow region just poleward of the dayside boundary. Events here have short time scales, less than five minutes, and are associated with the behaviour of magnetospheric boundaries. In addition, viscous-like interactions have been observed recently for the first time from the ground, using EISCAT in POLA mode. Determinations of the local time extent of this interaction and study of the driving mechanism require observations to the north of EISCAT by day, and roughly over EISCAT at night.

The proper study of the ionospheric flow-pattern associated with these mechanisms is thus a fundamental goal, which requires the deployment of a new Polar Cap Radar to the north of EISCAT, capable of making measurements over the invariant latitude range 75° to 80°. This would normally encompass the dayside cusp at noon, whereas on the nightside it would lie within the polar cap, though it would sometimes be engulfed by the poleward expanding bulge of aurorae during substorms.

New and significant results can be obtained by operating such a ground-based system on its own, but its value will be greatly and mutually enhanced if properly coordinated with space-based observations, such as those to be undertaken by the CLUSTER spacecraft both at the magnetopause and in the tail.

Routine observations are required in areas threaded by magnetic field lines which map to the dayside magnetopause; these provide data on the primary influence of magnetosphere-ionosphere-solar wind interactions and the generation of ionospheric convection. This requires sub-minute time resolution (ideally around 10 seconds) and spatial resolution better than 10 km.

There is great advantage, for all such studies of spatially structured, time-dependent plasma flows, in making joint observations with the EISCAT radars. This allows convection studies to be performed simultaneously on both large- and small-scale phenomena, including dayside magnetopause - solar wind coupling, nightside magnetotail phenomena and substorms. These scientific goals set the requirement that the radar should be able to look both to the west and to the south at low elevations from Svalbard.

An ancillary, bistatic coherent radar, with a viewing area covering that of the Polar Cap Radar, would allow novel investigations using real time guidance of the polar incoherent scatter radar to track significant boundaries. In this case the need for both rapid scanning and measurement of the full velocity vector would be reduced. These observations require low elevation look directions towards the magnetic north, with limited scanning, 10-15 second resolution and a range resolution of better than 20 km (to match that of the coherent radars). The coherent radar could also provide a spatial grid of flow vectors with high temporal resolution around the points studied in detail by the incoherent scatter facility.

1.(b) Birkeland Currents

Electric coupling between the magnetosphere and ionosphere takes place through large-scale and filamentary field-aligned current systems, as first suggested by Birkeland in 1908. Statistical studies using low-altitude polar-orbiting satellite data reveal five distinct Birkeland current regions, including: (1) the Region One and (2) the 'cusp' region systems, and (3) the polar cap 'NBZ' system, occurring when the IMF is directed northward; the Svalbard radar would be ideally situated to study these three regions.

Many important questions remain regarding the structure and origin of these high-latitude Birkeland currents. Satellite studies of Birkeland currents are limited in that they provide only snapshots of field-aligned current structure and are frequently misleading because of spatial/temporal ambiguities. Information on two-dimensional spatial structure and on how current sheets evolve with time requires continuous large-scale monitoring possible only with sophisticated ground-based radars. Thus field-aligned current densities may be determined by direct measurements of the differences in the field-aligned bulk flows of the ions and electrons. This would allow study of the relationship of the large-scale currents, due to quasi-steady reconnection and viscous-like interactions, to the filamentary currents required to drive the transient ionospheric flow bursts shown in Figures 2 and 3.

High-latitude Birkeland currents also provide unique information about other important processes in the magnetosphere. For example, studying the occurrence and local-time extent of the cusp Birkeland currents may provide: a) a quantitative check on the occurrence of quasi-steady reconnection at the dayside magnetopause, thereby allowing the conditions under which it takes place to be determined, and b) information on the length of the magnetopause reconnection X-line. Polar Birkeland currents also provide key information about the nature of time-dependent reconnection phenomena such as flux transfer events. Another significant area that the Svalbard radar would address is how Birkeland currents relate to the dayside aurorae. Even such basic questions as whether these aurorae are associated with downward- or upward-directed currents remain unanswered.

Existing data provide conflicting evidence for the behaviour of ionospheric flows associated with magnetic field reconnection at the polar cap boundary and in the low-altitude signatures of FTE's at the magnetopause. To resolve this uncertainty, scans are required over some hundreds of km in the vicinity of the dayside cleft, with adequate spatial resolution.

With an incoherent scatter radar, ionospheric currents can be measured in two ways. First, from convection measurements and the integrated conductivities, the Hall and Pedersen currents can be derived and the divergence of these perpendicular currents can be used to estimate the field-aligned currents on the large scale. This has been demonstrated using EISCAT and Figure 4 shows the distribution of the parallel currents.

The second technique uses simultaneous measurements of the ion lines and plasma lines to determine the drift of the electron and ion population separately and hence the current. This technique has been used successfully at Chatanika and has recently been implemented at EISCAT to measure the field-aligned currents in the vicinity of an auroral arc. This technique is more suitable for monitoring small-scale features and rapid variations in the currents.

Observations by the new radar in the throat region of the ionosphere are most important because this region cannot normally be seen by the EISCAT radars. The CLUSTER mission will make detailed studies in the magnetospheric counterpart of this region, which will be well matched to the new radar's data set. Real-time data analysis is required, allowing effective interactive control of the radar to ensure that the beams are directed accurately into the throat region.

1.(c) The Cusp/Cleft Ion Fountain

In the dayside cleft region the cleft ion fountain is present at all times, irrespective of magnetic activity, and is a significant contributor to the total plasma content of the magnetosphere. An important property of this source is its ability to modulate the plasma composition of the inner magnetosphere because, unlike the classical polar wind, it is rich in O^+ ions and has even been observed to inject molecular ion species into the polar magnetosphere. The source is highly localised in the pre-noon auroral oval, but influences the magnetosphere over large regions because convection can move heavy ions over great distances due to their long times of flight. The magnetospheric observations require ionospheric upflows which are at least an order of magnitude greater than those of the classical polar wind.

A few observations have been made of large upflows in the cleft ionosphere from low-orbiting satellites but the driving mechanism for the outflows is still unknown. Ion heating may make an important contribution, especially on the morning side of the cleft where the rapid westward ion drifts of the dusk convection cell meet eastward neutral winds driven by the dawn convection cell. Alternatively, large electron temperatures, known to occur in the cleft, can drive heavy ions upward by increasing the ambipolar charge-separation field. At present it is not even known whether the source is continuous or intermittent and extensive observations of this complex source region are essential to our further understanding of these processes.

The proposed new radar on Svalbard would allow the first accurate observations of the field-aligned plasma flow along the cleft field lines in the ionosphere. Furthermore, the temporal evolution of the upflows could be monitored, especially for the large upflows of O^+ ions which originate at a low enough altitude to be measured directly by an incoherent-scatter radar.

2. Polar Cap Potential and Convection Pattern

2.(a) Polar Cap Convection

It is well known that the pattern of plasma convection in the polar cap and auroral zone is very sensitive to the magnitude and direction of the interplanetary magnetic field. When the B_z component is southward, there exists a two-cell pattern. However, there is no way in which the pattern as a whole can be observed. Thus EISCAT statistics over many years have indicated only the equatorward part of the convection pattern in the northern hemisphere for different levels of Kp varying from quiet to active. The simultaneous operation of an incoherent-scatter radar on Svalbard will permit a much larger part of the pattern to be displayed, especially when the ionospheric electron density in the polar cap has an average or above-average value (see Figure 5), in which case measurements at low elevation will be possible up to an invariant latitude of about 85°. EISCAT measurements have also revealed rapid time-variations in the convection pattern and for this reason the beam-swinging technique with a single antenna is inadequate. A similar reservation applies to the tristatic technique if a scanning procedure is adopted to gain latitudinal coverage. However, if it were possible to make simultaneous velocity measurements in three directions using the polar-cap radar and a fourth, intersecting-beam direction using EISCAT, this problem would be largely overcome and it would be possible to monitor the relationship between changes in the IMF and the response of the convection electric field over a range of latitudes.

When B_z is northward, the convection pattern becomes more complex and indeed is still a matter for debate. Under most conditions, magnetic reconnection should dominate cusp flows in the vicinity of noon, the exact location being modulated by IMF B_y (another topic requiring investigation). Away from noon, however, viscous-like processes may dominate the flow from the auroral zone into the polar cap. Unlike reconnection, such processes may produce weak, smooth, northward flows across a boundary where otherwise the shear flow is reversed (see Figure 6).

The analysis of these flows provides an estimate of the voltage associated with this source. Present indications are that the potential associated with viscous-like processes is of the order of 10 kV, much less than that associated with subsolar reconnection when IMF B_z is small or southward (50 to 150 kV). However, when IMF B_z takes significant northward values, above about 2 nT, subsolar reconnection appears effectively to cease so that the viscous-like mechanisms may assume greater significance, at least in the equatorward part of the contracted flow pattern.

It has been possible to observe viscous-like interaction using EISCAT, but not on the dayside or when the polar cap is contracted. Observations from low-altitude spacecraft have indicated that a new 'reversed' twin-cell pattern of flow forms at the highest latitudes on the dayside during northward IMF, as indicated in Figure 6, though some authors have interpreted the observed flows in terms of a highly-distorted, twin-cell flow pattern. In either case, the observed sunward-directed flows are found to increase in strength as IMF B_z becomes increasingly northward, suggesting reconnection between the northward-directed IMF and tail-lobe flux tubes located poleward of the cusp.

It is of great importance to 'map' the complex flows in the polar cap for IMF $B_z > 2$ nT. This will require the collaboration of several radar systems, using both incoherent and coherent radar techniques, with the new Polar Cap Radar on Svalbard playing a central role, especially as part of a meridional chain of instruments across the auroral zone and polar cap, involving EISCAT, Svalbard and twin coherent radars operating at HF or VHF.

2.(b) Polar Cap Precipitation

The precipitation in the area poleward of the auroral oval is normally characterized by a low-energy, structureless, diffuse rain or drizzle, originating from plasma which relatively recently entered the magnetosphere on open field lines. Absence of internal magnetospheric acceleration, such as Fermi acceleration, on these field-lines explains the diffuseness of the precipitation and, without primary structures and associated field-aligned current flow, other field-aligned acceleration mechanisms cannot develop.

However, from optical observations it has long been known that, particularly during magnetically quiet times, auroral arc structures (earlier called un-aligned arcs) can exist in the polar cap regions. Recently, global images from high-altitude, polar-orbiting satellites such as DE-1 and Viking have revealed that sun-aligned arcs, in fact, extend over the whole region of the polar cap, connecting the dayside auroral oval with the nightside. Measurements of global convection patterns with the help of satellites and ground-based instrumentation have shown that these arcs, now renamed transpolar arcs or theta aurora, are associated with major distortions of the normal two cell convection pattern. Sometimes the data can be interpreted as being produced by multiple convection cells with sunward convection over the central polar cap. The existence of transpolar arcs was found to be strictly associated with northward directed interplanetary magnetic field, and asymmetries in the location of the auroral features and associated convection patterns are strongly dependent on the IMF B_y component.

A number of attempts have been made to explain these observations in terms of the existence of new merging regions on the frontside magnetospheric lobes or the increased importance of viscous-type solar wind magnetosphere interactions. Recent Viking observations, supported by EISCAT measurements, have revealed that the transpolar arc is often connected to either the morning or evening side of the auroral oval by a region of precipitation which shows no clear evidence for open field lines. The transpolar arc seems in many cases only to be a far northward boundary of an expanded auroral oval. This view could be tested by model calculations implementing field-line mapping according to the Tsyganenko magnetic-field model.

A more clearly identifiable intrusion of structured precipitation into the polar cap is observed to happen in a late stage of auroral substorm development, when the whole region of active aurora suddenly contracts poleward (poleward leap). This feature is certainly no polar-cap aurora, but might be associated with the formation of a plasmoid in the far tail. Recently, the substorm recovery phase has been recognized as the least understood part of the substorm development, and will certainly receive a lot of attention in the future.

A region of true polar-cap, structured precipitation is located around and poleward of the dayside cusp, where strong auroral brightenings and rapid poleward motions of auroral structures are observed in close association with dynamical changes in the solar wind plasma parameters. At present, it is unclear whether these precipitation events and associated extremely high ionospheric plasma flows stem from processes in the plasma mantle or whether they are associated with direct plasma intrusion in the cusp region.

In recent years it has become clear that the polar cap is poorly described in terms of regions of homogeneous low conductivity but, in fact, often contains structured aurora, stemming from direct plasma intrusions or complicated distortions of the 'normal' magnetosphere. The limitation of ground-based instrumentation in the polar cap region has led to an under-representation of polar cap phenomena in our understanding of the solar wind - magnetosphere - ionosphere system. A combined polar cap - auroral oval radar system should produce a vast amount of new data both on direct solar wind - magnetosphere interaction and on the more complicated magnetospheric energy storage and release process associated with substorms.

2.(c) Coupling between Auroral and Polar Zones

The polar cap boundary is located at latitudes intermediate between the auroral radar, EISCAT, and the proposed Polar Cap Radar. It is formally defined as the boundary between two classes of magnetic field lines: closed lines with both ends connected to the ionosphere, and lines still connected by one end to the polar ionosphere but with the other 'open' extending into the solar wind. As a result, it also separates two components of the convection motion, sunward for closed lines, antisunward for polar open lines.

Simultaneous observations by both radars would provide the complementary measurements required for a precise analysis of the topology and dynamics of the polar cap boundary as a function of the solar wind parameters and of magnetic activity conditions. In particular, the dynamics of this boundary during disturbed times, associated with the ionospheric signature of particle precipitation, electric fields and currents, also inferred from simultaneous operations of both radars, would improve the presently poor understanding of substorms.

Finally, on a global scale, the extended range of latitudes simultaneously explored in the auroral and polar ionosphere is connected by magnetic field lines to huge parts of the equatorial magnetosphere extending from the inner magnetosphere and the plasma sheet inner boundary (a few terrestrial radii), up to the cusps and the dayside magnetopause, or to distant tail regions on the nightside. Therefore, observations of ionospheric electrodynamics will provide information on the global structure of parameters such as electric fields and field-aligned currents in the connected magnetospheric regions.

3. Ionosphere-Magnetosphere Plasma Exchange

3.(a) Large Upward Flows in the Midnight Sector

Large upward ion fluxes have been observed on several occasions in the midnight sector near the polar-cap/auroral-zone boundary. The magnitude of the observed thermal O^+ fluxes is at least an order of magnitude greater than that required to support the light ion outflow at greater altitudes. Tristatic flow data show that these fluxes occur in regions where a strong electric field drives the plasma eastward in the dawn convection cell against the prevailing westward flow of the neutral atmosphere, and where particle precipitation creates enhanced Pedersen conductivity with consequent strong Joule heating. Figure 7 shows examples of observed field-aligned velocity profiles during heating events, indicating the large upward fluxes at greater altitudes.

Examination of examples occurring on the Tromsø field line suggest that strong upwelling of the neutral atmosphere due to Joule heating in the E-region, enhanced plasma pressure due to frictional heating in the F-region and the hydromagnetic mirror force associated with non-thermal ion distributions, all contribute to the upward acceleration which drives the plasma at speeds of over 500 ms^{-1}. However, the large majority of such events occur several degrees to the north of EISCAT, and can only be studied using tristatic data from the northernmost positions of EISCAT Common Programme Three (a wide latitudinal scanning programme which computes a full scan every 30 minutes). These data give an estimate of the field-aligned velocity at one height only, with large errors due to the poor measurement geometry, well outside the triangle defined by the three EISCAT stations.

An incoherent scatter radar on Svalbard would allow a proper study of these events. Coplanar observations of a single scattering volume by EISCAT and the Svalbard radar would be within a few degrees of the magnetic meridian plane at F-region heights and would give an accurate measurement of the true field-aligned velocity component in the polar cap and auroral oval. The relationship between electric fields and large up-fluxes of thermal ions, and estimates of the effect of these upward fluxes on the thermal balance of the plasma, could be examined with such data.

Other studies of field-aligned flows, field-aligned currents and non-thermal plasmas require multiple reception channels and an adequate system bandwidth to include both the up-shifted and the down-shifted plasma lines. Although field-aligned observations do not require very high spatial resolution, temporal resolution on the order of seconds is required to observe locally-heated, transient plasma populations.

3.(b) Polar Wind

For the polar ionosphere, the plasma pressure in the distant magnetosphere becomes insufficient to balance the pressure of the ionospheric plasma source. Light ions of the topside ionosphere, for which the gravitational energy is nearly balanced by the thermal energy, may thus escape from the ionosphere in a supersonic field-aligned flow. This was first suggested by W.I. Axford, who called this phenomenon the polar wind. A hydrodynamic theory predicted the existence of the polar wind for light ions. Subsequently, satellites have provided direct measurements of the ion fluxes above the auroral and polar regions, showing that the global picture of plasma outflow from the ionosphere is much more complicated than initially anticipated.

It was realised that the polar wind might not be limited to the polar cap and might extend to the auroral and subauroral regions at certain times and places. Indeed, a supersonic flow can exist even in a magnetic flux tube which is not open, when the pressure at the apex is below a critical value. The refilling process of magnetic flux tubes may then proceed via a period of supersonic flow. It is therefore of great interest to try to determine the relative extent of subsonic and supersonic flows in altitude, latitude and time.

The discovery of a large number of oxygen ions in the magnetosphere, which are necessarily of ionospheric origin, shows that ion escape is not restricted to light ions.

Several questions arise from the observations, especially those from satellites:

- where in latitude and altitude does ion escape occur?
- where and when do subsonic flows become supersonic?
- what is the influence of magnetic activity, season and other geophysical parameters?
- ultimately, what is the importance of the ionosphere as a source of plasma for the magnetosphere?

Theory has predicted the polar wind but so far the experimental evidence is limited.

Satellite measurements, made at an instant of time in a restricted volume of space, give useful information on the types of ions, their fluxes, their energies, but they give a limited picture of the escape process because they do not indicate what happens at lower altitudes, where variations in thermal pressure and/or other mechanisms take place.

Because an incoherent scatter radar can make measurements along a magnetic flux tube with short time resolution, it is a powerful tool to study the polar wind.

Provided its sensitivity is high enough to reach 1500 to 2000 km for the measured parameters, it might be possible to answer some of the questions listed above. Moreover, observations from radars at different locations, scanning from subauroral latitudes to high latitudes into the polar cap, can give precise information on the time and latitude occurrence of the supersonic flow and might shed some light on the emptying and refilling of the magnetosphere during the different phases of a storm.

Figure 8 shows the recent measurements by the EISCAT VHF radar of the ion outflow up to 1100 km. The O^+ ion velocities were measured by EISCAT and the H^+ velocities were derived by theoretical calculations from ionospheric parameter measurements.

4. Polar Ionosphere

4.(a) Ionization, Composition and Thermal Structure of the Ionosphere

An early task of an incoherent-scatter radar on Svalbard will be to establish the basic topography of the ionosphere in the cusp region and in the polar cap. There are strong indications that in the polar-cap ionosphere parameters such as electron concentration and electron and ion temperature often vary more than at any other latitude. For example, the measurements made by the Dynamics Explorer satellite DE-2, while scanning in latitude, show that the electron concentration at 500 km often shows a maximum or a minimum in a narrow zone centred at invariant latitude 75° N, whereas the electron temperature shows a sharp maximum in the same zone.

Many factors can be invoked to explain why the average behaviour of the ionosphere at very high latitudes should display such variation:

i) In the cusp region the balance of ionisation in the ionosphere is strongly affected by both precipitation and strong plasma upflows.

ii) At high latitudes the solar illumination shows a very large seasonal variation with long periods of total darkness in winter balanced by even longer periods of total illumination in summer. However, in the polar cap the simple balance of ionisation and recombination is strongly modulated by the very rapid convection of plasma in the polar cap, which transfers flux tubes from illuminated regions on the dayside into the midnight sector, while other flux tubes "stagnate" for long intervals in regions of darkness. The high plasma velocities associated with this convection will generate frictional heating of the ion population and if this is large enough it will, in turn, cause a sharp increase in the plasma recombination coefficient.

iii) A third factor that is unique to polar cap latitudes is the effect of open magnetic field lines on the ionosphere. Such field lines allow the total escape of plasma upwards, such as observed in the polar wind: at the same time they provide a channel of high thermal conductivity linking the cold plasma of the ionosphere with the much hotter plasma of the magnetosphere.

A radar on Svalbard will provide an unique data set, giving a continuous record of the polar-cap ionosphere over a height range from 90 to 1500 km at all times of day, for all seasons and all geomagnetic conditions. The ability to determine electron concentration, electron and ion temperatures and ion composition will provide scientists with the first truly comprehensive picture of the high-latitude ionosphere.

4.(b) Patches, Blobs and Irregularities

In addition to large variations in the average properties of the ionosphere, substantial evidence exists, both observational and theoretical, suggesting that 'patches' of enhanced ionisation form an important component of the dark polar-cap ionosphere in winter. Ionosonde studies, from Thule, Greenland, have shown increases in peak electron density by up to an order of magnitude above background on timescales of minutes to tens of minutes. Similar abrupt changes in total electron content, often much greater than the normal average diurnal range of this parameter, are a dominant feature in the post-noon sector. These temporal changes can be mapped to localised patches of ionisation, 100 to 1000 km in horizontal extent, which convect in an anti-sunwards direction across the polar cap with speeds up to a few kms^{-1}. These patches have been shown to exist for a wide range of magnetic conditions but they appear to be associated primarily with the southward-directed interplanetary magnetic field. Various types of blobs have been identified; boundary blobs located at the equatorward edge of the auroral oval coinciding with the precipitation zone and isolated blobs at the poleward edge of the boundary blobs in the auroral zone. Considerable uncertainty still exists about the generation, development and decay of these blobs.

Recent EISCAT observations have provided evidence that density enhancements are produced at high latitudes and low altitudes and drift towards low latitudes and high altitudes. High electron temperatures in the early stages of their development, which subsequently decrease, point towards particle precipitation as a generation mechanism, as suggested by earlier Chatanika and scintillation measurements. Other data favour generation by solar EUV and transport across the polar cap. Modelling studies have indicated how enhanced plasma densities in the dark polar cap could result from extended transit of relevant flux tubes through regions of significant solar production south of the cusp, prior to convection as patches across the polar cap. A patch is generated when there is an abrupt increase in cross-tail potential with consequent expansion of the polar cap radius, the horizontal extent of the patch being related to the time during which the new convection pattern is operating. Recent EISCAT observations of transient bursts of plasma flow into the dayside polar cap (see Section 1.(a)) are of great interest as examples of polar-cap plasma patches produced by this particular mechanism. In addition, the convection of patches out of the polar cap into the high-latitude nightside auroral ionosphere is of interest. Cross-polar-cap transport of patches requires study in relation to the structure of the nightside F-region auroral plasma.

The patches are also of importance in smaller-scale irregularities that are responsible for the scintillation of transionospheric propagating signals, which can severely disrupt space-borne radio systems at high latitudes. The abrupt changes in electron concentration are associated with steep localised gradients which may be unstable; if the plasma is convecting faster than the neutral atmosphere, the trailing edges of the patches would be unstable to the ExB gradient-drift mechanism. Some limited evidence has been found indicating scintillation due to sub-kilometre scale irregularities, associated with the trailing edges of patches. Irregularities have also been found near the leading edges and in the interiors of some patches, so that other types of generation mechanism may also be operating. A dependence of scintillation occurrence in the polar cap on solar activity has been found; since scintillation is related to the irregularity perturbation in electron concentration, a key factor in scintillation occurrence is the magnitude of the electron concentration in the polar cap, itself strongly dependent on solar activity. An incoherent scatter radar, located to observe from sub-cusp latitudes into the polar cap, would be an important tool in experimental studies of the birth of patches, their detachment from the dayside boundary, transport out of the cap and their role in generating blobs and irregularities, though this implies a need for multiple beams in order to resolve ambiguities between spatial and temporal effects.

Studies of irregularities in the ionosphere require detailed observations of sub-kilometre structures. In particular, there is a need to study the trailing edges of 'blobs' in fine detail, measuring electron density gradients and E fields with a temporal resolution of about 20 seconds. The blobs themselves have time scales (in the beam) of about ten minutes, travel at a few kms^{-1}, and have horizontal extents of 100-1000 km.

F-region fine structure with horizontal scale sizes from sub-kilometre to about 20 km would be well measured using simultaneous, multiple beams and provision for cross correlation between the beams would allow accurate velocity determination.

An important modelling requirement is to attempt to relate local irregularity structures with global structures. For this purpose, many parameters must be measured over a wide area and observations using either simultaneous, multiple directions or very fast scan patterns are required.

This work is not only important for studies of topics in basic science, but it also has spinoffs in several applications areas such as radio propagation and direction finding.

5. Thermospheric Studies

5.(a) Thermospheric Response to IMF

Within the polar cap, neutral winds in excess of 300 ms^{-1} are observed at altitudes around 300 km under almost all conditions. The peak velocities tend to follow the general trend of geomagnetic activity, with velocities in excess of 1 kms^{-1} being reported under very disturbed conditions. Generally, these winds are directed anti-sunward and result from a combination of mechanisms. These include global day-to-night pressure gradients, due to low-latitude solar heating, local ion-drag forcing the thermosphere over the polar cap, and continuity of the neutral flow driven by ion-drag in the dawn and dusk sectors of the auroral oval.

During periods of strong northward-directed IMF, the conventional pattern of anti-sunward wind breaks down. There is still uncertainty regarding the overall large-scale flow patterns within the polar cap at such times, while flow-mapping into the magnetopause and magnetotail regions during such conditions is still the subject of conceptual debate. However, it is clear that regions of sunward plasma flow do occur, as do regions of sunward neutral flow, aligned closely with the ion flow. There are, however, no quantitative global models of particle precipitation equivalent to those available for more usual conditions, and the state of the ionosphere at times of strong northward IMF is still not understood.

There are also cases of observation of sunward winds over the polar cap which appear uncorrelated with northward IMF. These observations are from both incoherent scatter radars and Fabry-Perot interferometers at Søndre Strømfjord, Greenland. Normally the meridional wind, as observed from that location, is directed equatorward throughout the night-time period. Occasionally, however, there are periods of 1 to 3 hours, during the night, when the meridional wind reverses so that poleward winds are observed. Since changes in the IMF appear to be unable to explain these observations, they remain a problem for the future.

Combined mapping of large-scale plasma and neutral atmosphere characteristics over the polar cap would be necessary to describe the underlying physical cause of such events. An incoherent scatter radar station within the polar cap, augmented by complementary neutral-wind observations, would be ideally situated to study these structures and to map the ionospheric response to changes in IMF-B_y (Figure 9).

The first-order response of the polar-cap plasma convection to the orientation of the y-component of the IMF has been established. The main response of the F-region convection pattern to a change in IMF-B_y is in the polar cap: the antisunward ion flow is stronger on the dawn side of the polar cap for positive B_y and stronger on the dusk side for negative B_y. The details of the plasma flow, the effect on the distribution of plasma densities, and the dynamical, as well as chemical, response of the neutral atmosphere are all areas of great interest. Numerical simulations indicate that the distribution of F-region plasma concentration over the polar cap responds to the change in convection, and that this response is dependent on season. In winter the neutral atmosphere at F-region heights is primarily atomic oxygen and the lifetime of the dominant O^+

ion is many hours. In this situation, transport of plasma plays a major role in the large-scale distribution, and 'tongues' of increased ionisation can form over the polar cap, creating structures that depend strongly on the detailed shape of the convection pattern. In summer, the neutral atmosphere contains significantly more molecular nitrogen at these altitudes, reducing the lifetime of the ions and consequently decreasing the influence of transport. Model predictions indicate that the summer-time polar cap distribution of ionisation is generally correlated with the composition of the neutral atmosphere, while the neutral composition itself is controlled partially by the neutral wind, driven by the B_y-dependent convection pattern.

It is also important to study tides at high geographic latitudes. These studies would normally require tristatic capability from the new radar; however, three beams from one site, rather than three separated receivers, would be acceptable.

6. High-Latitude Plasma Physics

Although most of the science which is discussed in this report may in a broad sense be called space plasma physics, we have collected in this section some discussion of phenomena in which plasma microprocesses also play an important role.

6.(a) Extraction of Ionospheric Plasma by Magnetospheric Processes

Most of the transfer of magnetospheric energy into the thermosphere and ionosphere can be referred to one of the following three kind of processes:

- energetic particle precipitation from the magnetosphere into the upper atmosphere,
- heating of the upper atmosphere due to the convection of the magnetospheric and ionospheric plasma in the large-scale electric and magnetic fields within the magnetosphere, and
- heating and acceleration of ionospheric plasma at higher altitudes and expulsion of it into the magnetosphere.

All of the above processes are associated with electric currents and are thought to be intimately related to the ejection of plasma from the ionosphere into the magnetosphere.

The global quantitative aspects of the first two processes had been estimated by the 1960s but the important role of the ionosphere in providing plasma to the magnetosphere was unknown and even unexpected by the space physics community as late as the formation of the EISCAT Scientific Association in 1975.

The polar wind has been estimated to supply the magnetosphere with a fairly steady flux of cold ionospheric ions from a few times 10^{25} ions s^{-1} to a few times 10^{26} ions s^{-1} outside of the plasmasphere. Sources involving acceleration of ions by electric and magnetic fields and waves contribute as least as much in total number flux as the polar wind. In terms of energy flux from the ionosphere to the magnetosphere, the polar wind contributes much less than the accelerated ions from the auroral zone and the polar cap. The extraction of ionospheric plasma from the ionosphere corresponds to a power flux of one to a few 10^9 W, which is one percent to a few tens of percent of the energy flux associated with the energetic particle precipitation (10^{10}-10^{11} W). Nonetheless, the extraction processes may affect the upper ionosphere significantly. Only with the Polar Cap Radar will it be possible to investigate such effects in the polar cap and the cusp/cleft region.

The question of which physical mechanisms play the major role in the energization and ejection of ionospheric plasma into the magnetosphere is a front-line item of research in space physics. Both magnetic field aligned and perpendicular acceleration mechanisms are certainly important. The S3-3 satellite provided the first direct observations of strong field-aligned upward-moving ion beams above the ionosphere but it also recorded the very frequent occurrence of acceleration of ions transverse to the magnetic field, producing the so-called ion conics. The perpendicular acceleration has been associated with ion cyclotron waves. It has been observed down to 400km altitude and it should widen the ion spectrum seen by the Polar Cap Radar.

The question of whether the waves accelerate the ions into beams or the beams cause the ion waves has recently been answered tentatively. At intermediate altitudes, the beams generate the ion waves, but waves are generated only when the cold electron density is not too high. These studies will need to be extended during the next decade and the Polar Cap Radar will provide important data from the upper ionosphere, which is the source region for the heavy magnetospheric ions.

Field-aligned electron distributions moving in the same direction as field-aligned ions were first reported from near the equatorial plane. Similar distributions have recently been observed at heights between 2500 and 13500km, which were the minimum and maximum altitudes of measurement of the Viking satellite. These phenomena have been found to be strongly correlated with slow electric field fluctuations with a power density spectrum that peaks below 1 Hz, i.e. below all characteristic frequencies of the ion species present in the upper ionosphere and lower magnetosphere. An example of a strong correlation between ion beams and electric fields is shown in Figure 10. The roughly perpendicular electric field component is shown in the middle frame. In the periods when ion beams (06:28:15 - 06:29:15 UT) and ion conics (from 06:30:25 onwards) were observed, there were also fluctuations in the electric field component of the order of magnitude 100 mV m^{-1}. Such large-amplitude fluctuations were not seen outside these time intervals. In the same period the plasma density was strongly reduced, as is illustrated by the two lowest frames (V_{fg} is the floating ground potential, which is proportional to log ($n_e \sqrt{T_e}$)) measured by means of the electric field experiment on Viking. When the electric field fluctuations were very large in amplitude, Viking generally recorded ion conics instead of beams. In cases of strong electric field fluctuations with elevated ion conics, the power density reaches 10^3 (mV $m^{-1})^2$ Hz^{-1}, which is some three orders of magnitude higher than the "normal" values characterizing situations with no measurable fluxes of upward flowing ions. When the slow electric field fluctuations are so large that the ions show conical distributions (elevated or not), narrow upward-directed electron beams of energies of the order of hundreds of electron volts are also frequently seen.

The example shown in Figure 10 was obtained at an altitude of about 7500 km, but Viking has made similar observations down to 2500 km, as mentioned before. The electric field fluctuations sometimes reach down to the DE2 satellite in the upper ionosphere, although with reduced amplitudes.

The cusp/cleft region has been found to be a particularly intense source region of slightly accelerated (suprathermal) ions (the cleft ion fountain). There are strong reasons to believe - but it is not definitely proved - that the acceleration of both the ions and electrons is caused by the electric field fluctuations mentioned. They affect the heavy ions more than the light ones. An important task for the Polar Cap Radar will be to investigate these upward flowing ions at very high magnetic latitudes.

The source of the slow electric field fluctuations is unknown but probably it is located in generator regions within the magnetosphere and the waves most likely travel to the ionosphere as some sort of Alfvén waves.

A particular feature of the slow electric field fluctuations is, as mentioned, that they may also give rise to strongly field-aligned beams of electrons, with energies of the order of hundreds of electron volts, streaming out of the ionosphere. For this to happen the fluctuating electric field has to have a small component directed along the magnetic field lines. Although it has not been possible to definitely measure this parallel electric field component with the Viking double-probe experiment, there are good general reasons to expect that it mostly exists when the strong perpendicular electric field fluctuations are observed. Assuming this and that the parallel acceleration region has a limited height extension of one or a few thousand kilometres, observations can be understood as caused by slow electric field fluctuations with a small parallel component. Whereas the ions move only short distances up and down along the magnetic field lines in the fluctuating field, the electrons, which move much faster, may be "shot" out of the acceleration region while the parallel field component points in one direction.

The key parameter in the estimation of a possible effect on ionospheric density caused by the expulsion of ionospheric plasma into the magnetosphere is, as mentioned above, the upward flux of ionospheric ions along the magnetic field lines. The first measurement of this flux was made by means of the S3-3 satellite at intermediate altitudes (below 8000 km). Characteristic fluxes observed at altitudes of about 1 R_e were

10^8 ions $cm^{-2}s^{-1}$ and the most intense fluxes were about an order of magnitude higher. A flux of 10^8 $cm^{-2}s^{-1}$ at 1 R_e corresponds to ~$8 \cdot 10^8$ $cm^{-2}s^{-1}$ at ionospheric altitudes.

Measurements with EISCAT of upflowing ions in the nightside auroral oval ionosphere have only recently become available. Cases have been found in which strong electric fields increase the ion temperature and cause Joule heating. The upward ion flows observed in the upper ionosphere under such conditions may be caused by the pressure increase associated with the electric field heating. Other recent observations by means of EISCAT at altitudes of up to more than 1000 km have shown large upward field-aligned flows of the bulk ion population, primarily within auroral arcs and in the absence of strong perpendicular electric fields. The ions (mainly O^+) have been found to reach field-aligned velocities of more than 1000 m s^{-1}, corresponding to ion fluxes of up to $2 \cdot 10^{10}$ $cm^{-2}s^{-1}$. No enhancement of the ion temperature has been observed during these ion outflow events. The field-aligned velocity increases with increasing altitude. We thus see that the largest ion fluxes observed at intermediate altitudes, as described earlier, can also be traced down to the F-region when no heating by electric fields is present. How these high fluxes in the upper ionosphere are produced is far from clear. A magnetic-field-aligned, electric-field component is one possible cause. It may also be an effect of a density cavity at greater altitudes on auroral field lines, a so-called auroral plasma cavity, which has been found to extend sometimes to altitudes as low as 1000 km.

The new EISCAT results mentioned above seem to connect the intermediate altitude observations with observations in the auroral-zone ionosphere in a promising way. However, it still remains to be understood how the high-density, low-velocity beam into the upper ionosphere is transformed to a low-density, high-velocity beam at a few thousand km altitude. In the investigation of that question, the Polar Cap Radar at Svalbard has a very important role to play.

The observed high rate of expulsion of ionospheric ions into the magnetosphere, mentioned above, implies that the upward flow of ions may strongly reduce the density above the F-layer peak. This should be easily observed with the Polar Cap Radar.

6.(b) Non-Thermal Plasmas

The high-latitude ionospheric plasma is frequently characterized by a strongly anisotropic high-energy tail. This may, however, not affect significantly the plasma bulk-properties as seen by incoherent scatter radars in the main part of the ionosphere, except when specific resonance conditions are met which create structures of the "right scale". However, at great altitudes at auroral and polar-cap latitudes, where the plasma density may be very low, the proportion of the non-thermal, energized plasma component may be much larger and the assumption of a Maxwellian distribution may not be applicable. Recent EISCAT observations have revealed the effects in the main part of the F-layer of supersonic plasma drifts through the neutral gas with which the ions collide. The resulting non-Maxwellian ion-velocity distributions can produce characteristic forms of the spectra measured by an incoherent scatter radar. As well as causing non-Maxwellian ion-velocity distributions along the line-of-sight, these effects also render the three-dimensional ion-velocity distribution anisotropic. Large temperature anisotropies ($T_{perp}/T_{para} > 2$) have been deduced from tristatic EISCAT observations.

One possible approach to analyzing incoherent scatter spectra under these circumstances has been to add a simple shape-deformation factor to describe the ion-velocity distribution function. Although the exact form of this is purely empirical, the distribution function is derived from the relaxation model of ion-neutral collisions, which are a mixture of polarisation elastic scatter and resonant charge exchange, and are computed using Monte-Carlo techniques. The results show that the aspect angle dependence of the line-of-sight ion-velocity distribution is more complex than predicted by the relaxation models. Furthermore, even the simulations do not allow for the effects of instabilities which are driven by, and subsequently act on, the distorted distribution function. There is evidence for instabilities driven by large electric fields with considerable k-vectors along the magnetic field. The ion-cyclotron instability is the prime candidate for such effects but the Post-Rosenbluth instability may also be important at certain plasma temperatures.

It is vital to make observations of the three-dimensional ion-velocity distribution both in and above the main F-region and to assess the role of various interactions and potential instabilities. An individual incoherent scatter radar can only gain information about the line-of-sight distribution function, whereas the viewing geometry for the EISCAT tristatic system gives aspect angle differences between the three directions - at appropriate ranges - which are too small (<30°) to be of use. An attempt has been made to overcome this problem by using a latitudinal scan across a region over which the plasma and thermospheric parameters (including ion drift and the neutral wind) are assumed to be roughly constant (see Figure 11). However, this assumption severely limits any conclusions that can be drawn. A better solution is to study the same volume of plasma independently, with two radars, to give information on the aspect angle dependence of the distribution function, whilst deriving improved ion-drift parameters.

The Svalbard radar offers the ideal viewing geometry for studying the non-thermal ion-velocity distributions created by the very large flow bursts observed north of EISCAT (See Section II C.1(a), above). A wide range of aspect angles (essential for the study of non-Maxwellian spectra for which the angular difference between the direction of observation and the local magnetic field is crucial), from parallel to almost perpendicular, would be available. In one configuration, for example using both Tromsø and Svalbard in transmitting and receiving modes, it would be possible to make two independent, bistatic measurements of the velocity component parallel to the magnetic field, and also two measurements at an aspect angle of 54.7°, where the observed ion temperature corresponds to the theoretical mean value.

The importance of these studies should not be underestimated. In many areas of ionospheric physics an isotropic Maxwellian ion-velocity distribution has been assumed but recent observations indicate that non-thermal effects are often present in EISCAT data, over large areas of the auroral oval, even for moderate magnetic activity. At present, analysis of ion temperatures can only be carried out for one specific aspect angle by assuming some form of the 3-dimensional ion-velocity distribution function. Indeed, for a temperature anisotropy of 2.5, which is both predicted and experimentally confirmed for large auroral electric fields, parameters derived from observations made close to the field direction can be wrong by as much as 100%, if an isotropic distribution is assumed.

The Polar Cap Radar would allow ion temperatures to be measured over a range of latitudes which would not be subject to this uncertainty - and the results of this work would allow the appropriate corrections to be made to EISCAT observations, including, of course, the existing data base. Furthermore, the observations possible with such a radar open up a whole new area of studies of plasma instabilities driven by large field-perpendicular ion drifts in the presence of ion-neutral collisions. The same principles apply to the effects of other instabilities driven by, for example, auroral precipitation and field-aligned currents.

These non-thermal plasma studies require time resolutions of the order of 1 minute, and the system must be capable of making observations in a common volume with EISCAT. Bistatic observations between Tromsø and the Polar Cap Radar (with cross reception of each radar at the other site) would then give unambiguous field parallel and field perpendicular data for non-thermal plasma velocity distribution studies.

The new radar would make fundamental contributions to many areas of plasma physics research, as well as in the more conventional geophysical areas.

7. MST Studies in the Polar Cap

The mesosphere can be studied with the incoherent scatter, as well as with the MST (mesosphere-stratosphere-troposphere), radar technique. In the lower thermosphere and mesosphere the incoherent scatter process is collision dominated. Incoherent scatter measurements of the lower thermosphere and mesosphere allow the derivation of electron density, ion-neutral collision frequency (neutral density) and temperature, ion (neutral) velocity, ion composition and the density of negative and positive ions, provided some assumptions can be applied. Occasionally coherent scatter from ionization irregularities can mask the incoherent scatter measurements, particularly in summer when Polar Mesosphere Summer Echoes occur.

On the frequencies used by EISCAT in Tromsø (224 MHz and 931 MHz), as well as on the anticipated Polar Cap Radar frequency of 450 MHz, the turbulence scatter contribution to echoes from mesospheric altitudes is usually negligible.

At frequencies as high as 450 MHz, observations of the troposphere and the lower stratosphere are certainly possible. These radars are known as ST (stratosphere-troposphere) radars. They are also called wind profilers, since they are applied in routine meteorological observations to measure wind profiles continuously. ST radar wind profilers measure the vertical profile of the three-dimensional wind vector, atmospheric stability and turbulence intensity, with a height resolution of some 100 metres and a time resolution as good as several seconds. Figures 12 and 13 present some results from MST radar observations, in order to prove the applicability of such measurements to the studies discussed in this section. Further examples are displayed and described in greater detail in a separate report entitled 'Polar Cap Radar: Research of the Polar Mesosphere-Stratosphere-Troposphere: A Proposal' by J. Röttger (hereafter abbreviated to MST-PCR).

7.(a) Coupling Processes Between the Lower Thermosphere and the Mesosphere

Particular phenomena in the polar atmosphere and the auroral ionosphere, namely particle precipitation, Joule heating, electric fields and Lorentz forcing, as well as vertical transport of constituents and momentum, which result from magnetosphere-ionosphere coupling, have an impact on the middle atmosphere. Furthermore dynamic processes, such as tides and gravity waves, which originate in the lower atmosphere (troposphere) and the middle atmosphere (stratosphere and mesosphere), propagate upwards into the thermosphere. These mutual coupling processes, which affect the structure, dynamics and aeronomy of the middle atmosphere and lower thermosphere, take place uniquely in the high latitude mesosphere, where the effects from the magnetosphere and ionosphere merge with the effects from the lower and middle atmosphere (see Figure 14).

The EISCAT UHF and VHF radars have already demonstrated their great value in studies of the coupling processes linking upper and lower regions of the lower thermosphere in the auroral zone. Several mesosphere/ D-region investigations have been undertaken with EISCAT, such as for instance the impact of precipitating electrons and protons on the D-region electron density and composition. How these coupling processes between the magnetosphere and the ionosphere, the thermosphere and the middle atmosphere take place in the polar cap region is so far unknown, since appropriate radar instruments are not operated at these high latitudes near 80°. For instance, the influx of solar protons into the polar-cap mesosphere and upper stratosphere clearly has an influence on the ozone budget and can be studied by the Polar Cap Radar. It would also be useful to perform simultaneous radar experiments in the auroral zone (EISCAT) and in the polar cap (Spitsbergen) to study the meridional variation of these effects and how their extension to lower altitudes in the middle atmosphere takes place.

Specifically, the Polar Cap Radar in the MST mode should be used to observe and study mesospheric temperature and winds, the possible auroral influences and the transport of nitric oxide, as well as solar proton events (SPE), the resulting polar cap absorption phenomena (PCA) and their impact on middle atmosphere ozone and dynamics. The extent of Polar Mesosphere Summer Echoes (PMSE) and their relation to Polar Mesosphere Clouds (PMC) and Noctilucent Clouds (NLC), Sudden Sodium and Sporadic-E layers needs to be studied in polar latitudes. The winter anomaly of absorption and its relation to stratospheric warming in the polar vortex is not known in the high latitudes of 80°. Also most essential is a climatological study of winds, tides and long period waves and particularly the climatology of atmospheric gravity waves (AGW) in the polar cap mesosphere, the supposed acceleration of the mean wind by AGW momentum deposition and the effect on the mesopause temperature. Details on these proposed research programmes are described in the separate report (MST-PCR).

For these obvious reasons, the Polar Cap Radar should have the capability to make detailed observations of the D-region and the mesosphere, in addition to the planned studies of the ionosphere and thermosphere.

7.(b) The Polar Stratosphere and Troposphere investigated by the Polar Cap Radar in ST Mode

There are also certain phenomena in the polar middle and lower atmosphere which need to be studied by radar, in addition to the multitude of other experiments that are already used for these studies in the Arctic and Antarctic, particularly those directed to the ozone problem. We will discuss only those phenomena that can be investigated with an ST radar (stratosphere-troposphere radar). These are the structure and dynamics of the troposphere and the lower stratosphere in the polar cap. The capabilities of ST radars for these studies are outlined in the separate report (MST-PCR) and the references cited therein.

With ST radar wind profilers it is possible to study dynamic processes in a wide scale range from planetary and synoptic-scale disturbances to small-scale gravity waves and clear-air turbulence. The wind field variations occurring in the polar vortex can be monitored continuously by an ST radar wind profiler, although only at one location and up to about 20-30 kilometres height. In polar regions it is of special interest to investigate with radar the exchange processes between the troposphere and the lower stratosphere, namely the variation of the tropopause height and the dynamics of tropopause foldings and fronts. The possibility of studying vertical transport between the troposphere and the stratosphere, and the transport within the stratosphere by means of the mean vertical motion and by turbulent diffusion, is challenging. The transport and deposition of energy and momentum by gravity waves in the lower stratosphere, which can be measured with ST radar, is also believed to have an impact on the mean stratospheric circulation and the polar stratosphere temperature. Furthermore, Polar Stratospheric Clouds, which are assumed to be related to mountain waves, exert control on the ozone depletion. The formation of mountain waves can be studied by ST radar and thus the dynamics in and around Polar Stratospheric Clouds can also be investigated by the Polar Cap ST radar. Such an ST radar, if it could be operated continuously, would also yield invaluable input data for meteorological modelling and forecasting. In summary, ST radar observations can contribute considerably to the study of the structure and dynamics of the polar cap stratosphere, as indicated in Figure 15.

It is necessary to understand the dynamics of the polar cap stratosphere before a complete picture of the ozone depletion phenomenon can be obtained. Expert scientists propose that further acquisition and examination of a broad range of chemical as well as dynamical observables will be necessary to address the challenging and important question of whether the processes leading to the Antarctic/Arctic ozone hole can also occur in other parts of the Earth's atmosphere.

The ST radars detect echoes which are scattered back from irregularities of humidity and temperature in the troposphere and irregularities of temperature in the stratosphere. The technique has developed to a stage which allows its routine application for operational meteorology. There are basically two frequency ranges that are used for these applications, namely the 50-MHz and the 400-MHz bands. The lower frequency band has been used from the beginning and most of the desired evolution has been achieved. Moreover, great scientific expertise has developed in using the VHF radars in the 50-MHz band. A network of wind profilers is now being implemented by operating UHF radars in the 400-MHz band. The sky noise level as well as the antenna area is smaller on 400 MHz than on 50 MHz, which is the main reason for the choice of the 400-MHz band for wind profiler networks. The upper altitude reached is slightly smaller than on 50 MHz, which is explained by a reduction of atmospheric irregularity amplitudes at 400 MHz as compared to 50 MHz.

However, the Polar Cap Radar, operated in the incoherent scatter mode with 3 MW peak power and 40 dB antenna gain, will be about three orders of magnitude more powerful than the troposphere-lower stratosphere 400-MHz wind profiler radars, which obtain wind profiles up to some 15 kilometres. It is estimated that the full-power Polar Cap Radar on 400 MHz would reach altitudes above 20 km. This can be confirmed by the troposphere- stratosphere observations with the Arecibo 430-MHz radar.

Several of the listed research topics need continuous data sets for climatological applications. It needs to be pointed out here, that the operation of a 450 MHz system for continuous routine observations is restricted, because of its primary application to ionospheric research. Certain research topics, such as the climatology of turbulence, gravity waves and wind fields will thus be hampered, or be impossible, with this system configuration. One may envisage, however, that the continuous operation of a subunit of the total system would allow us to obtain some data sets that could be used for climatological studies. The 450 MHz system has to be configured from the beginning in a way that will allow such observations.

It also needs to be noted here that certain measurements are not possible on 450 MHz because of the frequency-dependent properties of the scattering medium. For instance, more regular mesosphere studies, investigations of tropopause and frontal structures in the troposphere, and probably also observations of stratospheric layering, cannot be performed on 450 MHz.

8. Other Subjects of Study

One of the exciting features of any scientific discussion of a proposed incoherent scatter radar on Svalbard is that the number of fields where important studies can be made increases continually. In the discussion above, we have concentrated on seven fields of study in which members of the EISCAT community have been working for a number of years. We are very aware, however, of several other subjects of study where the prospects are equally exciting.

As examples, we would list the following:

(i) Solar wind-magnetosphere-ionosphere interaction studies require observations of MHD waves, with sources near the magnetopause providing energy coupling between the magnetosphere and ionosphere. In addition, the polar cap appears to be populated by MHD waves of unknown origin. There is much interest in such wave fields in the vicinity of the cusp; also, of course, in association with FTE phenomena. PC-2's, with periods of a few tens of seconds, are perhaps the least understood, while PC-1 observations would require sub-second temporal resolution.

(ii) Atmospheric gravity waves (AGW's), with sources in the polar cap and the auroral oval, provide a route for energy flow between the thermosphere and ionosphere. Observations of northward propagating waves generated by auroral sources would be most interesting - particularly if EISCAT also observed equatorward propagation from the same source. Five minutes resolution (or even shorter time scales), generally not scanning but with tristatic measurements for gravity-wave studies, is required; three beams from one site would be an acceptable alternative.

(iii) Sporadic-E and gravity-wave studies require high time and spatial resolution, coupled with simultaneous observations at multiple positions - for example, parallel and perpendicular to the local magnetic field. Atmospheric gravity waves are already known to be very prevalent in the vicinity of Svalbard, perhaps with tropospheric or stratospheric sources, and data acquired during the International Geophysical Year showed Sporadic-E to be common at Longyearbyen, the proposed site for the new radar.

(iv) Studies of the newly observed and poorly understood phenomenon of the turbulent heating of the E-region, through unstable waves in both the polar cap and auroral zones, will require high height and time resolution. This type of turbulence causes a tenfold increase in electron temperature in a narrow altitude range and is likely to modify significantly the E-region chemistry. This has the result of altering the electron density, which in turn determines the heating rate of the neutral atmosphere.

(v) Field-aligned plasma irregularities give rise to coherently backscattered signals and these irregularities are normally generated by the electrojet but may be also associated with field-aligned currents leading to instability. The rate at which the amplitude of coherent echoes falls off with increasing off-perpendicular angles from the local magnetic field is observed to be slower than theoretically expected. The new radar would enable this phenomenon to be observed routinely under a wide range of ambient conditions.

(vi) Many modelling projects require the new radar to provide detailed point measurements for the evaluation of existing, and new, models. Important parameters are the size of the polar cap, the positions of the polar cap boundary, the convection and precipitation boundaries, the Harang discontinuity and temperature and heating effects. Detailed mapping of trough features is important as are measurements in the ionospheric topside - the lowest acceptable altitude would be around 700-800 km in the winter nightside ionosphere. Data from further north are also required for modelling studies. These observations cannot be made by EISCAT because they are located so far to the north that 3D measurements are impossible. However, the Tromsø and Svalbard meridians are almost coplanar, which would allow an excellent determination of field-aligned flows using the two radars together.

(vii) The possibility of observing the perturbed plasma produced by the MPI RF heating facility at Tromsø with a radar located on Svalbard would provide new insights into plasma processes. The heated region has only been probed in the field-aligned direction using the current EISCAT system. An active system on Svalbard offers an unique opportunity to study the plethora of predicted effects at large aspect angles

III. SITE DEFINITIONS AND LOGISTICS

III.A. Sovereignty, Administration, Population, Weather and Climate

The Treaty of Svalbard dated 9th February 1920 gives Norway sovereignty over the archipelago and surrounding territorial waters. By the Act of 17th July 1925, Svalbard became part of the Kingdom of Norway. The signatories of the Treaty of Svalbard have the right of access and residence as well as equal rights in stipulated commercial, industrial, and research activities. As a research facility an IS radar on Svalbard is permitted by the Treaty. The islands Bjørnøya (Bear Island) and Hopen are Norwegian territory with exclusive Norwegian rights.

The administrative centre of Svalbard is Longyearbyen which is a mining community with about 1000 inhabitants and located on the largest island Spitsbergen. The Governor (Sysselmannen) is the Government's highest representative in Svalbard. He is also the Chief of Police, and is responsible for enforcing the legislation applying to Svalbard.

Longyearbyen is a well developed community with public services and amenities such as kindergarten, schools at different levels, hospital, church, bank, post office, shop, travel agency, restaurants, cinema, museum, library, engineering workshops, taxi and car rental etc. Svalbard Airport has passenger flights to Tromsø on the main land 4-5 times a week, depending on the time of the year. Longyearbyen is also the centre of telecommunications on Svalbard with connections to mainland Norway via satellite. Other smaller communities are Ny-Ålesund (research station), Sveagruva (mining), Isfjord Radio, Hopen and Bjørnøya (radio and weather stations), and Hornsund (Polish research station). Barentsburg and Pyramiden are Soviet mining communities about the same size as Longyearbyen.

In the coldest winter months, January-March, the average temperature in the Longyearbyen area is -11° to -12°C. The temperature can drop to under -20°C at times. The summer temperature seldom rises above +15°C and is +4° to +5°C on average. There may be strong wind, particularly in winter. Fog is usual in summer. At latitude 78° N (Longyearbyen) the sun does not rise above the horizon from 28 October until 14 February. There is midnight sun from 21 April until 21 August.

III.B. Site Recommendation

The recommended site for the Polar Cap Radar is the plateau above Mine No. 7 (Gruve 7) in Adventdalen, about 15 km from Longyearbyen (see Figure 16). The size of the plateau is about 2 km × 2 km. The lower part (to the north) lies 400-450 m above sea level and the higher part (to the south) about 500 m above the sea. The results of various measurements discussed below will determine the exact location of the radar on the plateau. A location closer to Mine No. 7 will reduce the costs associated with the provision of a road and power cable.

A site on the plateau has the following favourable properties:

- A good horizon profile
- A well developed infrastructure in its vicinity
- Little interference with existing facilities
- No conflict with environmental regulations.

Detailed considerations on these points are given below.

III.C. Horizon Profile

Figure 17 shows the horizon profile measured at the cairn on the ridge of the plateau near the mine. Low radar elevations are allowed at all azimuth angles. Although the horizon profile is slightly better in the higher part (to the south), moving around the plateau does not change the profile that much.

III.D. Existing Infrastructure

A road connection already exists between Longyearbyen and Mine No. 7. The road is of good quality and is kept open for the whole winter. The extension (1-1.5 km) of this road on to the plateau will be cheap and straightforward. The road on the plateau can easily be kept open.

The existing power line to Mine No. 7 is a 24 kV line specified as 3 × FerAl no. 70 (3 conductors of Fe and Al with a square of 70 mm^2) and is strong enough that also the radar can be connected. The capacity of the transformer at the mine is 4 MW. The mine uses only 1.0-1.5 MW; thus, there is an unused capacity of 2.5-3.0 MW which is sufficient for the radar. However, a new transformer must probably be installed on the plateau in any case. Otherwise the losses after the transformer would be too great. Also the use of the radar would cause annoying disturbances on the current delivered to the mine.

The energy supply in the Longyearbyen area is provided by a modern coal-fired power station. The electricity is supplied by two generators each of 5.5 MW output. The normal consumption is 50% of this and the peak load is 80%. This leaves an unused capacity sufficient for the radar. The energy supply is as stable and regular as in mainland Norway. Four diesel generators with a total output of 5.5 MW are kept in reserve and can be started at 10 minutes notice.

The water needed for cooling, sanitary equipment etc. on the site can be supplied by road transport. There is already established such transport to the mine.

Longyearbyen has good capacity for the accommodation of single persons. Furnished flats of about 20 m^2 with a kitchen and toilet can be rented for a minimum period of 6 months. There is a shortage of family houses and the EISCAT Scientific Association may have to build its own houses. Land is available and can be rented at a low price.

III.E. Possible Interference Problems

Three different kinds of interference problems have been considered in detail.

The possible electromagnetic interference on instruments at the site from the machinery in the mine and other associated activities has been measured. The frequency bands 224 ± 15 MHz and 931 ± 30 MHZ were found to be quite clean. In the band 350-500 MHz the only activity was around 385 MHz and these signals were weak and hardly detectable on the plateau. In conclusion, it is unlikely that RF-interference will cause any problems.

The possible impact of the radar on the telecommunications has been discussed with the Area Manager of the Norwegian Telecompany on Svalbard. Various radio links exist in the area. The impact on these links will be further investigated when the radar frequency has been decided and more is known about sidelobes and the distribution of power in the various harmonics.

The most serious interference seems to be with the air traffic. Svalbard Airport has about 30 landings or take-offs per day. Most of them are by helicopters which on days of good visibility follow the valleys at low height where they will be shielded against the radar beam. Also, 70-80% of the other traffic follows the flight path in the direction over the sea and should not be affected. The flight path in the opposite direction along Adventdalen is shown in Figures 16 and 18. It passes a few km to the north of the plateau at a minimum height of 3000 feet, that is, 500-600 m above the plateau. Thus, aircraft may pass through the radar beam for certain directions of transmission. Also, there is a waiting path at 5000 feet over Adventdalen. The possible impact on the aircraft instruments is currently being investigated in cooperation with the Norwegian Air Traffic Control Authorities. Certainly, some kind of precaution has to be taken. The best solution seems to be to install a separate small surveillance radar which can detect nearby aircraft and switch off the main radar under certain conditions. Also, direct communication can be established with the control tower at the airport. The radar is not expected to have any effect on the beacon in Adventdalen, which has a much lower frequency (326 kHz) and is located down in the bottom of the valley.

III.F. Environmental Regulations

Very strict environmental regulations apply on the Svalbard islands. The general rule is that one should apply to the Governor's Office one year in advance to ask the permission of any activity that will have an impact on the nature. The permission to build an IS radar on the plateau will certainly be given, the area already being disturbed by the presence of the mine.

III.G. Wind and Icing

Wind and temperature measurements have been carried out at Svalbard Airport since 1975. Before that data were taken at Skjæringa in Longyearbyen and at Isfjord Radio. However, local variations are strong in this area and the data from these three stations are of limited use to evaluate the meteorological conditions on the plateau. Thus a weather station was installed on the plateau in the second week of October 1990. The station measures wind and also temperature and humidity, which will provide information on icing. The measurements will continue until 31 May 1991, with a possible prolongation after that. The station is being run under a contract between Norges Allmennvitenskapelige Forskningsråd (NAVF) and the Norwegian Meteorological Institute.

III.H. Building Conditions

The mining company "Store Norske Spitsbergen Kulkompani A/S" owns the land on the plateau, which can be rented at a low price.

An important question to be answered is whether antennas (and buildings) can be built on rock or have to be set up on permafrost. The only safe way to find this out is to perform test drillings. Drilling by pole drill, which can go down to 6 or 7 m, can be made by the mining company at a cheap price. It has been decided that test drillings shall be carried out in late October or early November this autumn when drilling conditions are good and also no special permission is required. Some test drilling has been undertaken earlier near the cairn at the ridge of the plateau, where the rock was found 2.5-3.0 m below the surface. It is safer and also cheaper to build on rock. Permafrost behaves as a very viscous fluid and moves, albeit very slowly.

III.I. Auroral Clutter

The problem of auroral clutter has been identified and thoroughly investigated in a separate report entitled 'Some considerations about auroral backscatter interference to an incoherent scatter radar on Svalbard' by K. Schlegel. The elevation of the horizon towards the north is considerably lower than at Ramfjordmoen, but the minimum aspect angle at 100 km altitude is only about 6° (see Figure 17). It is well documented in the literature that the backscatter power from auroral clutter decreases considerably with aspect angle. Using the information about backscatter coefficients and aspect sensitivity available in the literature, it can be estimated that the auroral clutter may reach the incoherent scatter power level if the one-way antenna side lobe suppression is less than 20 dB for UHF frequencies and less than 23 dB for VHF frequencies. The worst case has been assumed for these figures and they apply only for observations at very low elevations towards north when the clutter enters the antenna through the nearest side lobe. In all other cases auroral clutter should not be a problem, since the suppression of the far side lobes is usually much better.

III.J. Cost Estimates for Construction Work

The following table gives cost estimates for the construction of a building on the site and the extensions of the road and power line from the mine to the site.

TABLE 1

BUILDING (similar to the one at Ramfjordmoen, 12,000 NOK/m^2)	NOK 12.00 M
ROAD (1.2Km)	NOK 0.50 M
HIGH VOLTAGE CABLE (1 km)	NOK 0.25 M
TRANSFORMER STATION (2 MVA) etc	NOK 0.75 M
TOTAL	NOK 13.50 M

IV. INSTRUMENTATION

IV.A. Possibilities for Polar Cap Radar Antenna-Transmitter Systems

The scientific requirements for the Polar Cap Radar (PCR) demand antennas of at least 30 m diameter, more than one quasi-simultaneous beam direction and a wide range of steerability in elevation and azimuth. A transmitter power in the order of 2-3 MW is considered necessary, and a frequency in the range 400-500 MHz is regarded as optimum. During the deliberations of the Working Group, discussions with technical and scientific consultants and contacts with industrial companies, specifications were worked out as guidelines; these are summarized in Table 2. These specifications were followed as closely as possible, although it turned out in due course that some of the specified requirements had to be modified or even waived owing to excessive costs.

We will outline here the possible options and alternatives, which we were able to investigate in the short time period available for the completion of the present report. We will first discuss antenna systems and then possible transmitter assemblies. We will finally summarize the available systems and recommend certain configurations of antenna-transmitter systems, in particular taking the investment cost limitations into account.

It is to be noted that in this preliminary report the currency units DEM (Deutsche Mark), GBP (Great Britain Pound), SEK (Swedish Crown) and USD (US Dollar) are used interchangeably. This is done only for convenience in compiling this preliminary version. Ultimately, all currency units will be converted into SEK (Swedish Crown), which is the accounting unit for EISCAT financial procedures.

IV.B. Potential Antenna Configurations of the Polar Cap Radar

During the discussions in the Polar Cap Radar Working Group meetings, certain kinds of antenna configurations and constructions, which would serve the given purpose, were considered. It turned out that support from expert consultants was necessary because of the very specific requirements which were imposed. The PCR Working Group thus decided to request a pre-feasibility study from the company Elekluft, which had already supported EISCAT for two years on the Tromsø radio frequency interference and transmitter problems. The following summary and recommendations on antenna systems for the PCR result from intensive collaboration between some PCR Working Group members, further advisers and consultants and the engineers of the Elekluft company. It also contains a summary of the extensive pre-feasibility study which was delivered by the Elekluft company. The complete pre-feasibility study is presented in a separate report entitled 'Pre-feasibility Study of POCAR Antenna Systems', which is subsequently abbreviated to 'Antenna Pre-feasibility Study'.

Basically four different kinds of antenna construction are regarded as possible:

1. Phased array,
2. Single dish with multiple feeds,
3. Three dishes with
   - 3.(a) 32 m diameter,
   - 3.(b) 45 m diameter,
4. Triple cylinder antenna.

1. Phased Array

To comply with the specifications, a phased array would consist of 6400 single elements forming an array of 47 m diameter. The illumination has to be tapered by a Taylor function, small mutual coupling between single elements is required, the capability of bidirectional circular polarisation is needed, as is the required bandwidth. Crossed dipoles are considered to be acceptable and the single element gain is marginally adequate. Crossed Yagi-Uda antenna elements have higher gain and reduced coupling and would be suitable. Time delay steering is necessary for beam swinging and a complicated distribution network is necessary. This electronic steering with a phased array, however, will not allow beam separations larger than some 10 degrees. In order to fulfil the specifications to cover high and low elevation as well as a large azimuth angle range, the array platform needs to be moved mechanically.

The advantages of a phased array are:
+ very flexible means of beam steering,
+ negligible degradation for beams steered off-boresight for small steering angles (≤15°),
+ low sidelobes,
+ inherent capability of power handling,
+ graceful degradation if some modules fail,
+ multi-channel interferometer applications,
+ future growth potential.

The disadvantages of a phased array are:
- expensive design due to complex feed network and large number of feed elements,
- requires considerable design effort for hardware and software monitoring and control,
- needs complex computer system for monitoring, control, built-in tests and maintenance,
- multi-frequency use not feasible,
- difficult and very expensive to obtain low system noise at 450 MHz.

Possible configurations of the distribution and phasing networks for a phased array antenna system as well as computed antenna diagrams are found in the Antenna Pre-feasibility Study. In Figure 19 we show as an example a part of the feed network, which is regarded as optimum. The number of components for such a phased array network is given in the Antenna Pre-feasibility Study. In Figure 20 an artist's view shows what the mechanical construction of the movable platform structure, which would carry the phased array elements, might look like.

2. Single Dish with Multiple Feeds

The requirement for three quasi-simultaneous beams using a dish antenna with primary or secondary feed systems is a very stringent one. Difficulties with beam switching with one (quasi-)fixed reflector dish result from the defocussing properties of the reflectors for rays inclined with respect to the central axis. The consequences are a broadening of the main beam, reduction in gain and an increase in the sidelobe level. A performance improvement is gained by off-set antennas, since the off-set section of a paraboloid can have better focusing properties than the centre section for certain beam directions. Additionally, the blockage by the feed element or the subreflector is avoided and the feed can be located at the optimum focusing point. Such a configuration with off-set feeds is similar to the present EISCAT VHF antenna, but with three feed systems and a symmetric reflector dish. It is assumed that a small phased array (2x40 elements) should be considered for feed systems, since the phase and amplitude could then be matched to waists of the individual off-axis beams. Details of this antenna type can also be found in the Antenna Pre-feasibility Study. An artist's view of such an antenna construction is shown in Figure 21.

Advantages of a single dish with three feeds are:
+ compact design with only one reflector,
+ high gain for each beam,
+ no limitations on mechanical steering,
+ three (quasi-)simultaneous beams.

Disadvantages of a single dish with three feeds:

- high effort for design of three individual primary feed arrays matched to the three dedicated beam directions,
- it may be impossible to combine three beams into common directions,
- unknown high risk in design due to:
  - reflector deformation by wind and mechanical steering,
  - influence of cross polarization and beam squint at off-axis directions,
  - insufficient shaping.

At present it is not known if such an antenna has been constructed before and the design risks are regarded as high. As is seen in Figure 21, the dimensions of this antenna type have also to be much larger than any of the other antennas considered.

3. Three dishes with 32 m or 45 m diameter

This configuration employs widely used antennas and combines a very simple design with high reliability. The antennas could use primary or secondary feeds.

The Cassegrain (secondary) feed system, as is used for instance with the present EISCAT UHF antennas, is available as standard. A hubroom in the apex accommodates the RF equipment, allowing proper environmental protection of sensitive equipment. Also, maintenance is easier due to access from behind the reflector surface. Disadvantages are high sidelobe levels and subreflector blockage, which is particularly pronounced due to the large ratio of subreflector to antenna diameter, resulting from the relatively low frequency of 450 MHz and the given (limited) antenna size. For these reasons, only primary feed dish antennas are considered practical. Primary feed antennas are standard antennas. Details can be found in the Antenna Pre-feasibility Study.

The advantages of primary feed antennas are:

+ design, construction, costs and operation reliability,
+ sidelobe suppressions of better than -25 dB and -30 dB for near and far sidelobes, respectively.

Disadvantages are:

- long waveguide,
- spill over causing increased system noise and clutter,
- high VSWR (mismatch of antenna feed port)
- feed not weather-protected (radome possible?)
- maintenance difficulties.

A 45m-diameter dish would yield 46.5 dB gain and about 1.1° beamwidth (3 dB) at 450 MHz. Figure 22 shows some typical antenna diagrams for the near main lobe directions and the far from main lobe directions, which demonstrate that the performance would meet the specifications.

A 32m-diameter dish would yield about 42 dB gain and about 1.5° beamwidth (3 dB) at 450 MHz. Figure 23 shows the corresponding antenna patterns.

Two or three of these dish antennas could be operated in a coherent transmission and reception mode, as indicated in Figure 24(a), which would increase the theoretical total gain by 4.8 dB (a correct value for a realistic configuration will be computed). However, there are two restrictions to be considered. These are firstly the mutual shielding of the radiation in certain beam directions (details are again found in the Antenna Pre-feasibility Study) and secondly the "interferometer" effect. This is caused by the complex superposition of the radiation pattern of single antennas located at a distance which is greater than the diameter of a single antenna. The result is that the main lobe of the combined antennas is split into sub-sidelobes, as is shown in Figure 24(b) for a particular example. Furthermore, the compensation for phase path variation as a function of pointing angle needs to be taken into account by hardware phase-shifters, as is shown in Figure 25. The distortion of the main beam in this configuration still exists and needs to be carefully computed for all required azimuth and elevation angles, since there even will be offsets of the real pointing direction, with respect to the mechanical direction, of the order of one beamwidth for certain directions. Disregarding these beam deformations, it is assumed, however, that the gain in a multitude of directions is acceptably larger than that of one antenna.

4. The Triple Cylinder Antenna

This antenna design follows, in principle, the present EISCAT VHF antenna. The steering in elevation is done mechanically. The (quasi-)simultaneous beams are obtained by electronic beam steering through a phased-array line feed up to a certain angle of, say, 15°. With three reflector sectors, each having a typical dimension of 32 m (or 45 m), three beams can be achieved simultaneously. To allow other main azimuth beam directions, the whole structure should be moved mechanically around a vertical axis. The principle of such a design is depicted in Figure 26.

Some other antenna types have been discussed and these are briefly listed in the Antenna Pre-feasibility Study, but will not be considered further here for reasons of impracticability.

IV.C. Costs for Construction of the Antenna Systems

The final decision on the antenna configuration will be determined by the operational requirements and obviously by the total permitted expenditure. It was difficult to obtain reliable cost estimates due to the as yet unclear system configuration. However, some relevant information on antennas and corresponding feed and control systems were obtained. The companies MAN and Krupp, who were involved in the EISCAT VHF antenna design, were approached and presented preliminary estimates. It is expected that they will deliver more detailed data towards the end of October 1990. Furthermore TIW, the constructor of the EISCAT UHF antennas, delivered a preliminary quotation as did Radiation Systems, also a US company. In addition to the companies mentioned in the transmitter section, the following companies were approached either directly by us or by Elekluft, with the object of obtaining cost estimates for the mechanical part of antennas: DX Antenna Co. Ltd., Kobe, Japan; GEC Marconi System Company, Chelmsford, UK; Fujimoto Metal Products Co. Ltd., Chiba, Japan; Harada Industry Co. Ltd., Tokyo, Japan; Krupp Industrietechnik GmbH, Duisburg, Germany; Mitsubishi Heavy Industries, Tokyo, Japan; NEC Corporation, Tokyo, Japan; Radiation Systems, Richardson, USA; Sumimoto Electric Industries Ltd., Tokyo, Japan; Thomson CSF, Paris, France; TIW System Inc., Sunnyvale, USA; and Vertex Communication Corp., Kilgore, USA. On the electrical components for the antennas, the following companies were contacted: ANT, Backnang, Germany; Omecon, Ottobrunn, Germany; Parzich GmbH, Pürgen, Germany; Spinner GmbH, München, Germany; and Telemeter, Donauwörth, Germany.

IV.D. Potential Transmitter Configurations of the Polar Cap Radar

We present here certain configurations of transmitters, which we regard as potential candidates for a Polar Cap Radar. We also briefly discuss the technical lay-out. Owing to the very short time in which this report to Council had to be completed, the price estimates cannot be absolutely accurate and we estimate an uncertainty of some ±20%. We were not able to undertake a complete market study and were not able to approach all possible equipment manufacturers, but endeavoured to get at least one price for each alternative. Furthermore, some capable and well-reputed companies have not yet replied to our requests.

Several arguments have to be considered in the selection of a transmitter system. At first glance the system installation investment seems to be of major importance, but in the long run other features such as the recurrent operating costs, reliability and system maintenance will be even more important. In this context the tube/active device lifetime and replacement costs are also of concern. A certain degree of redundancy ought to be designed into the system, allowing for a graceful degradation in output power in case of single amplifier failure. Finally the investment in the RF distribution system, the preamplifiers and the transmit/receive-switches is also highly dependent on the amplifier design as well as, of course, on the antenna system to be chosen.

The significant technical data of the various amplifier systems is summarized in Table 3. In the following sub-sections we briefly introduce the technical features of each alternative, considering our particular application, and also include the results of a market survey for each alternative.

1. High Power Klystron

High power klystrons are used for particle accelerators, S-band military radar systems and conventional incoherent scatter radars. For operating frequencies around 450 MHz and high duty factors, they are manufactured only in small numbers, and therefore the development of a suitable klystron would contribute considerably to the costs. A very high beam voltage (80-100 kV) and hard tube modulators are required. This fact and the large size of a klystron makes maintenance a tedious procedure. Compared with the EISCAT VHF klystron, the design of a 450 MHz klystron would be easier and less risky, but not quite straightforward. Klystrons of this kind exist as surplus but they are not accessible, nor applicable for the specified purposes of the Polar Cap Radar.

Advantages:

+ high gain,
+ uncomplicated, straightforward amplifier design
+ fairly compact full transmitter size.

Disadvantages:

- manufactured by a very small number of companies
- high development costs
- requires hard tube modulator
- difficult and risky to handle due to large dimensions
- tedious maintenance
- low system redundancy
- low efficiency
- narrow bandwidth.

Cost estimates:

Philips Components GmbH in Hamburg indicated a price of 717 kDEM for a 1 MW klystron at 352 MHz, and 585 kDEM for 400 kW at 500 MHz, both including cabinets and controls. Taking into account the fact that these klystrons are not designed for pulse operation, and considering EISCAT's experience with the 224 MHz klystrons, a safety factor of two should be considered in the price estimate for a new design. Based on this estimate, we have to anticipate about 9 MDEM for the klystrons for a 3 MW transmitter designed for the 450-500 MHz frequency range.

Thomson CSF and Varian are certainly also capable of manufacturing a suitable high power klystron, but responses are not available so far.

Total transmitter costs are assumed to be about 14 MDEM.

2. Low Power Television (TV) Klystron

Klystrons in the TV frequency range 470-860 MHz are operated at up to 70 kW sync (equivalent to about 50 kW CW power, CW = Continuous Wave (100% duty cycle)) output power in several hundred TV transmitters all around the world. For frequencies outside the TV band, the cavities would have to be slightly rescaled, which is not assumed to be risky and is relatively inexpensive because of the large number of klystrons required.

Advantages:

+ TV klystrons used commercially in large numbers
+ high redundancy, because of large number in system
+ offered by several manufacturers
+ good reliability
+ high gain (driven by a solid state amplifier).

Disadvantages:

- relatively low power of 70 kW per single module,
  hence there is a substantial investment in RF distribution system
- relatively large size of the total configuration.

Cost Estimates:

Philips Components GmbH in Hamburg specified the price for a slightly modified 70 kW TV klystron including cabinet and controls at 100 kDEM. To achieve 3 MW pulsed peak power as many as 48 such devices are necessary, summing up to 5 MDEM. The price for a spare or replacement 70 kW klystron is about 55 kDEM.

A complete Philips transmitter system for 3 MW with very conservative ratings would cost 14 MDEM.

Varian TVT Ltd. (UK) manufactures klystron-based TV transmitters. For quantities larger than 10, a complete 40 kW transmitter would cost about 500 kUSD (=340 kDEM). This means that a 3 MW Varian transmitter system would cost 25 MDEM.

Other TV klystron manufacturers are Thomson CSF and EEV, but quotations are not yet available.

3. Klystrodes

For several years, extensive efforts have been made to reduce the net power consumption of TV transmitters. This resulted in the development of the klystrode, which combines the advantages of grid tubes and klystrons. The first tubes have been operated at 60 kW sync output power for 2 years now. Although experience led to several modifications, basically in the transmitter design, a move among TV stations towards klystrodes is apparent. The leading manufacturer of klystrodes today is Varian, but other companies also seem to put more effort into that new tube now. Recently, Varian has delivered a klystrode rated for 500 kW at a duty cycle of 10% at 425 MHz and will this year deliver also a 250 kW CW klystrode for 267 MHz. Like a grid tube, the klystrode's operating frequency is determined only by the external cavities.

Advantages:

+ high efficiency up to 75 % (reduced operating costs)
+ intrinsic separation of DC and RF path
+ high isolation between RF input and output
+ single low power focusing magnet
+ compact and comparatively light weight device
+ external cavity allows simple rescaling (no redesign)
+ focusing magnet failure would cause no damage to the tube; it would even still operate as an amplifier
+ phasing the RF outputs of two klystrodes together is well proven and often done in TV transmitters
+ no hard tube modulator required.

Disadvantages:
- new tube type, non-negligible design risk
- hot cathode very close to grid
- experience with pulse operation negligible so far.

Cost estimates:

Varian can offer an 8 x 375 kW klystrode amplifier using their 500 kW klystrode. Their estimate for the complete transmitter system is 10 MUSD (= 15 MDEM). The transmitter construction would be done by Continental Electronics, a Varian division. A spare or replacement 60 kW tube costs 30 kUSD and a 250 kW about 175 kUSD.

Klystrode based TV transmitters are built also by Comark, a Thomson (US) division, but further information is not available.

Considering possible additional control and cooling systems the high power Varian klystrode transmitter would cost 22 MDEM and the low power klystrode version about 15 MDEM.

4. MSDC Klystrons

This modified klystron was developed by Varian as an alternative to the klystrode, but is presently more emphasized by Varian's competitors. In this multiple stage depressed collector (MSDC) klystron the beam electrons are collected at different voltage levels, depending on their energy. The net power consumption is consequently reduced considerably.

Advantages:
+ high efficiency
+ no high power hard tube modulator required
+ high gain, can be driven by a solid state amplifier

Disadvantages:
- several high voltage electrodes at collector
- new tube type, design risk
- probably high interpulse noise
- pulse operation not yet considered.

Cost estimates:

Philips Components GmbH in Hamburg have recently tested their first MSDC klystron but are at present unable to give any price estimates. However, it may be assumed that a complete MSDC klystron TV transmitter is about equal in cost to a conventional TV klystron transmitter. The higher tube price is probably compensated by the smaller power supply.

We estimate the total transmitter to cost around 16 MDEM.

5. Power Grid Tubes

Power grid tubes are used in very large numbers in broadcast transmitters, industrial RF generators and particle accelerators. The efficiency and power output drop rapidly above a certain frequency (for instance around several 100 MHz), which is determined by the distance between the electrodes.

Advantages:

+ straightforward cavity design
+ tube itself is not designed for a particular frequency
+ usually no high power hard tube modulator required
+ low plate voltage

Disadvantages:

- because of low gain, several transmitter stages are required
- narrow bandwidth in the cascaded amplifier chain

Cost estimates:

Burle Industries (UK) Ltd. submitted an estimate for a complete 2 x 1.5 MW amplifier using rather old, very high power triodes type 7835. This tube was ruled out in the EISCAT VHF transmitter design phase because random oscillations at microwave frequencies may occur when not driven with RF. The price including power supplies, cabinets, control, etc. but excluding cooling system is 7 MUSD (= 11 MDEM).

Thomson Components AB proposed three different solutions based on power grid tubes. The tubes and cavities for a 16 amplifier system with a final stage peak output power of 190 kW would cost 3.7 MDEM. The same system has been used since 1974 for a military radar.

Another alternative of Thomson Components AB employs 10 final amplifiers at 320 kW each. The final tube is a new type, which has already been used in particle accelerators. Tubes and cavities for this solution would cost 3 MDEM.

The third Thomson system delivers 95 kW per tube of a type which is also used in accelerators. The price for 32 tubes and cavities would be 4.5 MDEM.

Other manufacturers are Varian, ASEA Brown Boveri, Raytheon, GEC-Marconi and Litton, but information or quotations are not available.

Total transmitter cost based on the Burle estimate is 18 MDEM, and for the three Thomson proposals is between 12 MDEM and 14 MDEM.

6. Solid State Amplifiers

The most impressive feature of a solid state amplifier is its reliability and the possibility of using it in a phased array system. Special care has to be taken to protect the semiconductor against lightning and other discharges. A properly designed amplifier has an extremely high lifetime expectancy, limited only by component degradation and subsystem failure. The presently available standard device peak output power is only 500 W in the 450 MHz range. A large number of amplifier modules needs to be combined to achieve the designed total power. The development costs for the module itself are negligible and the price per device will most likely drop by 50% within 2 years. For phase steering, failure localization and determination, as well as for maintaining phase and power stability, a very complicated control and monitoring system would be required, but failure of single modules would not degrade the total system performance appreciably.

Advantages:

+ very high lifetime and reliability
+ low operating voltage
+ allows remote operation
+ graceful system degradation in case of failure

Disadvantages:

- low power per device module
- low overall efficiency
- extensive distribution and control system

Cost estimates:

Philips Components GmbH in Hamburg would be prepared to supply VMOS power transistors and cooperate in the amplifier production with SSB-Electronic in Iserlohn. The costs for the RF-semiconductors for a 1 kW module would sum up to 2 kDEM. This leads to an estimate of 6 MDEM for the semiconductors of the full 3 MW transmitter, excluding circulators, power and phase detectors, power supplies, etc.

Vilem Klir GmbH in München has already built power amplifier modules, phase shifters, combiners and PIN-diode T/R-switches for 1.5 KW at 450 MHz. They estimated the price of a 400 W amplifier module at 1600 DEM, a 1/8 power divider or combiner at 780 DEM, a 4 bit phase shifter at 980 DEM and a power supply for two modules at 1890 DEM. For an array with 6561 elements (81 x 81) this adds up to about 25 MDEM.

Several other semiconductor and system manufacturers are able to supply suitable solid state amplifier modules. Contacts have been established with SGS Thomson Semiconductors and Mitsubishi Electric.

The complete set of components for a solid-state transmitter system including cooling and control systems will certainly cost more than 35 MDEM. As an example, we got a price quotation from Mitsubishi Electric Corporation for a fully steerable complete 224 MHz semiconductor phased array system, based on the MU radar design, at a cost of 16 billion Yen, which is 130 MDEM.

IV.E. Recommendation for Transmitters

In Table 4 we have summarized the cost estimates for the different alternatives described earlier. We have separated these into two versions, a full power 3 MW and a reduced power 1.5 MW version.

It is also to be noted that reliable information on companies designing transmit-receive switches and other particular components such as high-power phase shifters etc. is still not available. Although these components may not have a major effect on the total costs, the special design, construction and testing may be time- and manpower-consuming.

We have not yet had sufficiently conclusive information from the various suppliers to enable us to recommend one particular transmitter system above others, particularly because the antenna system is not yet determined. However, high power klystrons should probably be ruled out because of the low redundancy offered by a system designed around them. The solid state alternative must probably also be discarded due to its disproportionately high cost, which is not offset by the potential gains in reliability and redundancy. The grid tube amplifier system tends to become complicated, because of the low gain per stage and the consequent cascading of cavities.

All other possibilities should be evaluated more carefully, although the widely used low power TV klystrons seem to offer the best trade-off in terms of reliability, redundancy, and investment. Both new tube types, the klystrode and the MSDC klystron, have not accumulated enough operating hours to eliminate all doubts regarding design and performance. But, in particular, the klystrode offers very promising features, and should be thoroughly considered. We recommend that a final decision should be taken only after careful investigations have been undertaken by expert project staff and consultants, allowing for the experiences of other users with existing transmitter systems. By no means should a decision be made only on the information made available by the manufacturers or distributors.

IV.F. The Antenna-Transmitter Alternatives and General Remarks

To obtain a general idea on the layout of different transmitter configurations we present in Figures 27, 28 and 29 simplified system block diagrams of certain configurations. Further details can be found in the Antenna Pre-feasibility Study.

Ultimately, we will have to consider the overall costs for the antenna-transmitter system investment and operation, but the as yet unclear system configuration does not facilitate either a careful evaluation or a clear recommendation. The final assessment must include the total expenditures for the amplifiers, antennas, receivers, system control and monitoring, transmitter hall, operating costs (electricity, maintenance etc.), spare parts and the staff salaries.

As a first assessment we have compiled the best estimates of the overall costs for the different system configurations that have been considered above. These are summarized in Table 5. It is to be noted that these are assumed to be the costs for the investment only. The additional expenditure for project manpower, supervisor consultancy and any overhead is not included.

Table 5 consists of input data, which were available through the most effective market survey we were able to perform in the short time period until 10 October 1990, which was the deadline imposed for the finalization of this technical part of the report.

We must emphasize at this point that the data in Table 5 should be regarded only as very approximate, owing to the fact that critical time restrictions and uncertain indications on the realization and funding of the project, as defined in the initial study, prevented more detailed responses from companies on antenna and transmitter designs. It should be noted that we were able to obtain some reliable data on transmitter klystrons, tubes and semiconductors. Representative price estimates for complete transmitters are, however, available only in a very few cases, when a fairly conventional and traditional design would be employed. It has not been possible so far to establish working relationships with companies prepared to construct a klystron transmitter. The Antenna Pre-feasibility Study by Elekluft was indispensable for the initial assessment of possible antenna configurations. Some of the antennas, namely the 32-m dishes, are structurally similar to standard antennas and the price estimates therefore have the smallest uncertainties. However, the final configuration of the antennas is still not known in detail, which accounts for the differences of the diverse quotations and the remaining uncertainties. Our estimates for transmitters are dominated by the cumulative costs of components and subsystems, but even these are only known approximately at the present time. The remaining uncertainty is strongly influenced by design and construction costs, which will still accrue to the project regardless of whether these tasks are contracted out to industry or handled by project staff.

In our opinion, truly reliable cost estimates for the antenna systems, as well as for the transmitters, can only be obtained either through a detailed technical study by paid consultants or independent experts, or through formal tender action after the funding of the full project is ascertained.

TABLE 2

Optimum Specifications for the Proposal of a Polar Cap Radar on Spitsbergen

Frequency:

Operation:	450 MHz
Optional operation:	350–500 MHz (to be decided according to transmitter availability and frequency allocation)
Receiving (option):	(224 MHz) or 931 MHz

Antenna system:

Beamwidth:	1° (1.6°) (one-way) at boresight, symmetrical
Gain (main lobe):	45 (41) dBi
Sidelobes (near):	25 dB down from main lobe (one-way)
Sidelobes (far):	30 dB down from main lobe (one-way)
Beam directions:	≥ 3 (2) (simultaneous or from pulse-to-pulse, i.e. within some ms) with minimum angular separation of 20° (15°)

Noise temperature (at the input of LNAs, defined without sky noise and without LNA noise):
6 dB down from sky noise or 100 K whichever is larger,
(70 – 80 K for dish antenna)

Bandwidth (-1.5 dB):	
transmit:	± 2 MHz at mid-frequency
receive:	± 10 MHz at mid-frequency (for phased array: at boresight only, other beam directions ± 2 MHz)
Polarisation:	
accuracy:	< 0.5 dB
transmit:	right-hand circular
receive:	left-hand circular (or v.v.)
VSWR:	
transmit:	≤ 1.2
receive:	≤ 1.6
Power capability:	
peak:	3 (2) MW
average:	400 (270) kW
pulse lengths:	0.001 – 2.0 ms

Highest operating frequency in receive mode
(for dish only): 3 GHz (3 dB efficiency loss compared to 450 MHz)

Antenna mechanical specifications

subdivided into the presently evaluated three types of configuration:

(A) 3 (2) standard parabolic dishes,
(B) 1 offset-feed dish (allowing 3 beam directions),
(C) 1 phased array platform (allowing electronic beam steering and beam forming):

Type:	(A)	(B)	(C)
Feed system: elements:	single secondary Cassegrain	triple (>15°) primary feed	array >6000
Foc.len./diam.	0.3	1.3	–
Diameter of array (m):	45	60 (geometrical) 45 (effective)	< 45
Slewing velocity (°/s):	0.3 (1.0)	0.3 (1.0)	0.3 (1.0)
Slewing range (°):			
elevation:	5–175 (110)	5–175 (110)	10–170 (110)
azimuth:	0–400 (540)	0–400 (540)	0–400 (540)
Surface accuracy (cm_{rms}):	1	1	stiff struct. deviation: 5
Pointing/tracking accuracy (°):	0.1 (0.2)	0.1 (0.2)	0.1 (0.2)
Windspeed (km/h):			
operational:	100	100	100
survival:	180	180	180
Temperature (°C):			
operational:	-40 – +20	-40 – +20	-40 – +20
survival:	-55 – +20	-55 – +20	-55 – +20
Rotary joints:	2	6	> 32
Equipment on azimuth platform:			
weight (kg):	4000	12000	12000
volume (m^3):	50	150	150

Icing: presently unknown, but radome may have to be considered.

---

numbers in brackets denote options

Transmitter (see also antenna specifications):

Frequency:	
operation:	450 MHz
optional:	350–500 MHz (t.b.d.)
bandwidth(-1.5 dB):	± 2 MHz
Transmitter modules:	8 to 32 (64?), phase coherent
Total power:	
peak:	3 (2) MW (max.)
average:	400 (270) kW (max.)
pulse length:	0.001 – 2.0 ms (3% (10)% droop) phase-coding
interpulse period:	0.1 ms (minimum)
VSWR:	1.2
Duplexer:	
isolation:	> 60 dB
recovery:	< 20 µs (to 99% full operation)
insertion loss:	< 0.2 dB
Operation:	Capability for fully automated operation and restart.

Receiver:

Frequency etc as given above and derived according to receiver/exciter configuration.

Input bandwidth:	±10 MHz (at -1.5 dB),
Baseband-width:	50 kHz – 2 MHz,

Multiple independent channels:

Type (A):	3 (2) coherent channels,
Type (B):	3 standard channels,
Type (C):	> 8 coherent channels;

Noise temperature: < 30 K,

Dynamic range: > 90 dB,

Higher order inter modulation products: < 120 dB,

Phase noise of oscillators (incl. transmitter exciter with respect to the carrier frequency:

< - 20 dBc at 1 Hz,	< - 40 dBc at 5 Hz,
< - 80 dBc at 100 Hz,	< - 120 dBc at 10 kHz,
< - 120 dBc at 1 MHz.	

TABLE 3

Summary of Amplifier Details

Amplifier type	power (kW)	gain (dB)	effic (%)	remarks
(1) H.P. Klystron	1000-2000	40	35	low redundancy, complicated support
(2) TV klystron	60-120	40	50	off the shelf tube
(3) Klystrode	60-500	20	70	lowest power costs, new tube type
(4) MSDC klystron	60-120	35	70	low power costs
(5) Power grid tube	< 1000	13	55	low gain, many stages
(6) Solid state ampl.	< 1	12	50	low power/module, needs many stages

TABLE 4

Summary of Transmitter (3 MW) Costs: (very preliminary)

(1) High power klystron:	
SRI: 4.9 MUSD/2 MW =	50 MSEK/3 MW
Philips:	50 MSEK
(2) Low power TV klystrons:	
Philips:	50 MSEK
(3) Varian klystrode:	
High power:	80 MSEK
Low power:	50 MSEK
(4) MSDC klystron:	
Philips:	50 MSEK
(5) Grid tube:	
Burle:	66 MSEK
Thompson:	55 MSEK
Average:	56 MSEK = 15 MDEM = 5 MGBP

NOTE: Experience shows that the specified transmitter power is always larger by about a factor of 1.25 compared to the finally achieved operational power. That means a presently ordered 3MW transmitter will very likely only allow 2.4 MW operational power.

TABLE 5

Presently Best Available Cost Estimates for Antenna-Transmitter Systems

Version:
(1a) Phased Array 45m (32 transmitters = 3 MW)
(1b) Phased Array 45 m (8000 transmitters = 3 MW)
(2) One triple-feed 60m dish (3 MW)
(3a) Three 32m dishes (3 MW)
(3b) Three 45m dishes (3 MW)
(4) Triple cylinder (3 MW)
(5) Two 32m dishes (1.5 MW)

Costs in MDEM (3 MDEM = 1 MGBP)

Version:		(1a)	(1b)	(2)	(3a)	(3b)	(4)	(5)
Mechan:	MAN	40*	40*	40		60*		
	TIW			38*	30*	77		20
	Krupp				30	45		20*
	Rad.Sys.				20			14
	Estimate						60*	

(* = used for costing)

	(1a)	(1b)	(2)	(3a)	(3b)	(4)	(5)
Dipoles/Feed	12	12	0.35	0.7	"	5	0.5
Waveg./Dis.Sys.	30	10	2	2.0	"	3	1.5
Rotary Joints			2	2.3	5.0	3	1.5
Low Noise Ampl.	11	10	0.35	0.1	0.1	0.1	0.1
T/R, hybrids and phaseshift	21		1.7	1.0	1.0	1.0	1.0
Design	1	1	10	1	1	3	1
TX-modules	15	40	15	15	15	15	8
Monit./contr.	5	15	2	2	2	2	1
Costs							
Total (MDEM):	135	128	72	54	84	92	35
Total (MGBP):	45	43	23	18	28	31	11

IV.G. Receiving and Signal Processing Systems for the Polar Cap Radar

1. Introduction

The receiver of the Polar Cap Radar is discussed here but it is too early to propose any final solution. The number of antenna elements or feed points dictates the number of independent receiver lines. The necessity for polarisers in the receiver system is partly dependent on the selected radar configuration. The number of IF frequencies also has to be decided. "Direct" reception without an IF stage is not proposed here, but the possibility of having only one frequency conversion must be studied. Finally, a decision is needed concerning the detector configuration. This will require tests to be performed. Cost estimates cannot be made accurately at this stage, but this part of the radar forms only 10-20% of the total costs of the system.

It is not possible to forecast exactly in 1990 what will be the most reasonable and cost effective solution in 1995. This is especially true of the computers and the signal processing part of the system. It is better to study the markets in detail in 1992-1993. Alternative solutions are proposed in outline. Detailed planning is not appropriate at this initial stage but will be needed in the near future.

2. Receiver

The receiver configuration for EISCAT was carefully considered and it can be used as a starting point. The receiver system can be a conventional single or double conversion receiver, but there are other solutions, too. The detector environment has to be considered carefully. The total bandwidth must be of the order of 20 MHz.

Simple circular polarization is probably sufficient, so costly polarizer arrangements are not necessary. Amplifiers for the receiver front end are commercially available for any possible Polar Cap Radar frequency, but they can also be made by EISCAT. Filters are available commercially. One or two channels per antenna or feedpoint are needed.

If the radar configuration is such that in some applications three receiver systems have to be added coherently, then the system has to have phase coherence maintained everywhere between the different receiver systems and the addition done in the digital part after detection.

The choice of first IF frequency depends on the chosen working frequencies. There are no essential component difficulties. The possibility of doing the channel separation in the first IF has to be studied, as does the possibility of doing the separation and receiver-to-receiver phasing for coherent addition completely in the digital part of the system. If the channel separation is done in the second IF, the receiver system will look much like EISCAT's. Eight receiver channels would be a flexible solution which would allow the use of "classical" multichannel experiments as performed currently on EISCAT. A higher number of channels could be envisaged for some experiments but not often.

In a multi-antenna system, the phase coherence between receiver lines must be maintained.

There are several different ways of achieving the design goals for the complex signal detection needed for experiments. A copy of the present EISCAT system has the advantage that it is a proven solution. One alternative is a fully digital detector followed by digital filters. It is also possible to have analog detection as in EISCAT, but with the low pass filtering done using digital filters.

The old "classical" solution has its benefits. It is relatively simple and it has been well developed in the EISCAT system. The fully digital solutions have their benefits as well, though. The whole filtering is programmable, both in gain and in filter characteristics, and an exciting possibility would be to have only one wideband receiver channel with a fast ADC and thereafter everything else, including channel separation and coherent addition of receiver lines, done by digital processing of this single time series of samples. The one problem with this is that very high quality construction and shielding is required. An interesting intermediate possibility would be something like the present EISCAT system, but with the last part of the post detector filters substituted by a digital filter.

The "digital" solution is certainly more state-of-the-art, but experience is needed with the systems involved. If this experience can not be obtained from other radar installations or comparable systems, tests of the concepts would have to be performed on the EISCAT receiving system.
The receiver control system is not complicated. Any one of a number of standard digital control systems would do. Several standard solutions exist. At each point it must be possible to read the hardware status, and/or digitally control it.

3. Real Time Signal Processing

There are elements in the processing, that are still beyond the capabilities of simple "personal computer" based solutions and are likely to remain so for some time. Thus, for real time signal processing, some hardware based solution is needed. It is not totally impossible that this situation will change before the design for the polar cap radar is finalized.

If the data is fast-sampled for the plasma-line or other wideband tasks, then the "natural" way of dealing with this would be to use FFT-processors, forming spectral estimates (and averaging them) directly from the set of complex samples.

Ion-line, or other narrow bandwidth sampling, can be practically handled somewhat differently as the universal solution is the formation of lag profile matrices. If the signal bandwidth is dictated by the target bandwidth, then the computation problem is always easy, and the present computational power of the EISCAT correlators is adequate. However, the final signal bandwidth is often modulation bandwidth dependent and this may be more so in future developments. In extreme cases (although ones which can already be envisaged), the computation power demanded would be more than one order of magnitude higher than in the present EISCAT system.

The correlator part is in principle simple. The correlator capabilities must match the demands of any new modulation schemes. Any correlator designed for incoherent scatter radar applications can always be considered as a combination of a complex multiplier (for computing the lag profile matrix) and FIR filter (doing the additive operations along the matrix diagonals) together with the necessary memory modules and interfaces. Three processes, all easily implementable in hardware, form the basis of the processing in the ion line computations:

1) FIR filtering
2) Lag profile matrix formation
3) Accumulation

The necessary hardware elements, together with their required memory modules, can be built into some standard bus system like the VME bus, or they can be plug-in boards in computer expansion slots. In the near future there will probably be fast enough hardware, with built-in ready-made software, available commercially to do this.

Every ion-line computation can be handled with the following sequence of operations:

1: FIR filtering in the amplitude domain within the coherence time (e.g. Barker codes).
2: Phase coherent integration between pulses if the target coherence time allows.
3: Lag-profile matrix computation.
4: Accumulation (integration) of matrices if the modulation is kept constant (not necessary except to save storage space).
5: FIR filtering of lag profiles of (integrated) matrices to decode, for example, alternating codes.
6: Final accumulation of filtered matrices and possible rearrangement of elements. The latter is probably unnecessary if the analysis system is properly written.

Every modulation can be handled in this way.

There are only two basic algorithms needed in the most general ion-line computation hardware optimally designed:

1) FIR algorithm.
2) Lag-profile computation algorithm.

A third algorithm needed in the additional case of computation of plasma lines:

3) FFT algorithm, which feeds blocks of data through a FFT processor.

It is assumed here that the high-speed real time computations are carried out in task-oriented hardware processors. These kinds of DSP-processors will probably be available as plug-in modules. The electronic components for them are already on the market.

4. Radar Controller and Timing

The radar controller distributes the commands that the radar system must execute exactly at a given time (microsecond accuracy). In future systems, the radar controller could deliver more information to the real time processing system than the mere "start compute" type interrupt. One example is the pattern of transmitted code. This would simplify the programming tasks in the other parts of the system and can make, for example, the use of true random codes possible.

The present EISCAT radar controller is too simple a device.

If it is necessary to receive the EISCAT signal, then a Cesium beam standard may be needed. If this receiving facility is not needed, cheaper and more maintenance-free solutions can be considered.

5. Computers, Experiment Design and Data Analysis

It is slightly too early to plan the computer system for the Polar Cap Radar in detail. The development of computer hardware in the class of computers needed for an incoherent scatter radar is proceeding very rapidly and is unlikely to be a problem.

The Polar Cap Radar must have a comprehensive experiment library designed by radar scientists and it must have modern tools for experiment design and modification. In data analysis, many new ideas will be taken into use during the coming years e.g. "full profile analysis" and analysis tools suitable for personal computers.

In the case of the Polar Cap Radar, we have a unique opportunity to put all these new ideas into practice. This includes experiment design tools, experiment libraries, data analysis packages of different complexity levels, remote control (monitoring) of the radar and a world-wide data distribution system.

V. CHOICE OF OPERATING FREQUENCY

A key question is the optimum frequency for the radar. It is clearly an advantage to choose a frequency where there is experience in design and operation, and equipment is available "off the shelf". This suggests that the frequency chosen should either lie near the EISCAT frequencies at 224 and 931 MHz or else lie in the band 400-500 MHz, which has been used by other incoherent scatter radars.

Factors in favour of a higher frequency are:

- A lower system noise. This ultimately depends on the sky temperature above Longyearbyen, which averages 140 K at 224 MHz, 25 K at 430 MHz but only 6 K at 931 MHz.
- a smaller antenna size for a given beamwidth, which also makes it easier to achieve full steerability and a high scanning rate.
- Less clutter from coherent echoes which are mainly due to field-aligned irregularities. The strength of these echoes will be about 12 times stronger at 430 MHz than at 931 MHz, and about 50 times stronger at 224 MHz.

Factors in favour of a lower frequency are:

- A smaller Debye ratio for a given electron concentration so that measurements can be extended to greater heights.
- Greater cross-section for MST work.

One final factor points to an intermediate frequency:

- At higher frequencies the bandwidth of the scattered signal is greater. This widens the bandwidth over which noise is received and if the system noise temperature is approximately constant (i.e. for frequencies > 400 MHz) this increases the total noise power in proportion. However, with a broader bandwidth the maximum lag which must be measured in the autocorrelation function is reduced. This allows the envelope of the transmitted signal to be shorter and hence allows observations to begin at shorter range.

At 224 MHz the high system noise seriously limits sensitivity, and the narrow bandwidth makes it very difficult to measure spectra from the E region, especially for observations near the zenith.

The Debye cut-off rules out 931 MHz as a suitable frequency for topside work, as experience at EISCAT has confirmed. Under normal conditions the Debye limit for 224 MHz and for frequencies in the range 400-500 MHz will lie well above 1000 km so that studies of the upward acceleration of plasma will be possible and, because of the lower system noise, the greatest heights will in practice be reached in the 400-500 MHz band.

It is, in fact, true in general that, for a given size of dish and a transmitter of given power, the maximum sensitivity is in the range 400-500 MHz and this is the frequency band recommended for the Polar Cap Radar.

Further details on the factors influencing the choice of a frequency in the band 400 - 500 MHz are presented in a separate document entitled 'Report on an Incoherent-Scatter Radar on Svalbard' by P.J.S. Williams.

VI. OPERATING MODES OF THE POLAR CAP RADAR

To judge the effectiveness of any proposed design to meet the scientific menu of an incoherent-scatter radar on Svalbard we must first define typical modes of operation. In defining these modes it is initially assumed that we have three parabolic dishes which can operate independently in three separate directions, or together pointing in a single direction and transmitting and receiving in phase. However, the analysis could apply equally to a phased array, mounted on a fully-steerable platform, which can scan electronically to make quasi-simultaneous observations in three pointing directions or remain pointing in a single direction.

If at the onset of observations only two parabolic dishes are available a modified version of these modes can be used: in most cases this will simply mean a poorer time resolution with measurements otherwise unchanged. In one case (Mode 3b), however, the observations will be limited.

If only one dish were available, the modes would be more seriously restricted. Measurements of scalar parameters would be possible, albeit with poorer time resolution, but accurate measurements of rapidly varying plasma velocities would not be possible for the following reasons.

Recent measurements at EISCAT have demonstrated that the strength of the electric field along the Tromsø field line frequently varies from small values to very large and back to small within a minute or so. If only a single dish is available, a beam-swinging technique must be used to measure three components of velocity. If, however, there are substantial variations in the velocity during the cycle of pointing directions then "mixing" occurs, whereby a time-variation in one velocity component is interpreted as a spurious component in another direction. In other words, not only does beam-swinging fail to record rapidly-varying plasma velocities : it does not even give a correct average value.

Tristatic observations, such as those made at EISCAT, have the advantage that they measure three components of velocity for a single volume at a single time and hence give an unbiased estimate of the true velocity vector. However, even a tristatic system has limitations : at EISCAT, for example, it is impossible to be certain from the radar data alone whether a rapid variation represents a sudden and instantaneous change in the whole convection pattern or a spatially-limited region of high velocity drifting through the EISCAT beam. It is for this reason that a three-antenna system will be so valuable when operating in the boundary region between the polar cap and the auroral zone.

VI.A. Single-beam Operation

Single-beam operation will be used for observations in which it is essential to utilise the maximum P×A. The antennas will point in the same direction, and the output from the transmitter will be divided in the switchyard to feed each dish simultaneously and in an appropriate phase, so that a phase-coherent signal is transmitted. If the received signals are also combined in phase before detection, the overall system has a total effective area almost as large as the combined area of the individual dishes. For moderately large dishes this is, in fact, the most cost-effective way of achieving a large collecting area, especially if the individual dishes are of a standard size, such as 32 m.

This mode would normally be used to study the topside, with all dishes pointing along the magnetic field line. Fortunately, at such high latitudes the field line is close to the vertical so that "shadowing" between the dishes is not a serious problem.

Obviously this mode can be used with 3, 2 or 1 dishes in operation: the only difference will be in the signal-to-noise ratio (SNR), which will be approximately proportional to the number of dishes employed, and the corresponding time resolution will be in the ratio 1:4:9.

This mode would be ideal for all studies of the polar wind or other large upward plasma flows at high altitude near the cusp or in the midnight sector.

VI.B. Multi-beam Operation

1. Joint Observations with EISCAT

Joint observations with EISCAT are possible even if the frequency of the system is not one of the EISCAT frequencies. In one mode, EISCAT would point at low elevation towards Longyearbyen, and one of the Svalbard beams would point at low elevation towards EISCAT, so that both radars observed a common volume approximately half-way between the two. With both acting as monostatic radars, it will be possible to determine unambiguously the two components of plasma velocity in the meridional plane : i.e. the field-aligned and the meridional field-perpendicular velocities. If two other antennas are available, they will also point at low elevation, one 15° to the west and the other 15° to the east of the meridional plane and they will help determine the zonal field-perpendicular velocity.

To operate efficiently in this mode, where the three beams are directed in different directions, the configuration of the switchyard must be changed to allow the total power of the transmitter to be switched from dish to dish between pulses. If this is done with three dishes it is equivalent to a $\sqrt{3}$ improvement in SNR when compared with the alternative switchyard configuration, which divides the total power equally and simultaneously between the three dishes. Appendix B describes a switchyard which would operate in this way, using phase-control of the output from the different units in a distributed transmitter to provide the two configurations.

If two dishes are in operation at Svalbard, this mode will not be seriously affected as the second beam, offset to east or west, will be adequate to determine the zonal velocity. Once again, it is necessary to switch power from dish to dish between pulses, but for two dishes this is an elementary procedure involving a single hybrid ring that can be fed in-phase or out-of-phase from the two halves of a distributed transmitter, so that the whole power output appears at one of the two other ports of the hybrid.

If, however, only one dish is available a choice will have to be made. Observations of a common volume with EISCAT will provide the two components of velocity in the meridional plane, but not the zonal velocity. The alternative mode will employ beam-swinging, possibly in synchronism with EISCAT. One compensating factor is that in this mode $P \times A$ is the same whether 1, 2 or 3 dishes are in use and so time resolution is not affected.

If, in addition, the antennas at Svalbard are designed to receive EISCAT transmissions, an extra measurement of the field-aligned velocity in the meridional plane will be possible. In determining the velocity itself, this will merely duplicate a measurement already available from the two monostatic observations but it will be an independent measurement and will reduce the necessary integration time.

A more important use of bistatic observations will be to measure the spectra scattered from a single volume of non-thermal plasma in two different directions, for example a bistatic measurement of the spectrum along the field line and two monostatic measurements at aspect angles close to 54.7°.

This mode will be used to study the transient response at the dayside magnetopause to changes in the interplanetary IMF, and plasma flow in the boundary region between the polar cap and the auroral zone. It will also be the ideal mode for studying the non-Maxwellian velocity distribution of ions in a plasma which has experienced strong frictional heating.

2. Polar Cap Scan

An alternative mode using three separate beams will scan the northern horizon at low elevation to monitor large-scale convection patterns in the polar cap. At the start of the scan the three antennas will point in three different directions forming an equilateral triangle with sides of length 15°, the base at an elevation of 15° and the vertex at an elevation of 28°. This will provide three components of plasma velocity in the ionosphere at ranges of up to 1400 km, so that a substantial portion of the polar cap - up to invariant latitudes of 85° -would be measured.

After a dwell time of 1 minute, the antennas will scan in azimuth to form a new triangle, and the measurements continued. After covering a total azimuth range of 120°, which will take about 10 minutes, the whole pattern will be repeated.

For two antennas, this mode could be modified so that the same pointing directions will be covered in the total scan, but only two at a time, and similarly a single antenna could cover the whole set of pointing directions. Once again, there is no serious loss of time resolution as the number of directions measured simultaneously is inversely proportional to the duty-cycle available at each. The real disadvantage is the problem of time-variation while a single antenna is scanning through three adjacent positions.

This mode is designed to study the whole pattern of polar-cap convection during periods when the interplanetary magnetic field is approximately constant, especially when the B_z component is northward. It can also be used to survey the distribution of precipitation across the polar cap.

3. Observations centred on the Field Line

In the final mode proposed for a three-antenna system, the beams point in three directions splayed symmetrically about the magnetic field line to make continuous measurements of the three components of plasma velocity. If the plasma velocity is truly constant with time, then this will be confirmed by the measurements made by the three antennas, and if there is a time variation this will be recognised. Hence the three-beam system will avoid the vulnerability to time-variation that limits the reliability of a single-beam system at high latitude.

Care will still have to be taken when there is a combination of temporal- and spatial-variation, but in this mode the three-antenna system has a major advantage. If it can be assumed that the pattern of plasma velocity remains constant as it drifts through the Svalbard area, then both scalar and vector parameters measured in the three beams can be cross-correlated to determine the horizontal drift velocity of the pattern. The three velocity measurements can then be combined with suitable time delays to give unbiased measurements of the total vector of plasma velocity at three points. Simulations of two characteristic velocity regimes moving steadily through the field of view are summarised in Figure 30; viz. a sharp reversal of plasma velocity at a boundary (e.g. the polar-cap boundary) and a narrow band of large velocity at the leading edge of an auroral arc.

In this mode, observations with two or one antennas will be handicapped as the need to employ beamswinging will prevent the cross-correlation technique being used unambiguously. With a two-antenna system it will be possible to use one antenna pointing along the field line and the other offset from the zenith in the zonal (or meridional) plane to provide reliable measurements of the field-aligned and zonal (or meridional) components of velocity, but no estimate of the other component. Alternatively, both beams could be offset from the field-line, one in the zonal and the other in the meridional plane; with this deployment both components of the field-perpendicular velocity can be measured on the assumption of a zero field-aligned velocity.

With only a single antenna, full beam-swinging must be used: Figure 30 shows how this can give misleading results whenever there are significant variations in velocity during the scanning cycle.

A second measurement in this mode will determine the field-aligned currents (FAC) at three points in the F-region. By monitoring both the ion lines and plasma lines in each of the three directions a component of the FAC can be measured in each case. Assuming that at F-region heights any current will be field-aligned, the full value of the FAC can be determined at a given height for each of the three pointing directions, and by repeating this measurement at different heights the two-dimensional distribution of FACs can be derived. In the same way, two antennas or a single antenna can make valid measurements of the FAC but give less information on the spatial variation.

With three antennas this mode can be used to study reversals of plasma velocity at the boundary of the polar cap and the distribution of electric fields near an auroral arc. A modified version, with the three antennas pointing in a single plane in the sunward direction, could be used for studying the movement of blobs in the polar cap.

Under conditions for which the convection can be assumed to be anti-sunward, a modified version of the same mode can be used if only two antennas are available, but these studies cannot be carried out with a single antenna for the reasons given above.

This mode will also be ideal for studying the propagation of tides and large-scale gravity waves in the thermosphere. Under quiet conditions, this work can also be carried out with two or one antennas but if there are rapidly varying electric fields the results will be affected.

4. Mesosphere-Stratosphere-Troposphere Mode.

Finally, a three-beam mode, with one beam vertical and the other two offset in two orthogonal planes, will be useful for all MST work, providing simultaneous profiles of three velocity components over the height range from which scattered echoes can be detected.

If three antennas are not available during the first phase of the project, then at least two beam directions are advisable to cover the two orthogonal planes. If only one dish is available, beam swinging is possible for this work.

Further information on the operating modes of the Polar Cap Radar can be found in a separate document entitled 'Report on an Incoherent-Scatter Radar on Svalbard', by P.J.S. Williams.

VII. MANAGEMENT PLAN

VII.A. Draft Proposal for Staff Complement Plan for the Construction of the PCR

```
Year:              :   1991  :   1992  :   1993  :   1994  :   1995

Position:

Project Manager[1] *************************************....................
Project Engineer[1] :  *****************************************************
Assist. Engineer   :           :    ***************************************
Digital Engineer   :    ***************************************************
Programmer 1       :          *********************************************
Programmer 2       :           :           :*******************************
Administrative Assistant  .................................................
Technician 1       :          *********************************************
Technician 2       :           :     **************************************
Technician 3       :           :           :*******************************
Scientific Advisor      ...............................********************
Site Engineer      :           ............********************************
Site Caretaker     :           :           ********************************
Secretary          : ......................................................
```

*** - full time   ... - part time

[1] - temporary positions during development of the Polar Cap Radar

General Comments on the Management Plan

This proposal assumes that the Polar Cap Radar will be an EISCAT project.

It is anticipated that all "Polar Cap Radar staff members" will act in close consultation with EISCAT staff members. However, it is not the purpose of this particular proposal to consider ways in which appropriate EISCAT staff could become directly involved in, or affiliated to, the "Polar Cap Radar staff organization".

It is expected that additional external consultants will have to be called upon to advise on certain well defined sub-projects.

The possible burden on the existing EISCAT staff of the additional workload associated with the implementation of the Polar Cap Radar should be alleviated by ensuring that the construction of as much of the equipment as possible is either contracted out or purchased as commercially available subsystems or components. Also, the availability of commercial software packages should be investigated.

The initial offices and laboratories of the PCR staff could possibly be in Tromsø or at other EISCAT sites. The on-site offices, laboratories and workshops will have to be established in due course.

Initial Job Descriptions:

1) Project Manager:

Requirements:

Graduate engineer or physicist with practical experience in radar operation and project management, preferably in remote regions.

Responsibilities:

Report to and collaborate with the Director of EISCAT. Report to the PCR Advisory Committee and related Working Groups.

Evaluate the introductory feasibility study for uncertainties and work out proposals for changes.

Evaluate the feasibility study for immediate actions and prepare a detailed implementation plan for the construction of the Polar Cap Radar.

Continue existing and establish new contacts with industry. Contact institutions being or becoming involved in the establishment of the Polar Cap Radar. Prepare detailed specifications for all instrumentation required for the Polar Cap Radar. Prepare all details for open tender action.

Supervise project group and total project during the design, construction, and acceptance tests.

Supervise and certify ongoing projects and contracts with industry. Administer the project budget.

The Project Manager should be installed on a five-year contract for the duration of the construction phase until routine operations commence. The Project Manager should attend the EISCAT Council meetings for reporting purposes. It could be envisaged that the Project Manager could delegate some of his management duties to the Project Engineer towards the end of the construction phase; thus he may only be needed part-time during the final period.

2) Project Engineer:

Requirements:

Graduate electronic engineer with experience in high power transmitters and antennas (incl. mechanics).

Responsibilities:

Report to and collaborate with the Project Manager.

Evaluate the present feasibility study and to work out technical details of specifications for the design of antennas, transmitters, and duplexers, as well as the receivers.

Evaluate technical feasibility of incoming offers.

Negotiate technical details with companies and become involved in contracts. Supervise, by in-factory collaborations with involved companies, the ongoing contracts and certify the fulfilment of specifications. Discuss and negotiate necessary technical modifications of specifications during the construction phase.

Supervise the technical developments of PCR staff.

The Project Engineer should be on at least a five-year contract and remain affiliated on-site until the complete system is in full and reliable operation. Towards the end of the construction phase it may be considered that some of the duties of the Project Manager can be transferred to the Project Engineer; the Project Manager then may only be needed part time on a consultant basis.

3) Assistant Engineer:

Grad. engineer with good general experience of analog and digital hardware. Assist Project Engineer in specific tasks. Responsible for interfacing of digital and analog parts of the system.

Basic knowledge and experience in ionospheric and atmospheric physics. Later to become 1. Engineer on-site and Deputy Site Leader.

4) Digital Engineer:

Assist Project Engineer on digital equipment design and implementation. Supervise digital part of the system and digital technicians. Later to become 2. Engineer on-site.

5) Programmer 1:

Design and implement special system software.

Later to become Digital System and Computer Supervisor on-site.

6) Programmer 2:

Design and implement general software.

Later to become Programmer on-site until complete development of software.

7) Administrative Assistant:

Part-time administration in budget matters in collaboration with Tromsø offices and EISCAT HQ. Office at Tromsø.

8) Technician 1:

Construct and implement special digital equipment.

Later to become 1. Technician (digital) on-site. Adviser during operation.

9) Technician 2:

Construct and implement special analog equipment.

Later to become 2. Technician (analog) and Mechanics on-site. Adviser during operation.

10) Technician 3:

Assist Technician 1 and 2 on given tasks.

Later to become responsible for general technical tasks on-site. Adviser during operation.

11) Scientific Adviser:

Consult on special operation programmes and prepare experiment operation schemes. Later to act as Scientific Adviser on-site and in Tromsø. Responsible for scheduling in cooperation with EISCAT Tromsø.

12) Site Engineer:

During construction responsible for all on-site matters including administration. Supervise building, antenna construction and system installation and tests on-site.

Later to become the Site Leader.

13) Site Caretaker:

Responsible for all mechanical hardware support and maintenance on-site.

14) Secretary:

Assist Project Manager and his staff on secretarial matters.

Final note:

This draft proposal takes into account experience gained from the original preparatory work for the present EISCAT systems. It also considers certain experiences and developments during the construction, operation and the management of the EISCAT radar systems and organization.

VII.B. Outline of possible Timing Plan (Milestones) for Construction of the Polar Cap Radar

```
Year:             :    1991   :    1992   :    1993   :    1994   :    1995
                  :           :           :           :           :
Install Proj.Mgr. :********************************************************
Install Proj.Eng. :********************************************************
Revised Report    **          :           :           :           :
Prel. TX quot.    : *         :           :           :           :
Prel. Ant. quot.  : *         :           :           :           :
Final Report      : **        :           :           :           :
General PCR spec's:   *       :           :           :           :
Frequency decision:   *       :           :           :           :
Antenna decision  :   *       :           :           :           :
Final Ant.spec's. :    *      :           :           :           :
TX decision       :    *      :           :           :           :
Final TX spec's   :    *      :           :           :           :
Tender request Tx, Ant  *     :           :           :           :
Install Dig. Eng. :     ***************************************************
Study Dig.Equipm. :     *******           :           :           :
Study Analog.Equipm.    *******           :           :           :
Study Computing   :     *******           :           :           :
Install Programmer 1          *********************************************
Comput.program developm.      *********************************************
Install Technician 1          *********************************************
Install Technician 2          :     ***************************************
Install Technician 3          :           *********************************
Install Programmer 2          :           :  ******************************
Construct dig./anal. equipment  *******************************************
Site prep's,freq.all. etc.....***************....     :           :
Receive TX tenders         *  :           :           :           :
Receive Ant.tenders        *  :           :           :           :
Decide TX, Ant.company      * :           :           :           :
Order TX and Ant. :          *:           :           :           :
Install Ass. Eng. :           :     ***************************************
First TX tested   :           :           *           :           :
Install Site Engineer         ............*********************************
Begin building construction   :     ......*********************************
Ant. constr. on-site          :    .....  :    *****  :    *****  :   *****
System tests on-site          :           :      .....*********************
TXs installed on-site         :           :           *********************
Test transmission :           :           :           :           *********
TX, Ant. acceptance tests     :           :           :           :   *****
First experiments :           :           :           :           :      **
```

VIII. SUMMARY OF SCIENTIFIC CAPABILITIES AND COST ESTIMATES

The different antenna designs discussed in Section IV have been assessed in terms of their ability to achieve the scientific goals defined in Section II.C. However, owing the high cost estimates for both a phased array radar and a single dish with multiple feeds (see Table 5), the scientific assessment has been restricted to four antenna configurations that are either affordable now or potentially achievable by a phased programme of implementation. The four antenna configurations evaluated are: (i) 1×32m dish; (ii) 1×45m dish; (iii) 2×32m dishes; and (iv) 3×32m dishes. Table 6 indicates the relative scientific capabilities of the four configurations, expressed as percentages of the scientific capability achieved with 3×32m dishes. The evaluation of the scientific capabilities is not a trivial task and the percentages presented in the table should be regarded merely as giving an approximate assessment of the relative scientific capabilities of the different antenna systems. Moreover, the ordering of the scientific topics in this table is exactly the same as that in Section II.C and does not purport to provide any indication of scientific importance. Despite these caveats, the topics listed in Table 6 encompass almost all the scientific objectives of the solar-terrestrial physics community. Indeed, this table provides a concise summary of the strong scientific reasons for building an incoherent scatter radar on Svalbard. The numbers in the table indicate that very valuable scalar measurements can be made with a single antenna, although the great scientific potential of the new radar will only be realized when at least two antennas are in operation. Therefore, it is confidently anticipated that excellent and worthwhile science will result from measurements made during the first phase of the project, even if only one antenna is available. However, it is strongly recommended that the goal should then be to enhance the initial system as soon as further funds become available, in view of the really major scientific advances that would result from the provision of two, or preferably three, antennas.

TABLE 6

**Relative Scientific Capabilities (%)
of Different Antenna Systems**

Scientific Topic	Antenna(s)			
	1×32m	1×45m	2×32m	3×32m
Dayside Auroral and Plasma-Flow Transients	20	20	60	100
Birkeland Currents	60	60	80	100
Cusp/Cleft Ion Fountain	25	70	75	100
Polar Cap Convection	30	30	60	100
Polar Cap Precipitation	70	80	95	100
Auroral Zone/Polar Zone Coupling	70	70	100	100
Large Upward Flows Near Midnight	25	70	75	100
Polar Wind	25	70	75	100
Ionization, Composition and Thermal Structure	80	85	90	100
Patches, Blobs and Irregularities	60	65	80	100
Thermospheric Response to IMF	50	50	80	100
Extraction of Ionospheric Plasma	25	70	75	100
Non-Thermal Plasmas	50	60	80	100
Lower Thermosphere/Mesosphere Coupling	20	30	50	100
Polar Stratosphere and Troposphere	20	30	50	100

Table 7 gives the best cost estimates available at present for the radar systems corresponding to the different antenna configurations presented in Table 6. Estimates are given for the preparation of the site, construction of a building, road and powerline, and for the purchase of the various components of the radar systems. For the transmitter and antenna(s), we also give estimates corresponding to reduced specifications, as explained in the footnote to Table 7. Manpower costs during the construction phase are excluded.

TABLE 7

Best Available Cost Estimates

Itemized Expenditure	Antenna(s)			
	1 × 32m dish (M DEM)	1 × 45m dish (M DEM)	2 × 32m dishes (M DEM)	3 × 32m dishes (M DEM)
Building, Road, Powerline, etc.	3.5	3.5	3.5	3.5
Groundwork for Antenna(s)	0.5	0.7	1.0	1.5
Transmitter	15 8*	15 8*	15 8*	15 8*
Antenna Dish(es)	11.7 10*	21.7 17.7*	23.4 20*	35.1 30*
Receiver and Computers	1.6	1.6	3.2	4.8
T/R, Hybrids and Phaseshift	1.0	1.0	1.0	1.0
Monitoring and Control	1.0	1.0	1.0	1.0
Design	1.0	1.0	1.0	1.0
Total M DEM	35.3 26.6*	45.5 34.5*	49.1 38.7*	62.9 50.8*
M GBP	12.2 9.2*	15.7 11.9*	16.9 13.3*	21.7 17.5*
M SEK	131 99*	169 128*	182 143*	233 188*

£1 = 2.90 DEM = 10.75 SEK

* Reduced specifications:

1. The reduced specification for the transmitter implies 1.5 MW rather than 3.0 MW.

2. The costs quoted for a 32-m parabolic dish were in response to a detailed specification. It may be possible to reduce the costs if the specification is relaxed on the following points:

   i) The original specification required the antennas to scan in elevation from horizon to horizon through the zenith. It would, however, be acceptable if the scan was terminated 15° beyond the zenith as this would still allow the antenna to scan from the northern horizon to a field-aligned direction without needing to scan 180° in azimuth.

   ii) The specification required the antennas to slew at a maximum speed of 1° per second. If more than one antenna is in operation, the need for beam-swinging is reduced and the slew rate could be reduced if this led to significant financial savings.

   iii) The highest operating frequency, which was specified as 1 GHz, could be reduced.

   For the relaxed specification the estimated cost of the antennas has been reduced by 15%.

Table 8 provides an approximate assessment of the annual costs that will be incurred once the Polar Cap Radar becomes operational. However, it should be emphasized that the numbers in this table are merely provisional estimates. The cost of electricity is about 25% of the value quoted in the UK Report because of a reduction in the price of electricity on Svalbard. The sum allowed for maintenance, spares and consumables is of the order of 10% of the capital expenditure and is based on budgetary experience gained in operating the EISCAT radars over the past decade. A similar comparison with EISCAT experience has been used to estimate the modest contingency funds. The staff costs have been calculated on the basis of the posts defined in Section VII.A. These posts are those considered necessary to implement and operate the Polar Cap Radar as an international research facility capable of making major contributions to scientific knowledge. It may well transpire that not all of these staff posts are distinct from, or additional to, existing EISCAT posts. Moreover, some of the posts (tasks) could possibly be filled (undertaken) by staff seconded from the member countries. Finally, it should be stressed that the staff costs would build up gradually and could be partly subsumed in the capital costs during the initial stages of the project. The full staff costs given in Table 8 would not apply until the Polar Cap Radar started to become operational. For example, in the first year of the project, the staff costs would be only about £0.1M.

TABLE 8

Recurrent Costs

Recurrent Expenditure		GBP
Electricity:	0.31 NOK/kW hour For 1.5 MW load for 2000 hours	0.08 M pa
Maintenance, Spares and Consumables		1.00 M pa
Staff	11 × £50,000	0.55 M pa
Contingency Funds		0.15 M pa
	TOTAL	£1.78 M pa

Appendix A

Scientific Achievements of EISCAT

When EISCAT was first proposed ('A European Incoherent Scatter Facility in the Auroral Zone', 1974), eleven specific scientific topics were identified which, it was thought, EISCAT would be able to investigate. It is now possible to confirm that EISCAT has made a substantial contribution to each of these topics, fully justifying the support given to the project. However, in almost every case the most important results have developed from totally unexpected discoveries, as summarised below. We sincerely believe that the same pattern will apply to the Polar Cap Radar. The facility will be able to study all the scientific topics listed in the main case, and they more than justify the support required. However, the whole field of the polar-cap ionosphere has been investigated so little that without doubt the most important results will again be totally unexpected.

1. *'By looking directly along field lines in the topside ionosphere, the system will measure the outflow of plasma along the magnetic field lines'.*

   Recent observations with the VHF system have monitored the 'classical' polar wind at heights above 1500 km. However, the most exciting results have been field-aligned flows as large as 1 kms^{-1} observed in the F-region. When these were first reported they were rejected as 'impossible' but now the mechanisms that drive the plasma upward are better understood.

2. *'Measurements of the ionospheric drift velocity along magnetic field lines at lower altitudes will give practical information about thermospheric winds'.*

   In the F region, the comparison of EISCAT measurements of plasma velocity and Fabry-Perot measurements of neutral wind velocity have given good qualitative agreement and so confirm EISCAT's ability to measure the meridional component of thermospheric wind at these heights. In the E region, EISCAT measurements have monitored the diurnal and semi-diurnal tides for different seasons and different levels of magnetic activity. The most important tide is semi-diurnal and below 115 km this shows the phase variation with height of a (2,4) mode but a (2,2) mode at greater heights.

3. *'The velocity of the plasma perpendicular to the magnetic field lines will also be measured and from this the electric field may be determined. The distribution of electric fields will give us information about the large-scale circulation of plasma in the magnetosphere'.*

   By systematically measuring tristatic plasma velocities over many years, EISCAT has provided unparalleled data on the average two-cell pattern of plasma circulation in the auroral zone as a function of the interplanetary magnetic field. The unexpected result is that the plasma velocity often varies dramatically over a time-scale of 10 minutes or so, indicating that the whole pattern of circulation is bursty and can be switched on and off rapidly.

4. *'The electric fields in the ionosphere can also produce currents, particularly at auroral latitudes, and these currents can also be measured directly'.*

   EISCAT has successfully measured electric currents in the auroral zone in two ways. By determining the Hall and Pedersen conductivities as functions of height and by measuring the applied electric fields, the Hall and Pedersen currents can be inferred. Recently the field-aligned currents (FAC's) have been measured directly in the F-region by comparing the mean Doppler shift of the ion- and electron-acoustic spectra (see point 7 below).

The surprising results were:- i) the Pedersen currents played a more important role than previously thought; and ii) the FAC's were occasionally much larger than anticipated.

5. *'The neutral winds and electric fields together produce ionospheric drifts and currents which have a very strong influence on the overall structure of the ionosphere'.*

Under magnetically quiet conditions, EISCAT has been able to monitor in a comprehensive way the effect of neutral winds and electric fields on the conventional ionosphere, including the servo-mechanisms that tend to maintain the F-region peak at a fixed height. However, under disturbed conditions many unforeseen effects became important. The movement of plasma through the neutral atmosphere at speeds greater than the ion thermal speed caused strong frictional heating of the ion population, accompanied by a change in the ion-velocity distribution to a non-Maxwellian form. These changes had profound effects on recombination coefficients and also created a strong enhancement of plasma pressure which, together with the 'hydromagnetic mirror force', accelerated the plasma upwards creating a deep trough in electron concentration and at the same time driving a significant quantity of plasma upwards towards the magnetosphere.

6. *'The input of energy by particles and electric currents at high latitudes is a major heat source for the thermosphere, rivalling that due to solar ionising radiation. The EISCAT temperature measurements will provide information which is vital to studies of the energy balance of the thermosphere'.*

EISCAT has been able, as a matter of routine, to measure the input of energy due to soft and hard particle precipitation, and the Joule heating caused by Pedersen currents. The main result has been that the energy input due to Joule heating is an order-of-magnitude more important than that due to precipitating particles. It follows that the time variation of total Joule heating - which only incoherent scatter facilities like EISCAT can measure - gives the most representative picture of the transfer of energy from the magnetotail to the ionosphere during substorms. The picture provided in this way often displays quasi-periodic inputs of energy which are more regular than the inputs of hard particle precipitation monitored by auroral cameras, magnetometers and riometers.

7. *'The plasma line phenomenon observed in incoherent scatter is intensified by the precipitation of energetic particles. EISCAT will thus provide information about particle precipitation'.*

Natural plasma lines are observed by EISCAT more often and more easily than had originally been anticipated. As it happens, not very much work has yet been done to use these lines to monitor the precipitation of energetic particles - though this has been done extensively in other ways. A very exciting development has been the use of the plasma lines, together with the ion lines to measure the FAC's directly. This promises to be one of the most important techniques in studying magnetosphere-ionosphere coupling.

8. *'Electron density profiles through the auroral D and E layers, using short time resolution, will also indicate the varying flux and spectrum of precipitating particles'.*

This technique has proved very effective and the spectra of precipitating particles can be routinely determined with the necessary short time resolution. In addition, however, electron density profiles have illustrated the very complex pattern of sporadic-E layers.

9. *'Measurements at the lowest height ranges will provide information about the effects of stratospheric warmings on the D region and similar lower ionosphere phenomena'.*

Owing to the long delays in bringing the VHF system up to specification, D-region studies have been limited. However, they have produced one totally unexpected result. Previous theory had strongly indicated that turbulence on the scale of 0.7m in the D-region would suffer viscous damping. Nevertheless, the EISCAT VHF system in summertime receives extremely strong echoes from one or more narrow layers located near the mesopause. It is now suggested that, at a low enough temperature, multiply-hydrated ions occur and these dramatically alter the plasma diffusion coefficient so that turbulence at 0.7m is in the inertial sub-range.

10. *'F-region storm phenomena and seasonal variations are largely the result of composition changes in the thermosphere, which are in turn caused by variations in the air circulation pattern. High latitude studies are very important for a proper understanding of these phenomena'.*

A combination of EISCAT measurements and the UCL-Sheffield ionosphere-thermosphere coupled model are providing a better understanding of the global response to F-region storm phenomena. A surprising result is that the composition changes brought about during storms in the auroral zone do not penetrate sufficiently to lower latitudes to bring about the anomalies that had previously been explained in this way. This remains an outstanding problem in global thermospheric physics.

11. *'The EISCAT system will enable gravity waves and travelling ionospheric disturbances, many of which originate in auroral regions during storms, to be studied near their source'.*

The World Atmospheric Gravity-Wave Study (WAGS) campaign in the European sector was a major success, due largely to the role of EISCAT in monitoring the source region. On two occasions, clearly defined auroral disturbances were identified as the source of specific large-scale atmospheric gravity waves seen propagating equatorward from the auroral zone. Once again there was an unexpected result. Previous theory had suggested that the sources were impulsive and the observed periodicity of the gravity waves was a result of filtering and dispersion in the thermosphere. The EISCAT observations indicated on both occasions that the periodicity was already implicit in the auroral disturbance. They also suggested that Lorentz forcing rather than Joule heating was the main mechanism for generating the waves.

The Future

We now find ourselves in a similar position in proposing to build an incoherent scatter facility on Svalbard. Many of the most exciting and topical phenomena - such as the ground signatures of magnetopause reconnection, very large upward velocities in the topside ionosphere and the generation of non-thermal plasmas - generally occur to the north of EISCAT. For the 1990s the logic points to another advanced radar, located within the polar cap, especially as this will allow joint studies with the Cluster spacecraft mission, which can collaborate with the existing EISCAT system to address these problem areas.

Appendix B

Switchyard for Pulse-to-Pulse Switching

Figure 31 shows the layout of a switchyard designed by A.P. van Eyken and P.J.S. Williams for the UK report on the Polar Cap Radar. Its purpose is to allow the full power of a distributed transmitter to be switched between antennas from pulse to pulse for 3-beam operation. In this way the effective sensitivity of the system is increased by a factor of $\sqrt{3}$ when compared with an equal division of power between the antennas for each pulse. (The reason for this is that while the average signal power received by each antenna is unchanged the noise power is only received for one third of the time.)

Mechanical switching is impossible between pulses as the time available is too short. Instead, the phase of the output from each unit in the transmitter is varied from pulse to pulse. If two similar transmitters provide an in-phase input to opposite ports of a hybrid ring, then at the third port the two signals will be in-phase and will add constructively while at the forth port the two signals will be out-of-phase and cancel each other. If the phase of one of the transmitters is now changed by 180° the pattern is reversed and the output appears on the fourth port. Figure 31 shows how this principle can be used to switch the transmitted signal from four units between three antennas. The dummy load is needed to provide a matched output but, of course, no power should normally reach the load and software protection is desirable to ensure this does not happen. However, if one of the transmitter units fails, or if the power provided by each unit is not equal then power will be directed to the dummy load.

Table 9 is the 'truth table' to show how the phase of the four transmitter units can be modified to switch the output from antenna to antenna.

In the alternative mode of the switchyard, for single-beam operation, it is necessary to divide the power equally between the three antennas during each pulse. In this case H1 and H2 must divide the output in a 2:1 ratio. This is possible by applying inputs of equal power but with a phase difference of 114.5° (or 294.5°) to each hybrid. The waveguide trombones are included in the path to two of the antennas to ensure that the transmitted signals from the three antennas are in phase whatever the pointing direction of the single beam.

TABLE 9: Phase of Units in Distributed Transmitter

DAC1	DAC2	DAC3	DAC4	ANTENNA SUPPLIED
0	0	180	0	A1
0	0	0	180	A2
0	180	0	0	A3
0	114.5	0	294.5	A1/A2/A3

Appendix C

Scientific Consultants

Dr. G.N. Taylor

Royal Signals and Radar Establishment, St Andrews Road, Malvern, WR14 3PS, UK

Dr. G. Wannberg

EISCAT Scientific Association, Box 812, S-981 28 Kiruna, Sweden

Dr. P.J.S. Williams

Department of Physics, University College of Wales, Aberystwyth, SY23 3BZ, UK

Contributors

Dr D. Alcaydé	(CESR)
H. Boholm	(EISCAT - Tromsø)
Prof A. Brekke	(University of Tromsø)
Prof. S.W.H. Cowley	(ICSTM)
S.R. Crothers	(RAL)
V.N. Davda	(RAL)
E. Ellingsen	(Tromsø Satellite Station)
Dr A.P. van Eyken	(EISCAT - Tromsø)
Dr A.D. Farmer	(RAL)
Dr D. Fontaine	(CRPE)
K.S.C. Freeman	(RAL)
J.-A. Hansen	(EISCAT - Tromsø)
Prof O. Havnes	(University of Tromsø)
S. Heck	(EISCAT - Kiruna)
Dr A. Huuskonen	(University of Oulu)
R. Jacobsen	(EISCAT - Tromsø)
Prof J. Kangas	(University of Oulu)
Prof H. Kohl	(MPI)
R.O. Larsen	(EISCAT - Tromsø)
Dr M. Lehtinen	(University of Helsinki)
Dr M. Lockwood	(RAL)
Mrs U.P. Løvhaug	(EISCAT - Tromsø)
Dr H. Opgenoorth	(IRF)
A. Orheim	(Svalbard Development Company)
K. Rinnert	(MPI)
Prof. H. Rishbeth	(University of Southampton)
K. Sandvik	(Barlindhaug Company - Tromsø)
Prof A. Siivola	(University of Helsinki)
C. Taieb	(CRPE)
Ms T. Telebond	(Svalbard Development Company)
Dr E.C. Thomas	(University of Leicester)
Mrs J. Foster	(RAL) Editorial and Secretarial Assistant

Appendix E

Acknowledgements

Financial support has been received from the following Institutions:

Centre National de la Recherche Scientifique (CNRS)	(Paris, France)
Institute för Rymdfysik (IRF)	(Kiruna, Sweden)
MPI für Aeronomie	(Katlenburg-Lindau, Germany)
Naturvetenskapliga Forskningsrådet (NFR)	(Stockholm, Sweden)
Norges Allmennvitenskapelige Forskningsråd (NAVF)	(Oslo, Norway)
Science and Engineering Research Council (SERC)	(Swindon, U.K.)
Suomen Akatemia (SA)	(Helsinki, Finland)
Svalbard Development Company	(Longyearbyen, Svalbard)
University of Oslo	(Oslo, Norway)
University of Tromsø	(Tromsø, Norway)

Appendix F

Reports

Additional scientific and technical information is available in the following separate reports:

'Polar Cap Radar: Research on the Polar Mesosphere - Stratosphere - Troposphere : A Proposal', by J. Röttger, EISCAT Scientific Association, Kiruna, Sweden.

'Some Considerations about Auroral Backscatter Interference to an Incoherent Scatter Radar on Svalbard', by K. Schlegel, Max-Plank-Institut für Aeronomie, Lindau, Germany.

'Pre-feasibility Study of POCAR Antenna System', by Elekluft Company, Bonn, Germany.

'Receiving and Signal Processing in the Polar Cap Radar', by T. Turunen, Geophysical Observatory, Sodankylä, Finland.

'Report on an Incoherent-Scatter Radar on Svalbard', by P.J.S. Williams, University College of Wales, Aberystwyth, Wales.

FIGURE CAPTIONS

Figure 1 Map of the Arctic, showing the position of some key polar scientific stations, including the EISCAT stations at Tromsø, Kiruna and Sodankylä. The blue circle centred on the geographic pole (GP) represents geographic latitude 77°, which is taken as the boundary of the region accessible to daytime auroral observations. Within this circle, the sun is > 10° below the horizon at noon at winter solstice. The red circle centred on the invariant magnetic pole (MP) represents invariant latitude 76°, the average locus of the ionospheric footprint of the polar cusp. Longyearbyen (Svalbard) is clearly an ideal location for combined radar and optical observations of the polar ionosphere.
(after Saunders, M.A., Antarctic Science **1** (3), 193-203, 1989.)

Figure 2 A rapid poleward flow burst observed by EISCAT in the POLA mode. The line-of-sight velocities are consistent with a transient, vortical flow pattern which may have been produced by the pulse in the solar wind dynamic pressure observed by the AMPTE-IRM and UKS satellites several minutes earlier (top panel). No clear trigger is seen in the interplanetary magnetic field data (middle three panels).
(after Sibeck, D.G., et al., Geophys. Res. Lett., **16**, 13-16, 1989a. and Todd, H., et al., Geophys. Res. Lett., **13**, 909-912, 1986.)

Figure 3 Examples of transient dayside auroral/flow-burst events, observed by the EISCAT radar, photometers and all-sky camera on 12 January 1988. Auroral luminosity is shown as a function of UT and zenith angle (positive to the north) by the (a) 630.0nm and (b) 557.7nm meridian scanning photometers at Ny-Ålesund (NA). Panel (c) gives the ion drift velocities observed by EISCAT, and (d) the potential across the north-south dimensions of the EISCAT field of view (Φ). The all-sky TV image at 09:20:55 is given in (e), which also shows the near simultaneous EISCAT flow data. The meridian scanned by the photometers (dot-dash line) and the locations of magnetometers at Hornsund (H) and Bjørnøya (B), the approximate zenith angles of which are also indicated at the top of (a) and (b).
(after Lockwood, M., et al., Planet. Space Sci., **36** (11), 1229-1253, 1988.

Figure 4 Field-aligned current deduced from EISCAT observations acquired during a 24-hour period in June 1982, displayed is a polar diagram based on magnetic local time (MLT)- invariant latitude coordinates (after Caudal, G., J. geophys. Res., **92**, 6000-6012, 1987). Latitudinal profiles are shown, with solid areas representing positive current (into ionosphere) and open areas representing negative current (out of ionosphere).

Figure 5 Schematic representation of a typical twin-cell, high-latitude convection pattern (solid lines) in the northern polar-ionosphere for a southward interplanetary magnetic field (adapted from Heppner, J.P. and Maynard, N.C., J geophys. Res, **92**, 4467-4489, 1987). The dashed line represents the boundary between open and closed field lines. The bold dashed circles show typical viewing areas for the EISCAT UHF radar (centred on the open circles) and the proposed Svalbard radar (centred on the solid circles) at four magnetic local times (MLT).
(after Cowley, S.W.H., et al., J. atmos. terr. Phys., **52**, 645-664, 1990.)

Figure 6 High-latitude convection patterns for (a) small or southward IMF B_z (B_z<2nT), and (b) 'strong' northward IMF B_z (B_z>2nT).
(after Cowley, S.W.H., et al., J. atmos. terr. Phys., **52**, 645-664, 1990.)

Figure 7 Height profiles of plasma velocity parallel to the magnetic field line during a large upflow event driven by ion-neutral frictional heating.
(after Jones, G.O.L., et al., Nature, **336**, 231-232, 1988.)

Figure 8 Height profile of the line-of-sight velocity of the O^+ ions, as measured by the EISCAT VHF radar, and the corresponding height profile of the derived H^+ velocity.

Figure 9 Results from the UCL/Sheffield University coupled model of the ionosphere and thermosphere, indicating the position of the auroral oval by its enhanced plasma densities and the strength and direction of the thermospheric winds (S = Svalbard, E = EISCAT) for 00, 06, 12 and 18 UT. The model input parameters are for magnetic activity Kp of ≈3 (courtesy Fuller-Rowell, T.J.).

Figure 10 Energy-time spectrogram and electric field data from a pass of the Viking satellite through the morning auroral oval. The top two panels show data from the ion and electron spectrometer, the pitch angle being given by the third panel. The fourth and fifth panels show the electric field component in a spinning (spin plane) frame of reference and the floating ground potential ($V_{fg} \propto \log (N_e \sqrt{T_e})$ measured by the electric field experiment (V1). The bottom panel displays electron densities computed for 50 to 200 eV and for 200 eV to 400 keV.

Figure 11 Observed spectra (solid line) with best-fits from non-Maxwellian analysis (dashed lines) for various aspect angles, ϕ, during a scan of the EISCAT CP-3 experiment. For positions 5-10 the ion drift was large and roughly constant at Mach 2. The data show predicted aspect angle dependence for observations of non-thermal ion velocity distributions.
(after Winser, K.J. et al., J. geophys. Res., **94**, 1439-1449, 1989.)

Figure 12 Wind velocity measurements in the troposphere and the lower and middle stratosphere (after (a) Larsen, M.F. and Röttger, J., Bull. Amer. Meteor. Soc., **63**, 996-1008, 1982: (b) Fukao, S. et al., Month. Weath. Rev., **116**, 281-292, 1988: and (c) Röttger, J., Preprint Vol., 20th Conference on Radar Meteorology, 22-29, publ. by Amer. Meteor. Soc., Boston, 1981). The arrows in all three panels represent the horizontal wind velocity vector. Panel (a) shows the turning of the wind velocity in the upper troposphere during a tropopause break (the thick lines labelled TP indicate the radar determined tropopause). Panel (b) demonstrates the strong wind variability during a stationary cold front, and Panel (c) reveals the horizontal and the vertical (contours) velocity in the stratosphere during planetary wave passages. These data were collected with the SOUSY VHF radar in Germany (Panels (a) and (c)) and the MU VHF radar in Japan (Panel (b)).

Figure 13 The spectrograms shown in this figure, which were recorded by the EISCAT VHF radar, reveal the existence of mesospheric gravity waves.

Figure 14 Physical processes coupling the lower thermosphere, ionosphere and middle atmosphere in the polar regions (after Forbes, J.M., Physics of the Mesopause Region, in: Solar-Terrestrial Physics; Principles and Theoretical Foundations, eds. R.L. Carovillano and J.M. Forbes, pp. 733-752, D. Reidel Publ. Comp., Dordrecht, Holland, 1983). The altitude regions that can be observed by specific techniques are indicated on the right hand panel.

Figure 15 Structure and dynamics of the polar stratosphere and troposphere investigated by the polar cap radar operated in ST mode.

Figure 16 Map of Adventdalen, Spitsbergen (courtesy Norsk Polarinstitutt, Oslo). Scale: 1:100,000. Contour interval: 50m (25m in the lowland). The straight red line shows the flight path to Svalbard Airport. The proposed radar site is indicated by a red dot.

Figure 17 The bold line shows the horizon profile measured at the cairn on the ridge of the plateau. The faint lines show the aspect angle to the magnetic field (IGRF at epoch 1995) at an altitude of 100 km.

Figure 18 Instrument Approach Chart of Svalbard Airport for the flight path along Adventdalen. Scale: 1:250 000. Advent, 326ADV denotes the beacon in the valley. The position of the proposed radar site is indicated by ★.

(Figures 19 to 29 are courtesy Elekluft, Bonn, Germany.)

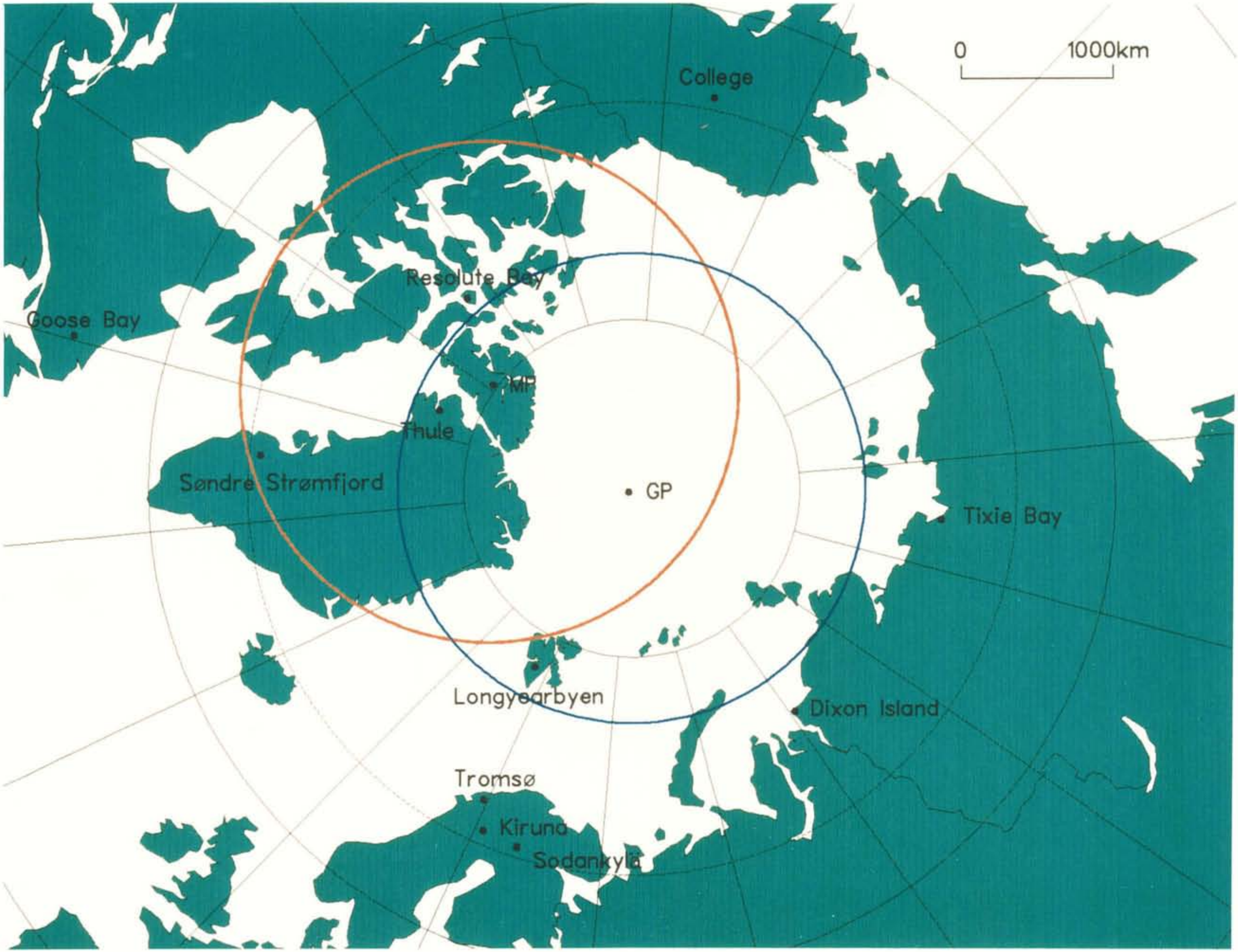
0
1000km
College
Resolute Bay
Goose Bay
MP
Thule
Søndre Strømfjord
GP
Tixie Bay
Longyearbyen
Dixon Island
Tromsø
Kiruna
Sodankylä

Figure 1

RAL

photoservices

Number 90FC6742

RUTHERFORD APPLETON LABORATORY
CHILTON, DIDCOT, OXON. OX11 0QX
Telephone: 0235 21900
ACKNOWLEDGEMENT REQUIRED

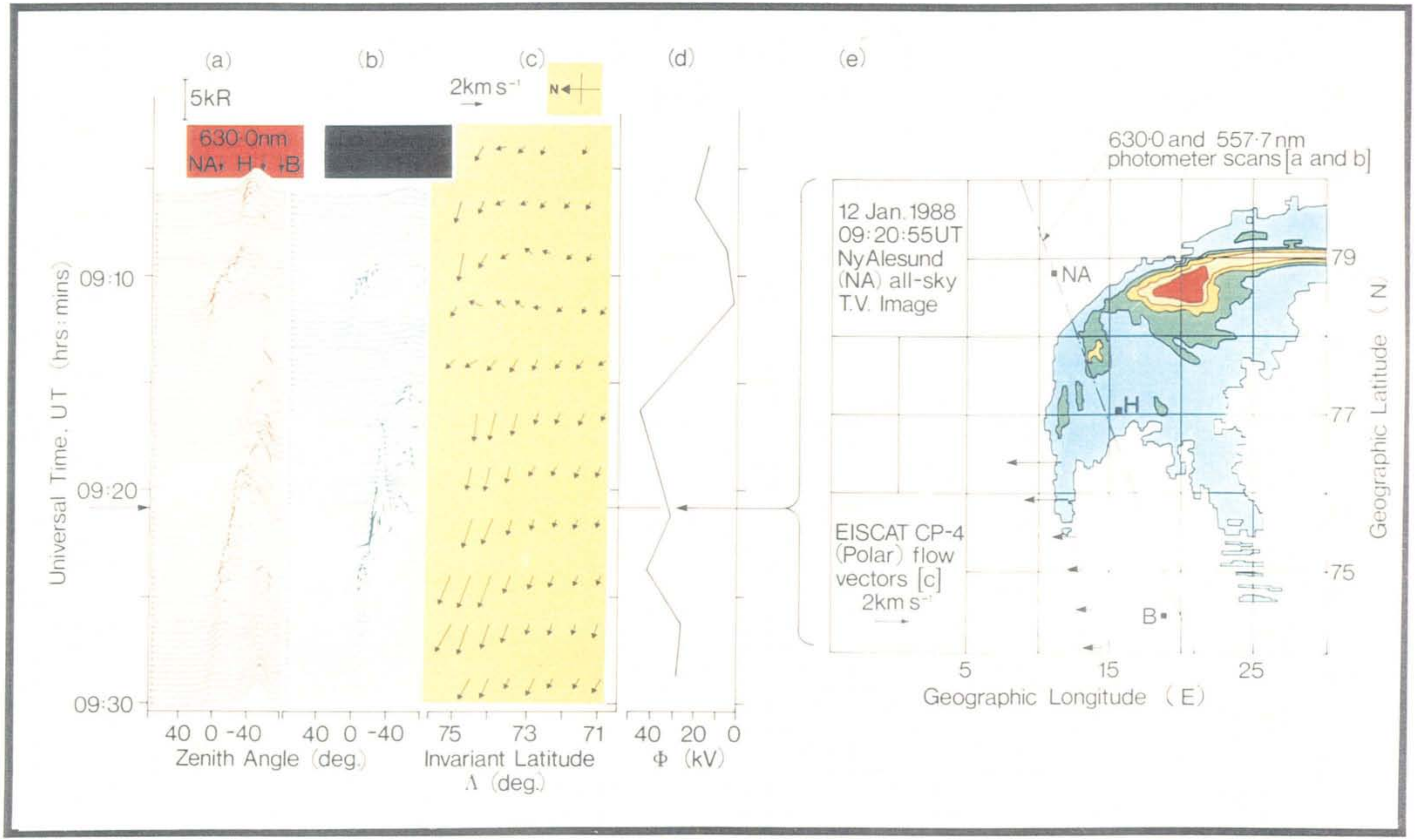

(a)
(b)
(c)
(d)
(e)
5kR
630·0nm
NA H B
2km s⁻¹
N
Universal Time, UT (hrs: mins)
09:10
09:20
09:30
40 0 -40
Zenith Angle (deg.)
40 0 -40
75 73 71
Invariant Latitude
Λ (deg.)
40 20 0
Φ (kV)
630·0 and 557·7 nm
photometer scans [a and b]
12 Jan. 1988
09:20:55UT
NyAlesund
(NA) all-sky
T.V. Image
NA
H
B
79
77
75
Geographic Latitude (N)
EISCAT CP-4
(Polar) flow
vectors [c]
2km s⁻¹
5 15 25
Geographic Longitude (E)

Figure 3

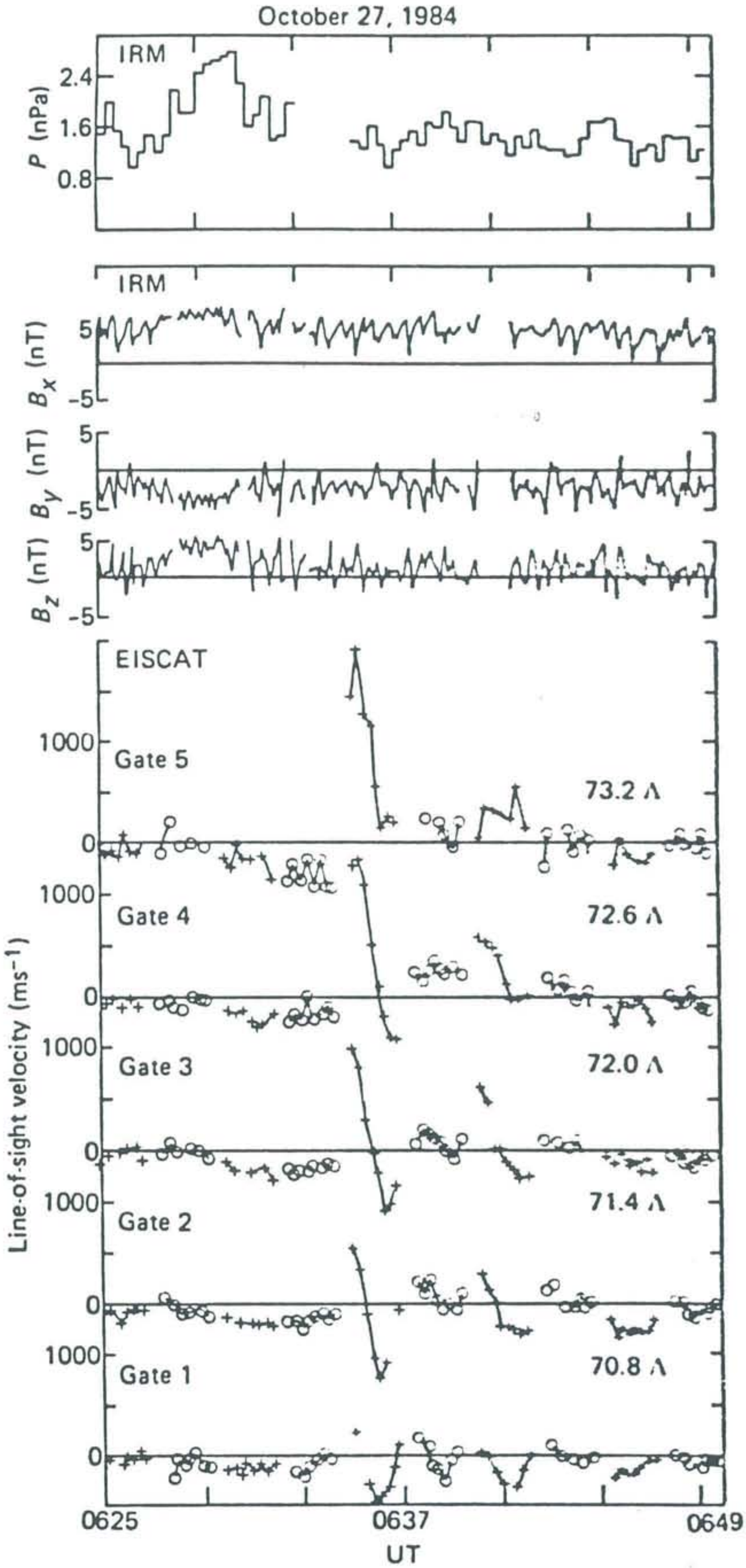

October 27, 1984
IRM
P (nPa)
2.4
1.6
0.8
IRM
B_X (nT)
5
-5
B_Y (nT)
5
-5
B_Z (nT)
5
-5
EISCAT
Line-of-sight velocity (ms^{-1})
Gate 5
73.2 Λ
Gate 4
72.6 Λ
Gate 3
72.0 Λ
Gate 2
71.4 Λ
Gate 1
70.8 Λ
1000
0
0625
0637
0649
UT

Figure 2

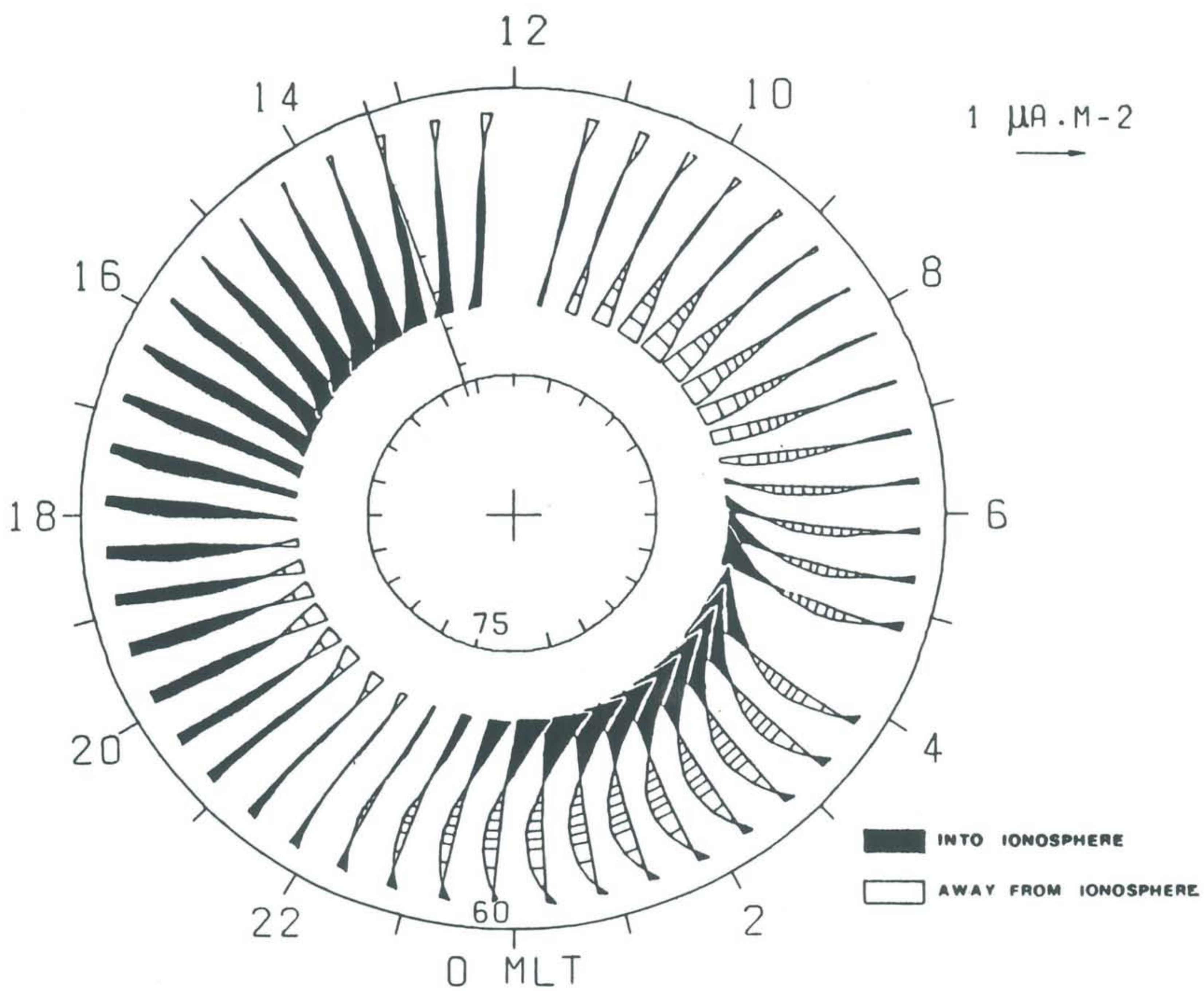
12
10
14
1 μA . M-2
16
8
18
6
75
20
4
INTO IONOSPHERE
AWAY FROM IONOSPHERE
22
60
2
0 MLT

Figure 4

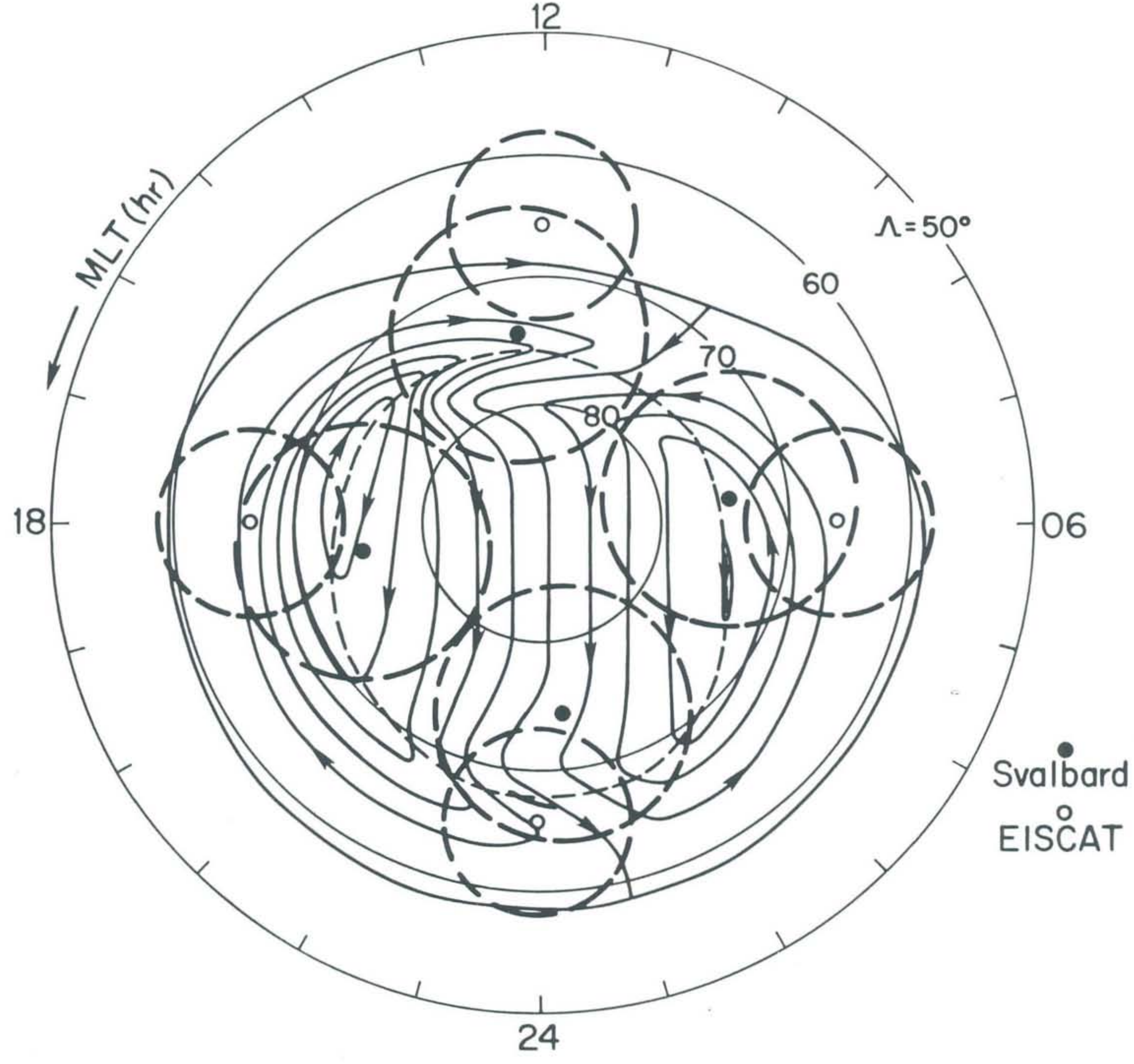

Figure 5

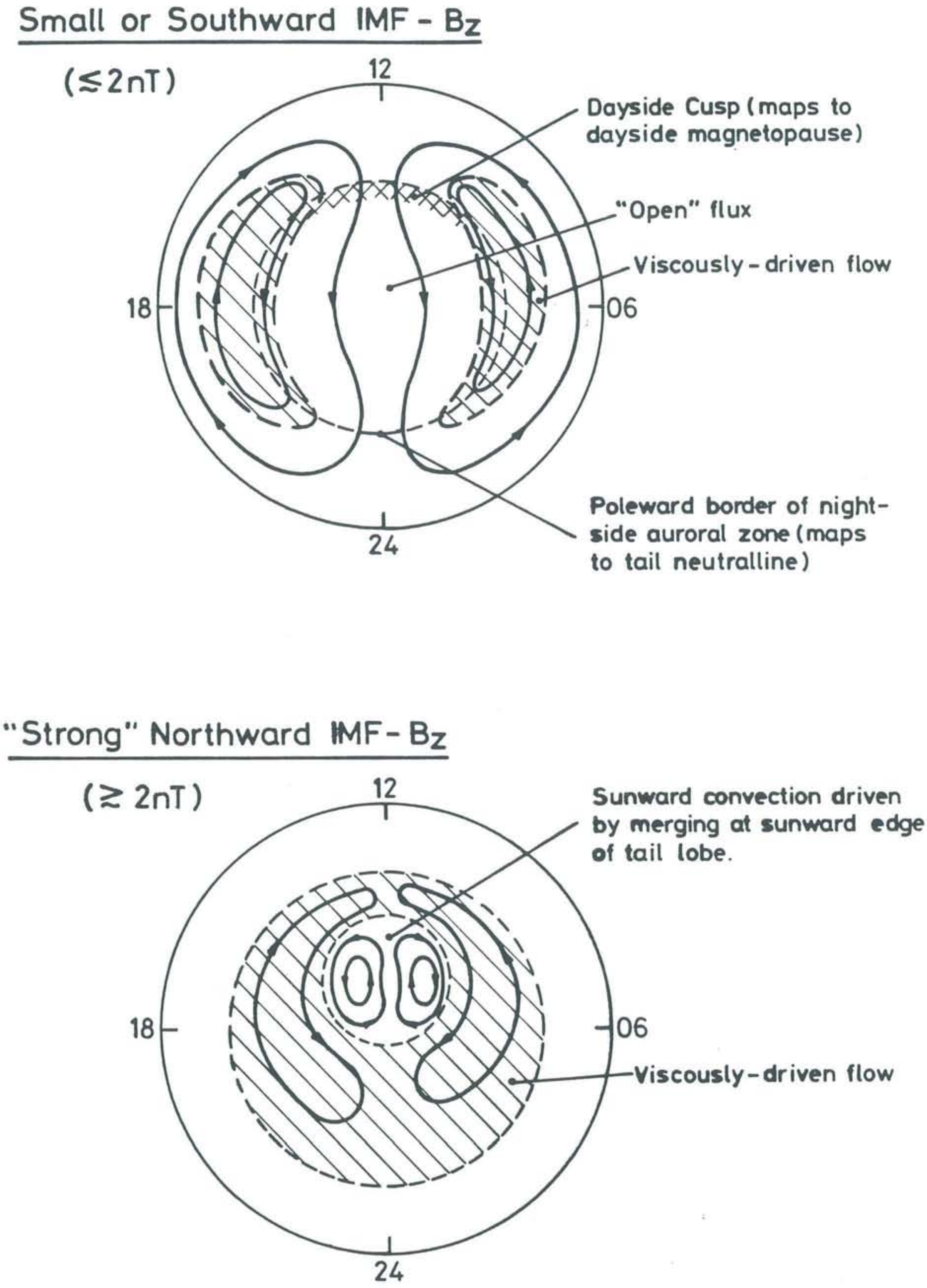

Small or Southward IMF - B_Z
($\lesssim$2nT)
12
Dayside Cusp (maps to dayside magnetopause)
"Open" flux
Viscously - driven flow
18
06
Poleward border of night-side auroral zone (maps to tail neutralline)
24
"Strong" Northward IMF - B_Z
($\gtrsim$ 2nT)
12
Sunward convection driven by merging at sunward edge of tail lobe.
18
06
Viscously - driven flow
24

Figure 6

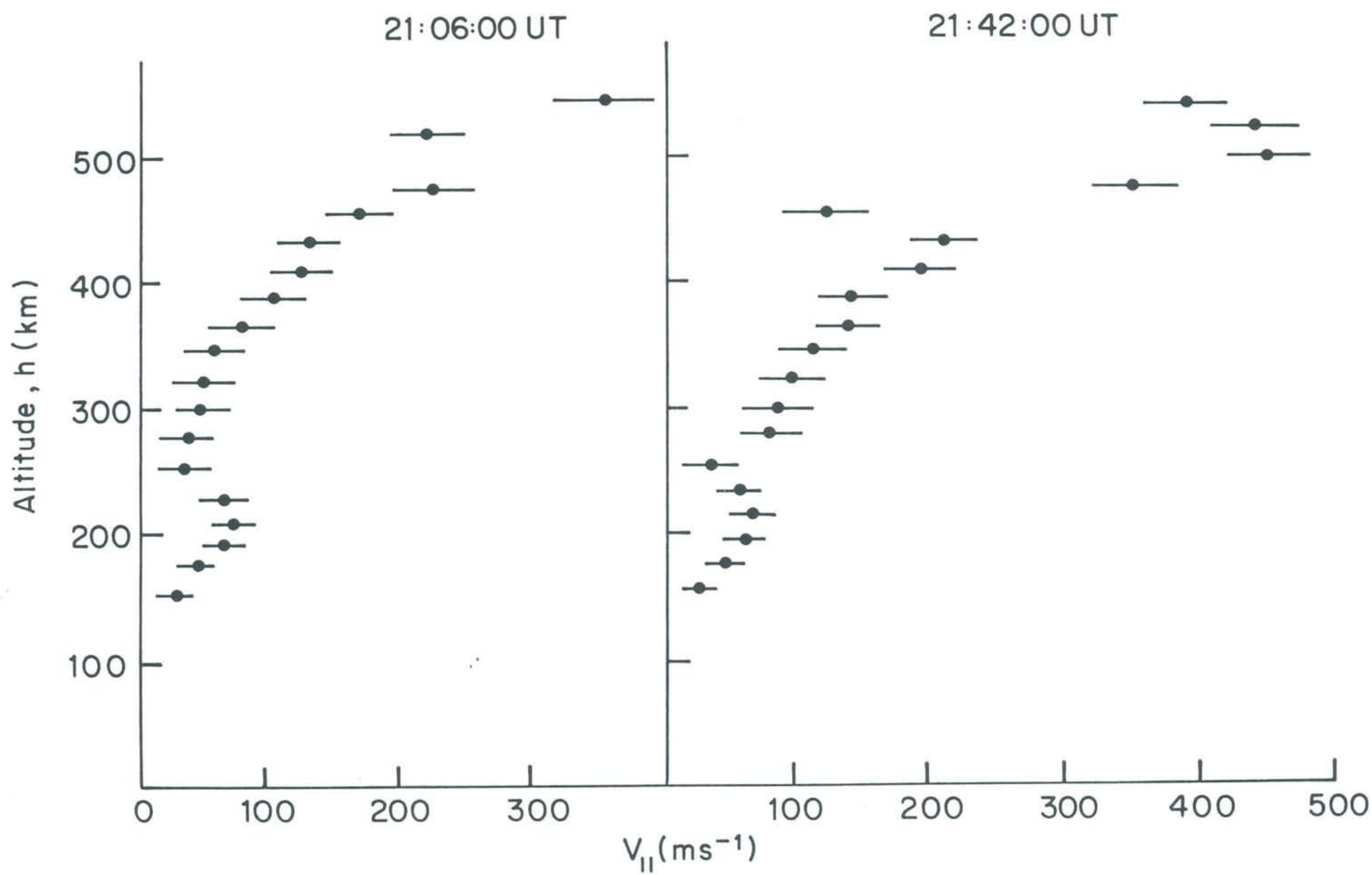
21:06:00 UT
21:42:00 UT
Altitude, h (km)
500
400
300
200
100
0
100
200
300
100
200
300
400
500
V_{II} (ms^{-1})

Figure 7

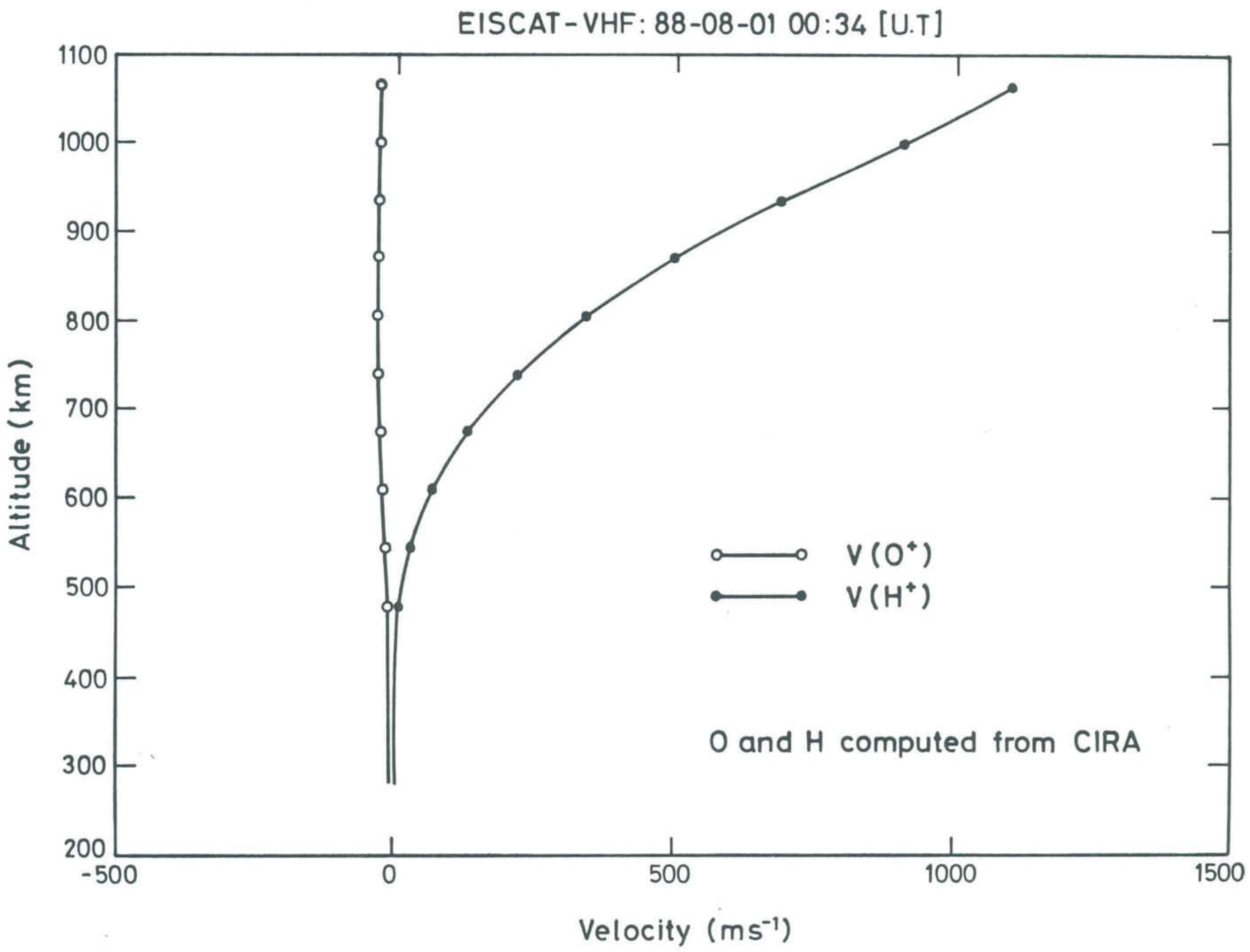
EISCAT-VHF: 88-08-01 00:34 [U.T]
Altitude (km)
Velocity (ms^{-1})
1100
1000
900
800
700
600
500
400
300
200
-500
0
500
1000
1500
V (O^+)
V (H^+)
O and H computed from CIRA

Figure 8

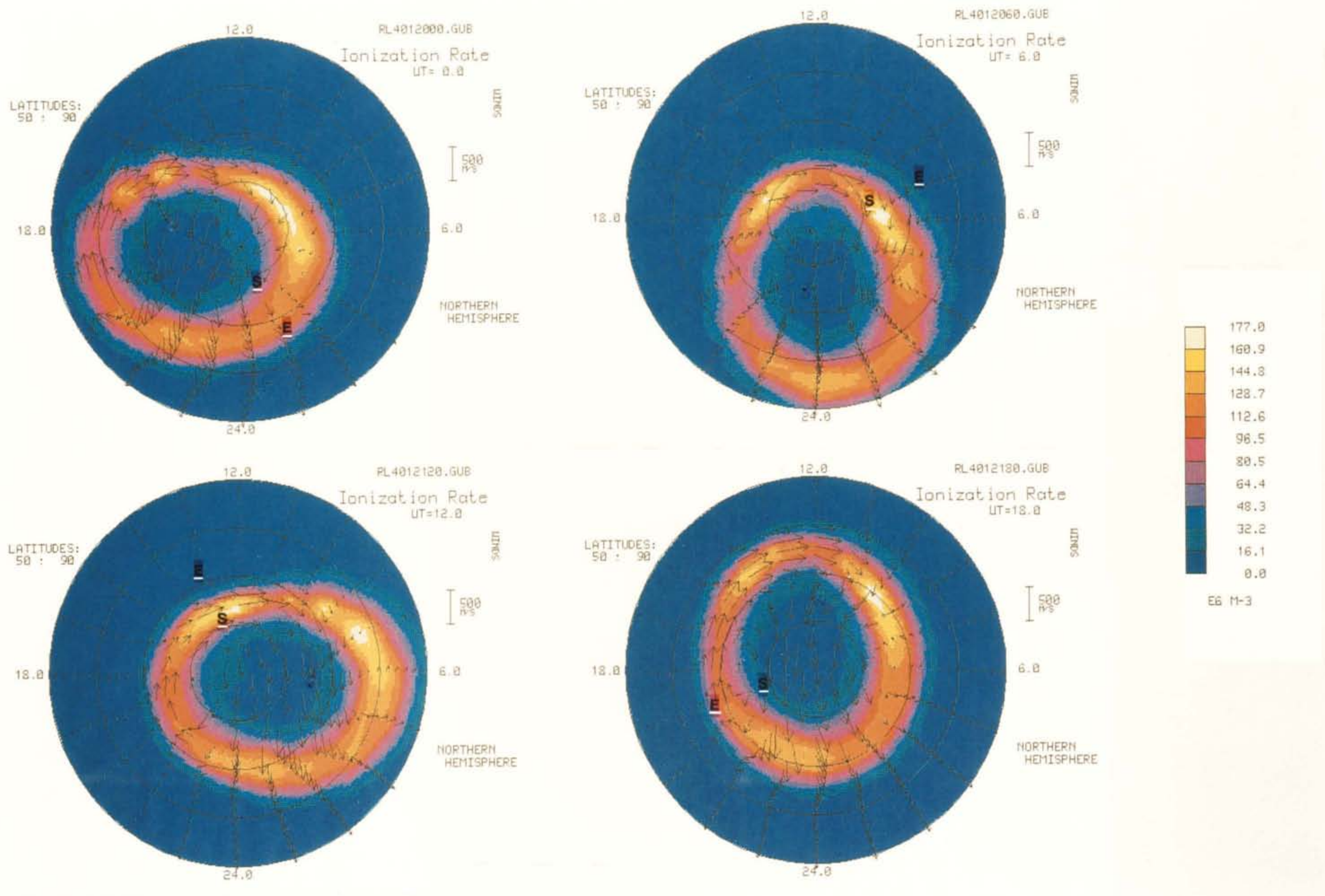

RL4012000.GUB
Ionization Rate
UT= 0.0
WINDS
LATITUDES:
50 : 90
12.0
18.0
6.0
24.0
500 M/S
NORTHERN
HEMISPHERE
S
E
RL4012060.GUB
Ionization Rate
UT= 6.0
RL4012120.GUB
Ionization Rate
UT=12.0
RL4012180.GUB
Ionization Rate
UT=18.0
177.0
160.9
144.8
128.7
112.6
96.5
80.5
64.4
48.3
32.2
16.1
0.0
E6 M-3

Figure 9

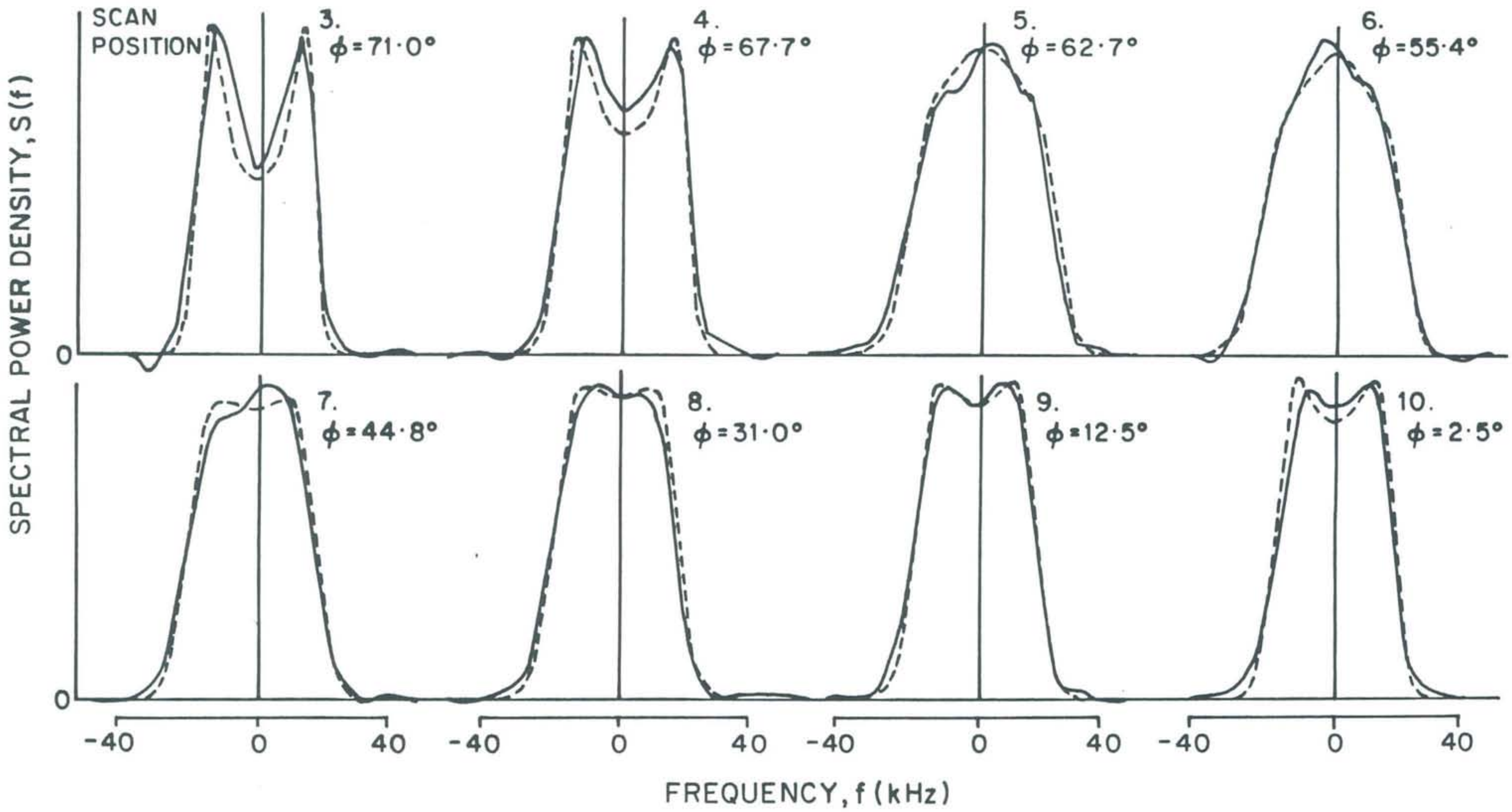
SCAN POSITION
3. $\phi = 71{\cdot}0°$
4. $\phi = 67{\cdot}7°$
5. $\phi = 62{\cdot}7°$
6. $\phi = 55{\cdot}4°$
7. $\phi = 44{\cdot}8°$
8. $\phi = 31{\cdot}0°$
9. $\phi = 12{\cdot}5°$
10. $\phi = 2{\cdot}5°$
SPECTRAL POWER DENSITY, S(f)
0
0
-40
0
40
FREQUENCY, f (kHz)

Figure 11

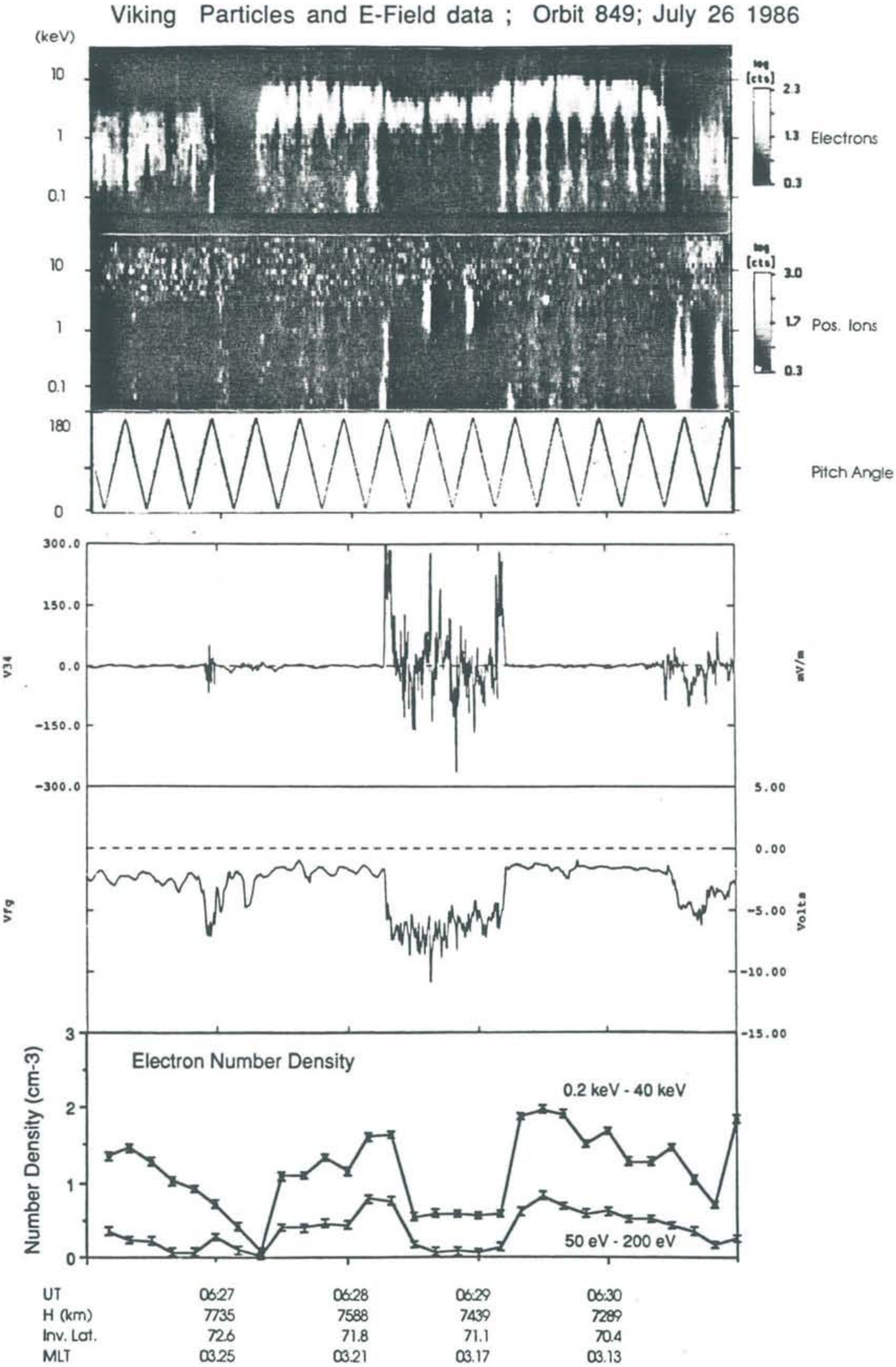

Viking Particles and E-Field data ; Orbit 849; July 26 1986
(keV)
10
1
0.1
10
1
0.1
log [cts]
2.3
1.3
0.3
Electrons
log [cts]
3.0
1.7
0.3
Pos. Ions
180
0
Pitch Angle
300.0
150.0
0.0
-150.0
-300.0
V34
mV/m
5.00
0.00
-5.00
-10.00
-15.00
Vfg
Volts
3
2
1
0
Number Density (cm-3)
Electron Number Density
0.2 keV - 40 keV
50 eV - 200 eV
UT 06:27 06:28 06:29 06:30
H (km) 7735 7588 7439 7289
Inv. Lat. 72.6 71.8 71.1 70.4
MLT 03.25 03.21 03.17 03.13

Figure 10

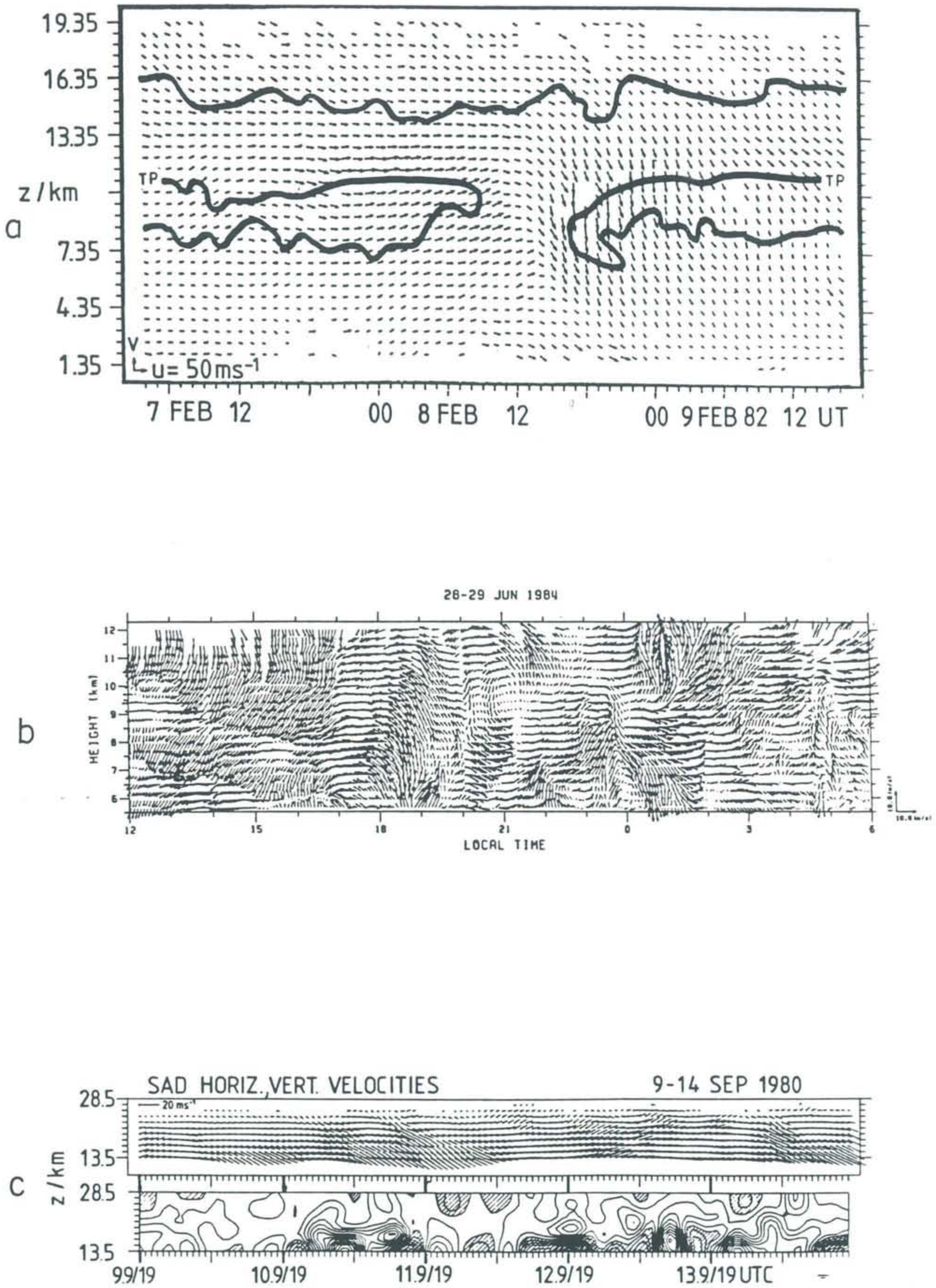
a
19.35
16.35
13.35
z / km
7.35
4.35
1.35
TP
TP
v
u= 50ms-1
7 FEB 12
00 8 FEB 12
00 9 FEB 82 12 UT
b
28-29 JUN 1984
HEIGHT (km)
12
11
10
9
8
7
6
12
15
18
21
0
3
6
LOCAL TIME
c
SAD HORIZ.,VERT. VELOCITIES
9-14 SEP 1980
20 ms-1
28.5
13.5
z / km
28.5
13.5
9.9/19
10.9/19
11.9/19
12.9/19
13.9/19 UTC

Figure 12

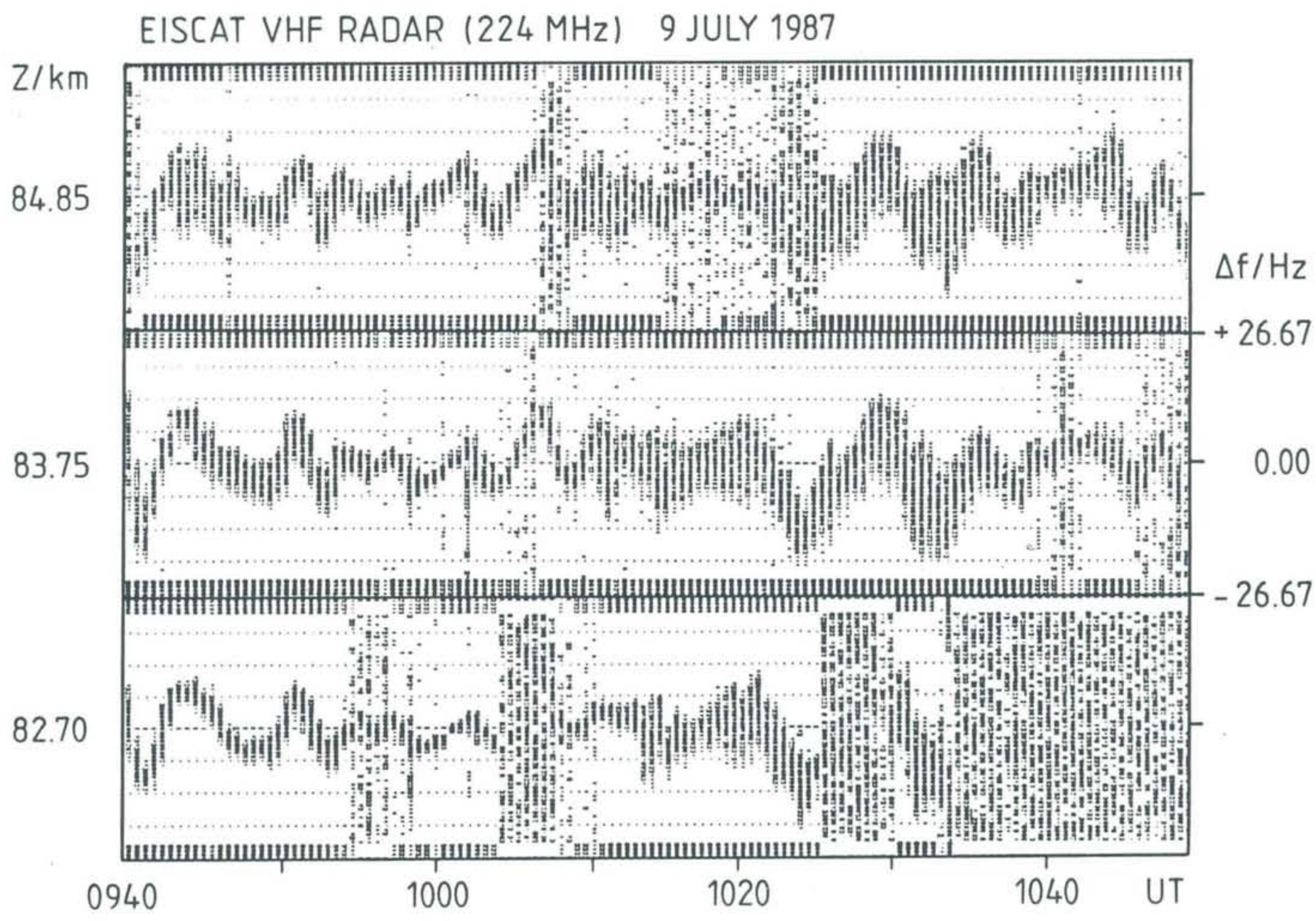

EISCAT VHF RADAR (224 MHz) 9 JULY 1987
Z/km
84.85
83.75
82.70
Δf/Hz
+ 26.67
0.00
- 26.67
0940
1000
1020
1040
UT

Figure 13

LOWER THERMOSPHERE - MESOSPHERE
COUPLING PROCESSES IN POLAR REGIONS

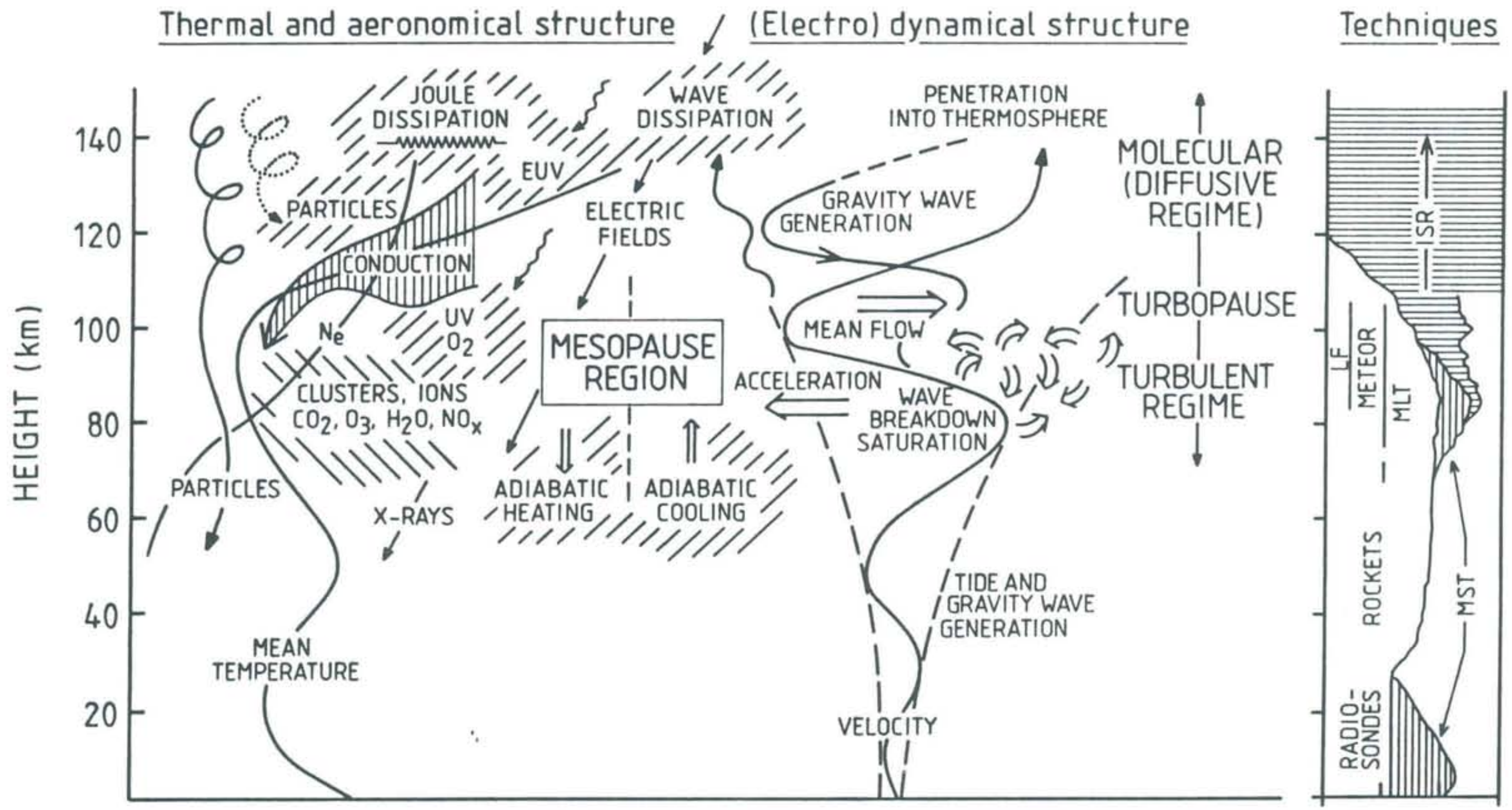

Figure 14

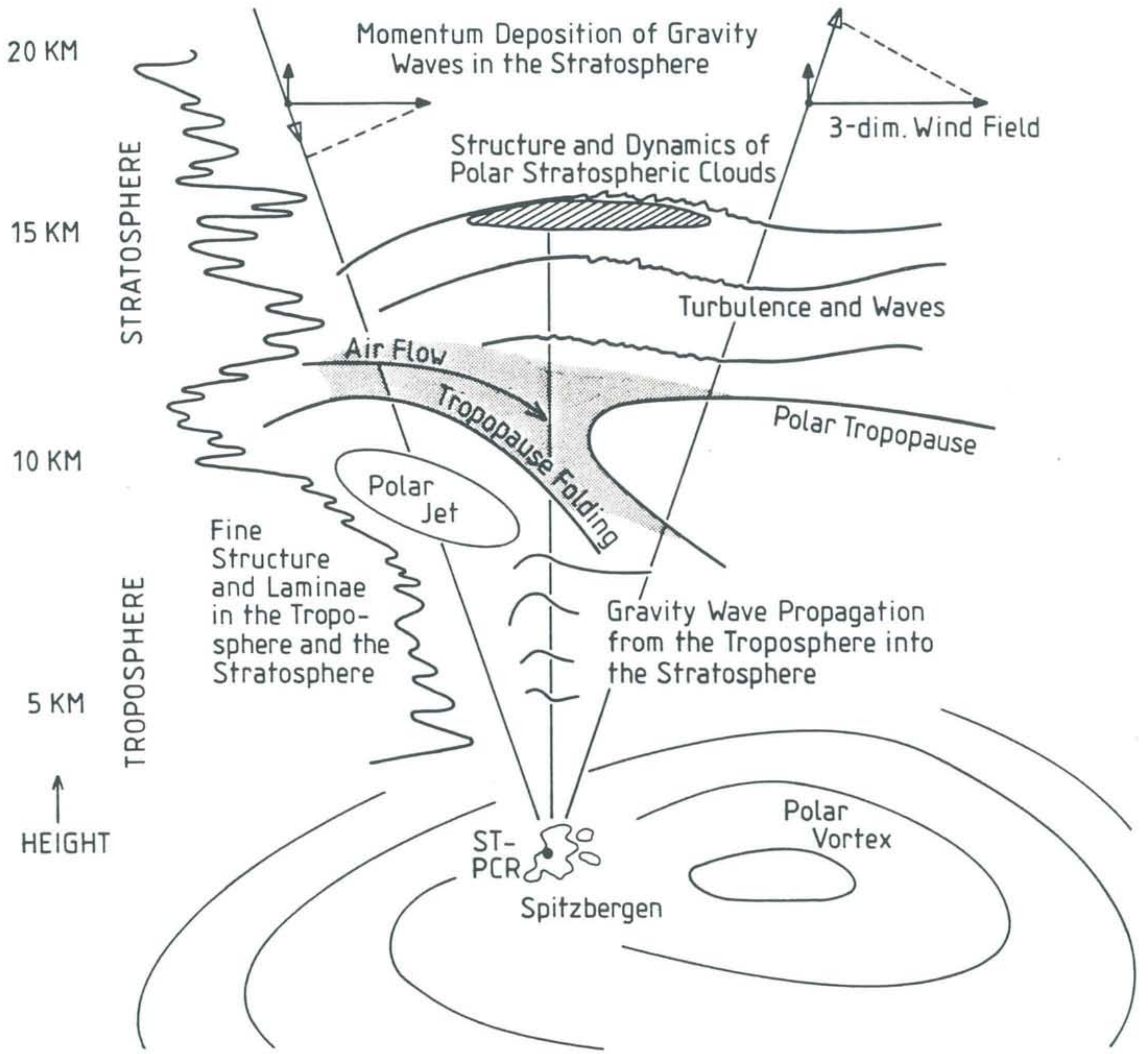

Structure and Dynamics of the Polar Stratosphere
and Troposphere Investigated by an ST-Polar Cap Radar

Figure 15

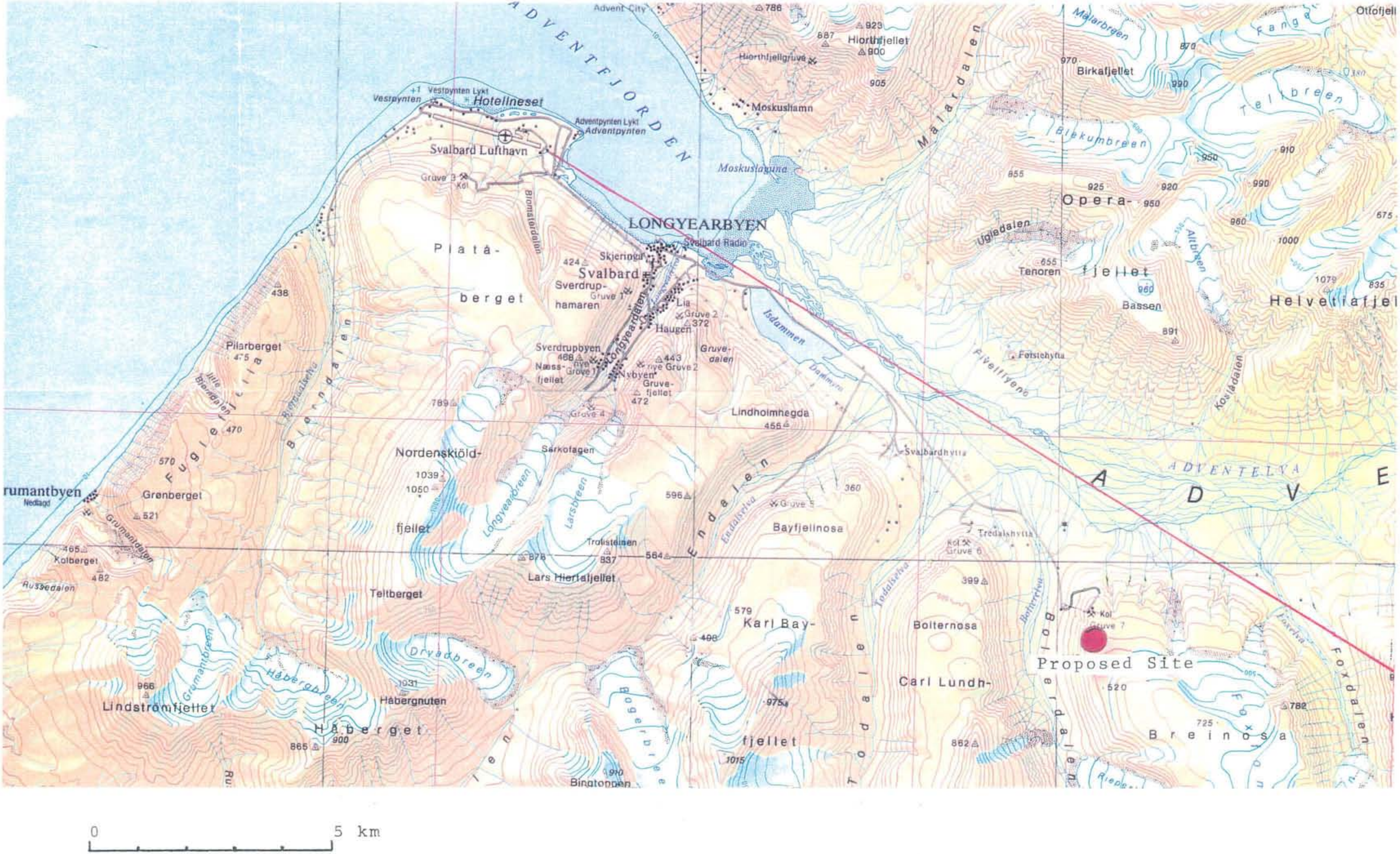

ADVENTFJORDEN
Advent City
Hiorthfjellet
Hiorthfjellgruve
Moskushamn
Mälardalen
Vestpynten
Hotellneset
Adventpynten
Svalbard Lufthavn
Gruve 3
Moskuslaguna
LONGYEARBYEN
Svalbard Radio
Platåberget
Skjeringa
Svalbard
Sverdruphamaren
Gruve 1
Lia
Haugen
Isdammen
Gruvedalen
Sverdrupbyen
Nybyen
Gruvefjellet
Lindholmhøgda
Svalbardhytta
Fuglefjella
Pilarberget
Bjørndalen
Nordenskiöldfjellet
Sarkofagen
Longyearbreen
Larsbreen
Endalen
Gruve 5
Bayfjellnosa
Grumantbyen
Grønberget
Kolberget
Russedalen
Trollsteinen
Lars Hierfaljellet
Teltberget
Karl Bayfjellet
Todalen
Bolternosa
Bolterdalen
Tredalshytta
Gruve 6
Gruve 7
Proposed Site
Carl Lundh-
Breinosa
Foxdalen
Foxelva
Dryadbreen
Håbergbreen
Håbergnuten
Håberget
Lindströmfjellet
Grumantbreen
Bogerbreen
Bingtoppen
Mälarbreen
Birkafjellet
Tellbreen
Blekumbreen
Operafjellet
Ugledalen
Tenoren
Bassen
Helvetiafjellet
Førstehytta
Fivelflyene
Koladalen
ADVENTELVA
ADVE
Ottofjell
0
5 km

Figure 16

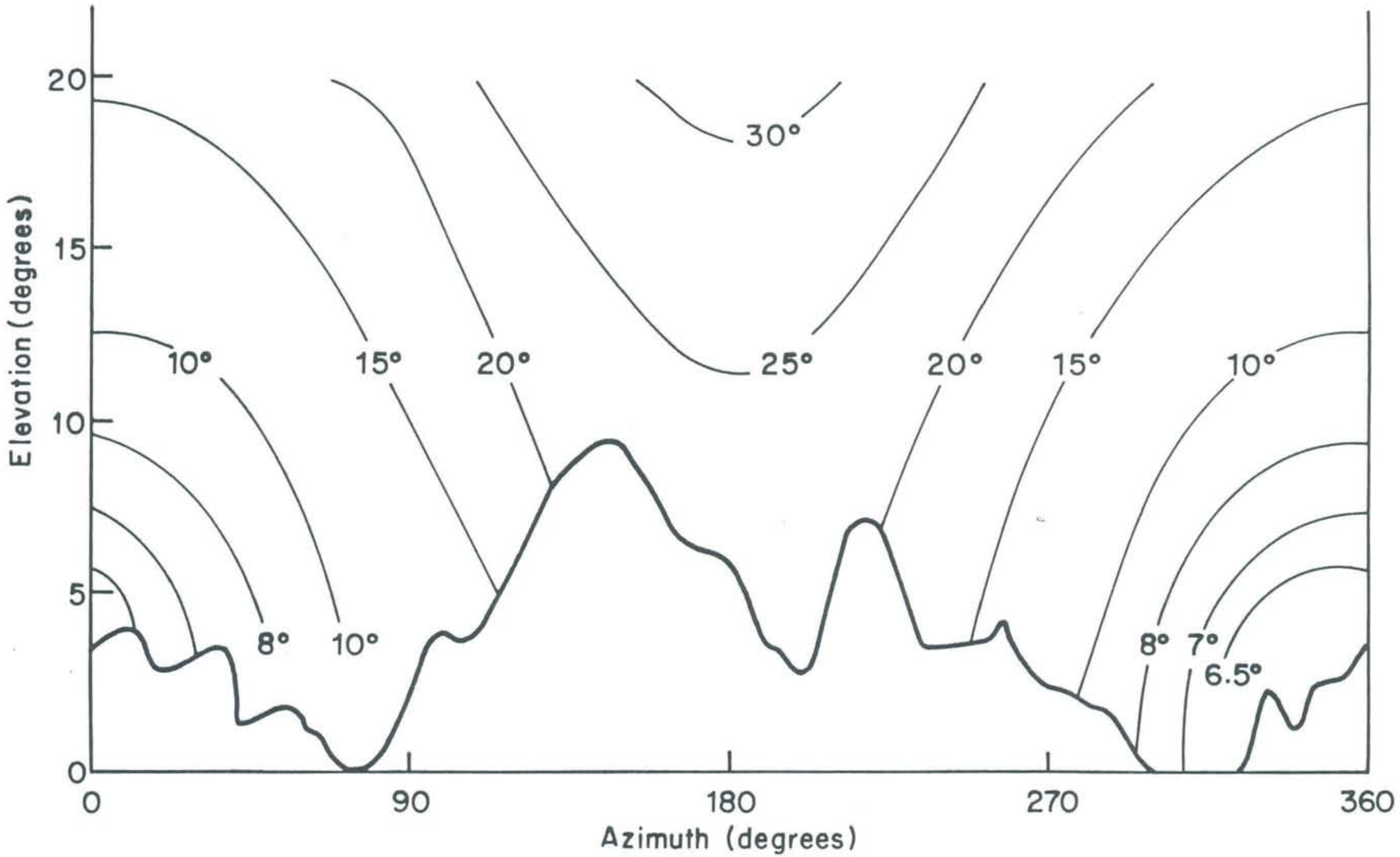
30°
25°
20°
15°
10°
20°
15°
10°
8°
10°
8°
7°
6.5°
20
15
10
5
0
Elevation (degrees)
0
90
180
270
360
Azimuth (degrees)

Figure 17

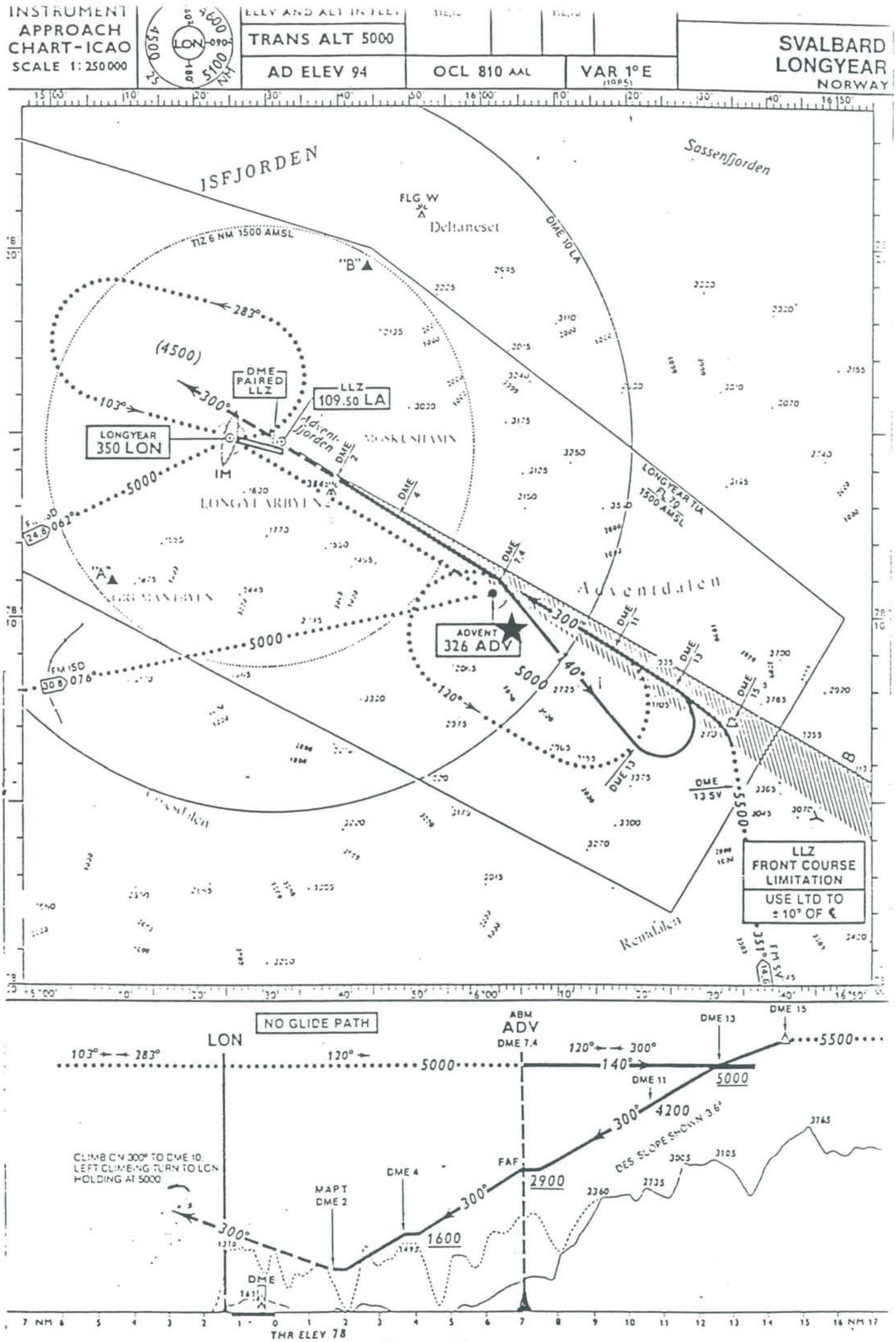
INSTRUMENT APPROACH CHART-ICAO
SCALE 1:250 000
TRANS ALT 5000
AD ELEV 94
OCL 810 AAL
VAR 1° E
SVALBARD
LONGYEAR
NORWAY
ISFJORDEN
Sassenfjorden
Deltaneset
TIZ 6 NM 1500 AMSL
DME 10 LA
(4500)
DME PAIRED LLZ
LLZ 109.50 LA
LONGYEAR 350 LON
IM
LONGYEARBYEN
ADVENT 326 ADV
Adventdalen
LONGYEAR TIA FL 70 1500 AMSL
LLZ FRONT COURSE LIMITATION
USE LTD TO ± 10° OF ℄
Reindalen
NO GLIDE PATH
LON
ABM ADV DME 7.4
DME 13
DME 15
DME 11
FAF
2900
MAPT DME 2
DME 4
1600
4200
5000
5500
DES SLOPE SHOWN 3.6°
CLIMB ON 300° TO DME 10, LEFT CLIMBING TURN TO LON HOLDING AT 5000
THR ELEV 78

Figure 18

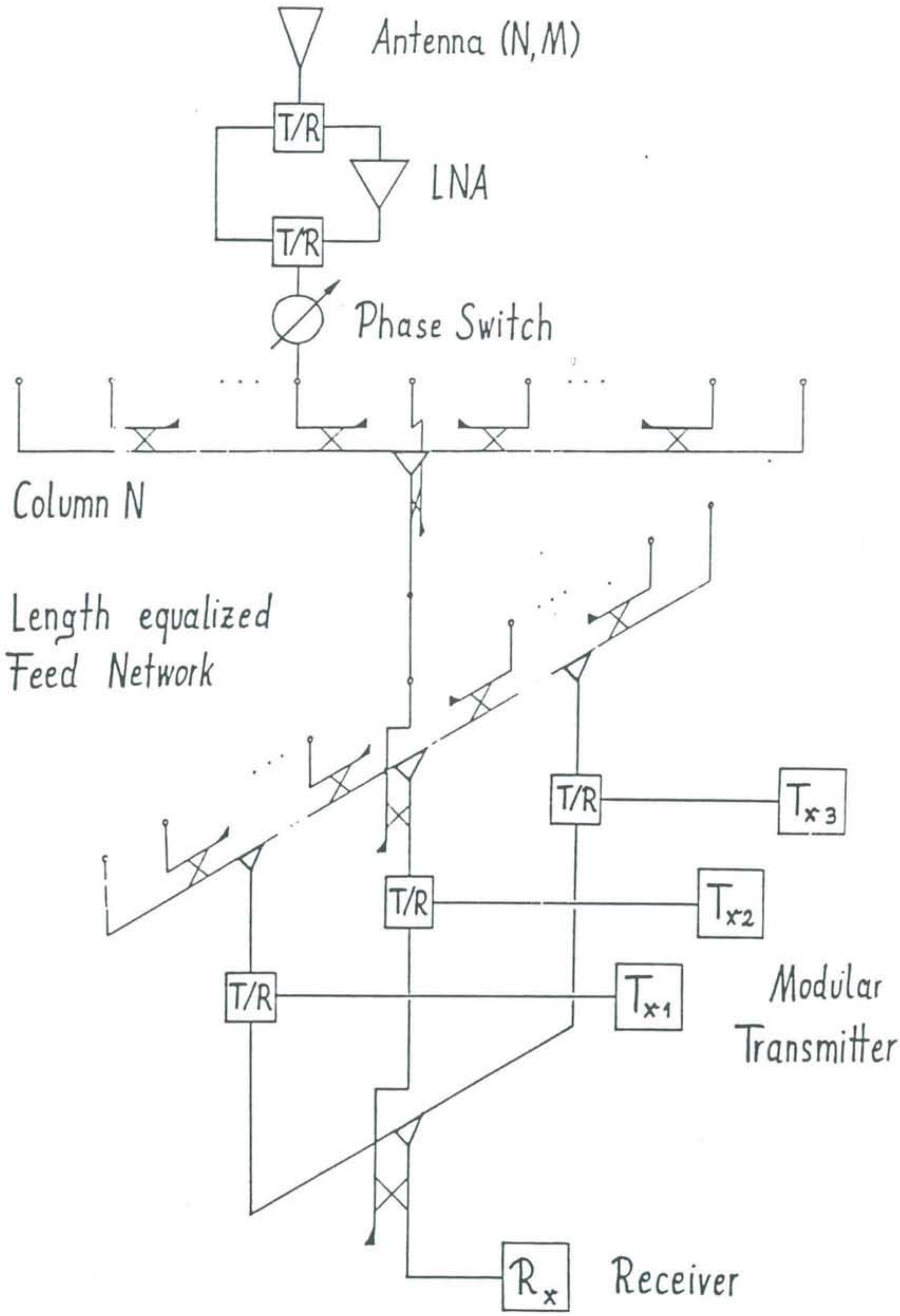

Antenna (N,M)
T/R
LNA
T/R
Phase Switch
Column N
Length equalized
Feed Network
T/R
$T_{x\text{-}3}$
T/R
$T_{x\text{-}2}$
T/R
$T_{x\text{-}1}$
Modular
Transmitter
R_x
Receiver

Figure 19

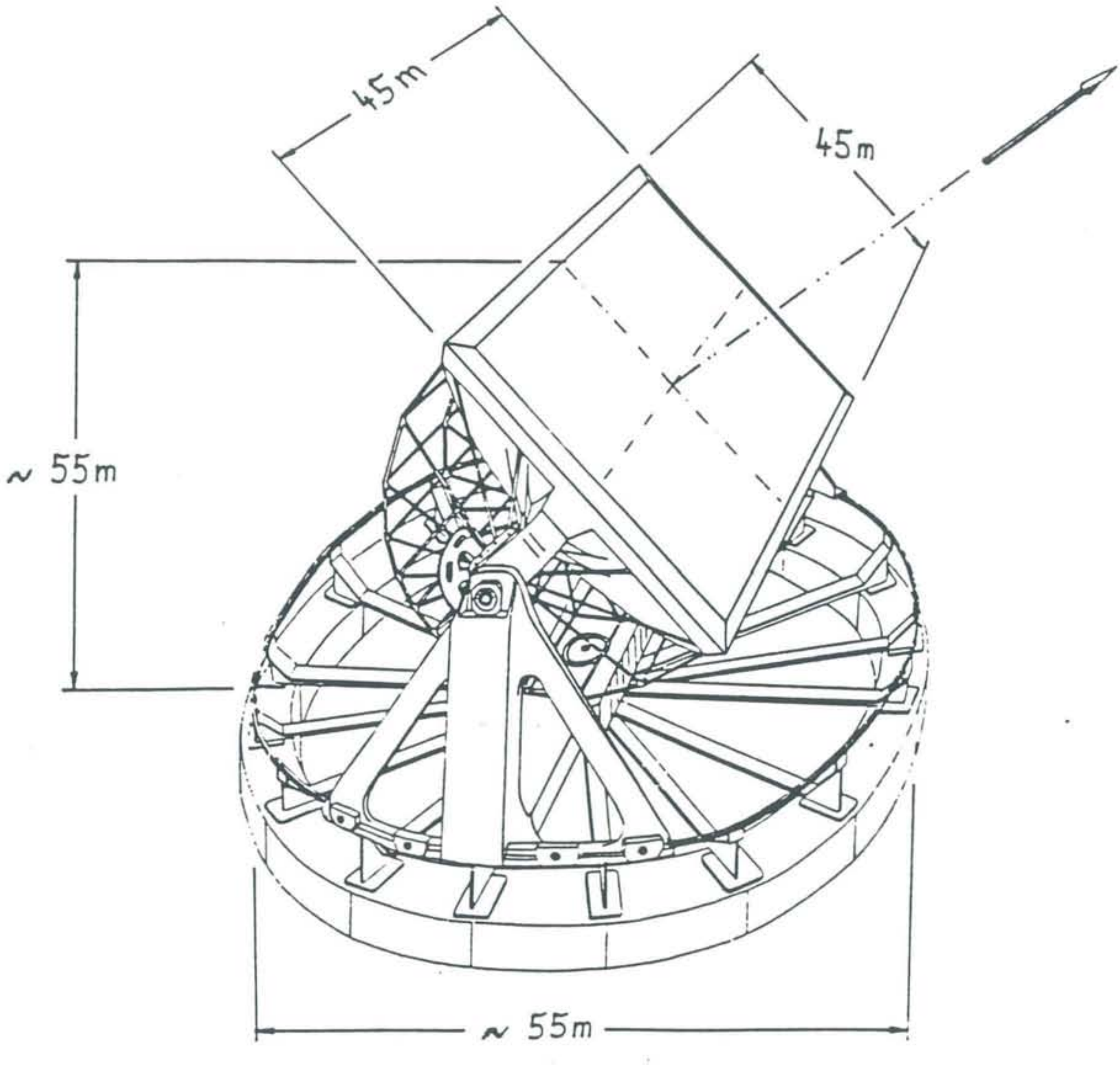

Figure 20

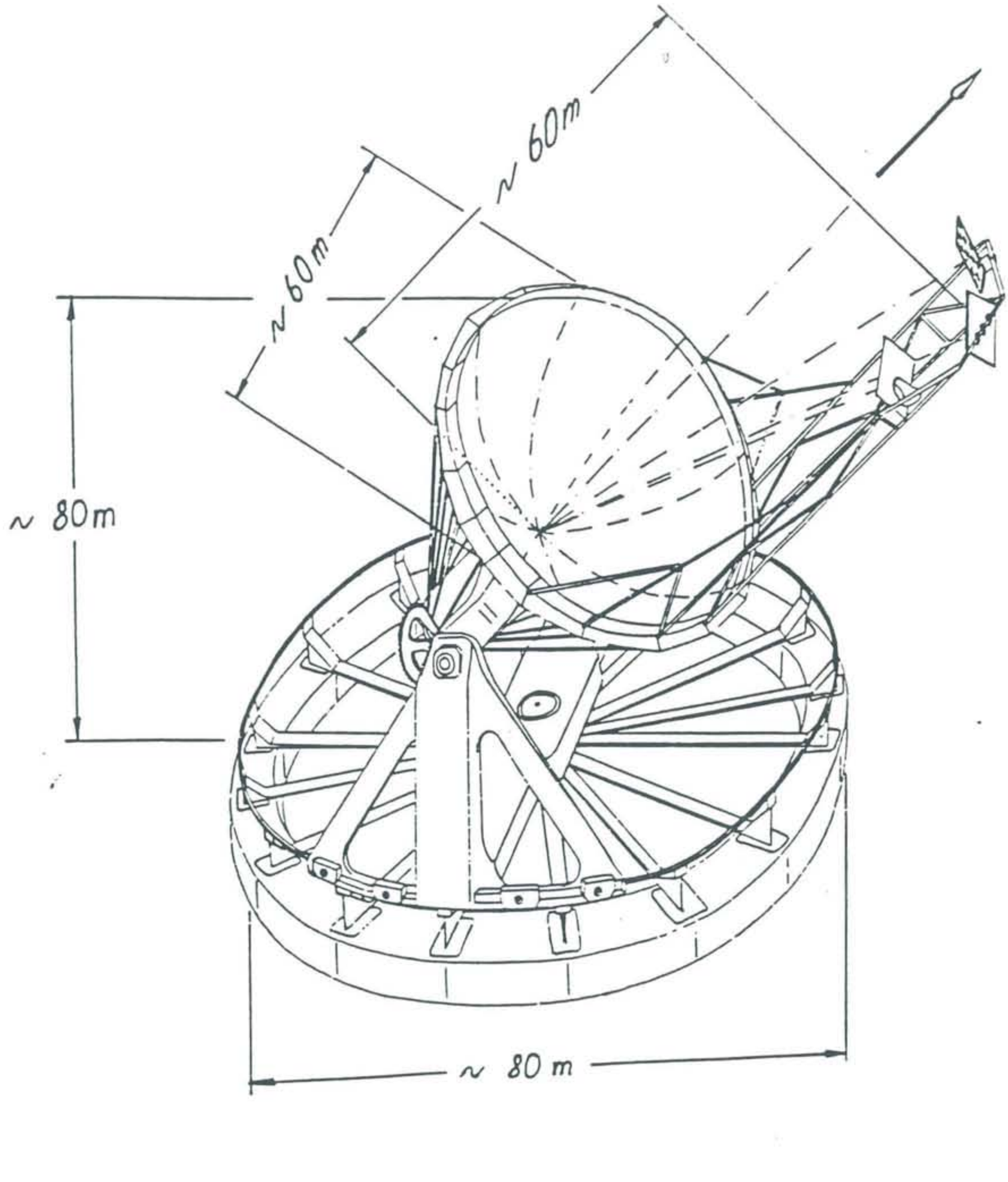

Figure 21

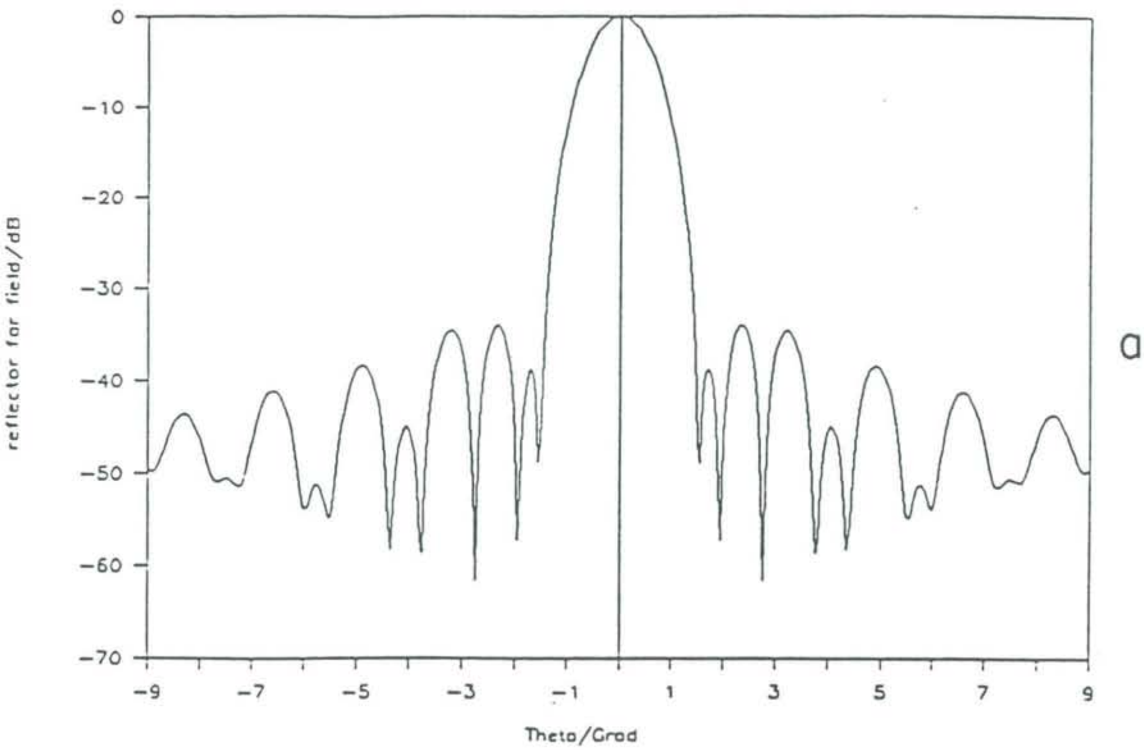

reflector far field/dB
0
-10
-20
-30
-40
-50
-60
-70
-9
-7
-5
-3
-1
1
3
5
7
9
Theta/Grad
a

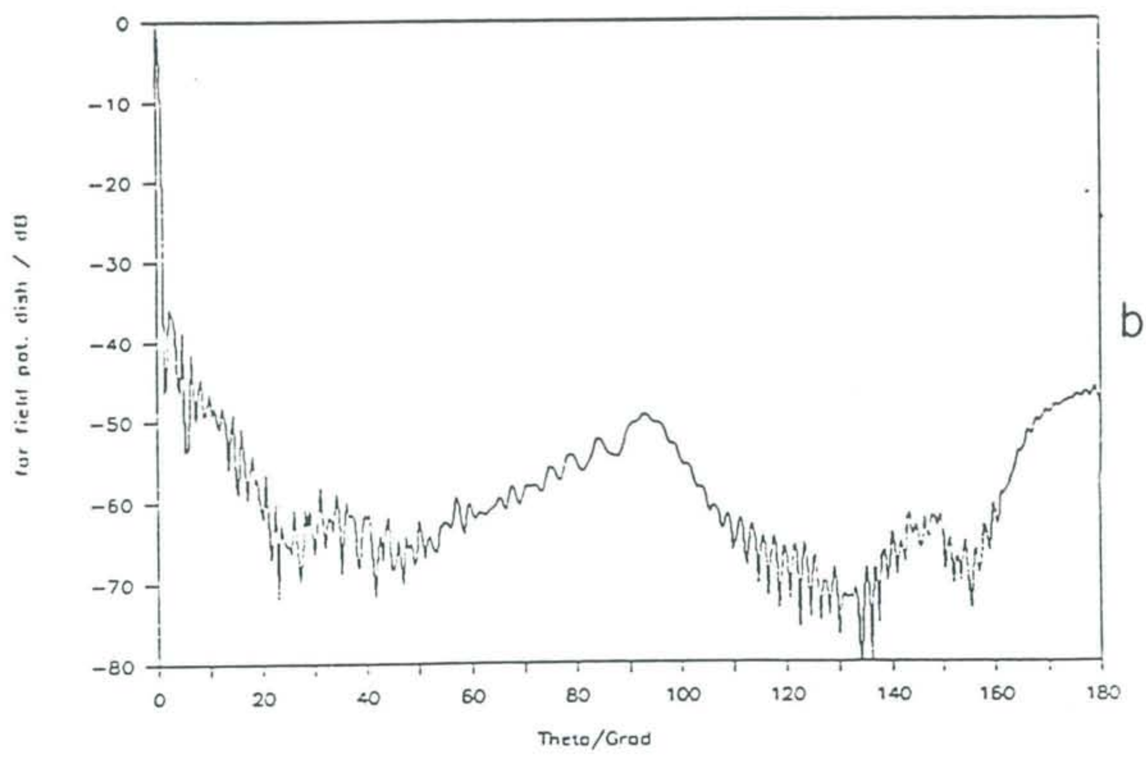

far field pat. dish / dB
0
-10
-20
-30
-40
-50
-60
-70
-80
0
20
40
60
80
100
120
140
160
180
Theta/Grad
b

Figure 22

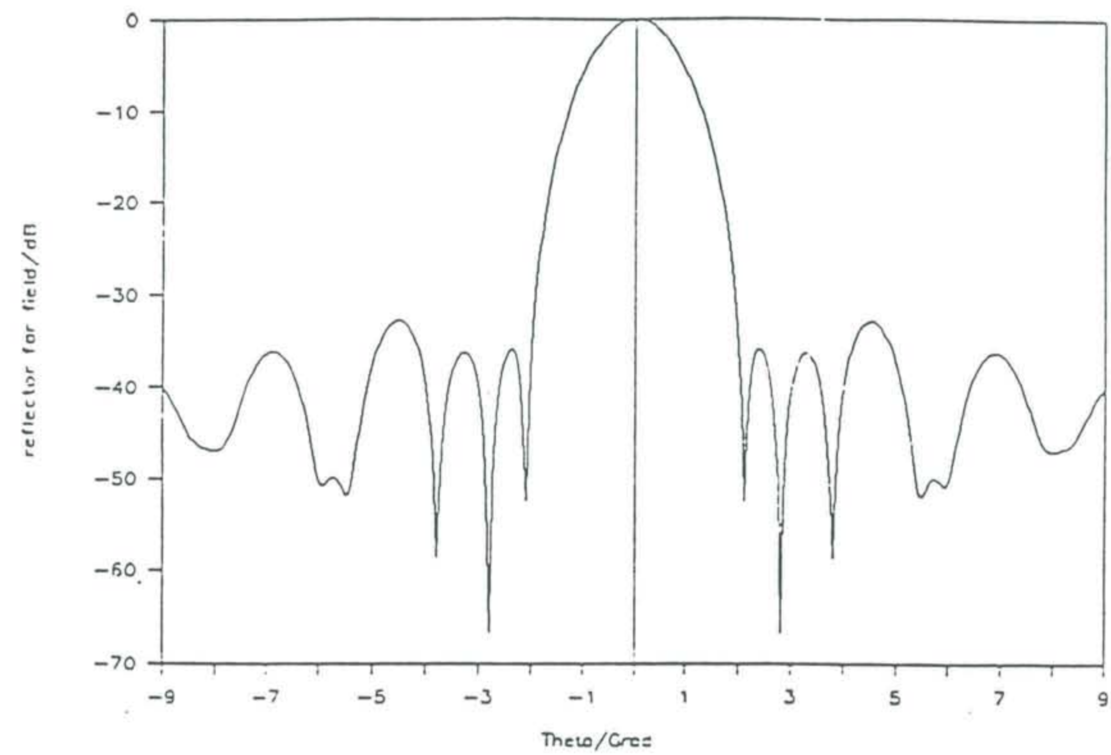
reflector far field/dB
Theta/Grad
0
-10
-20
-30
-40
-50
-60
-70
-9
-7
-5
-3
-1
1
3
5
7
9

a

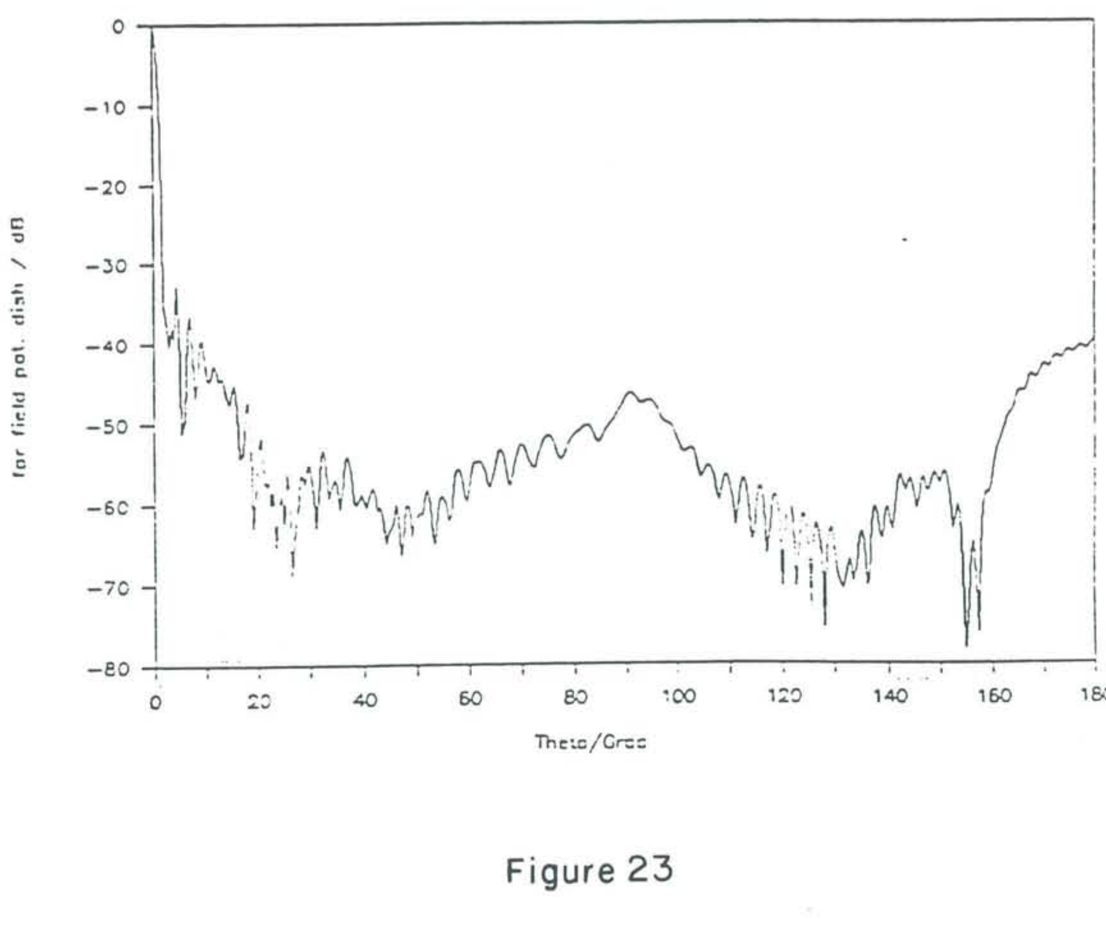
far field pol. dish / dB
Theta/Grad
0
-10
-20
-30
-40
-50
-60
-70
-80
0
20
40
60
80
100
120
140
160
180

b

Figure 23

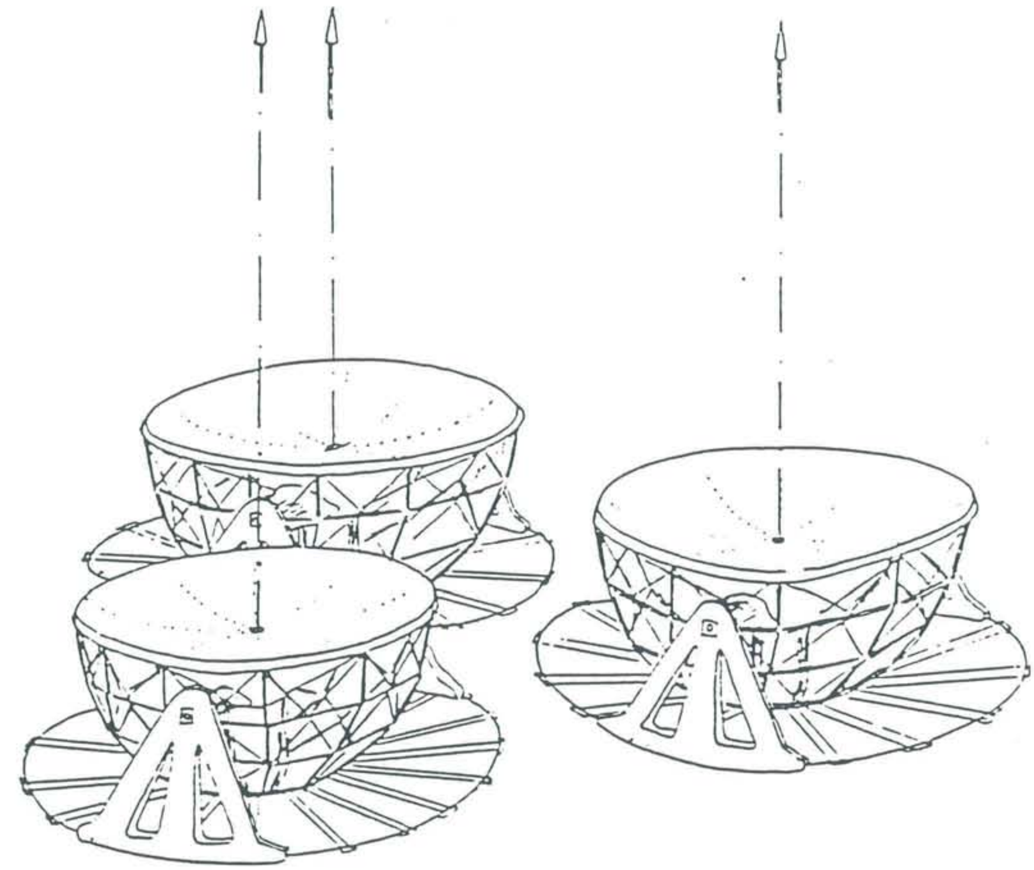

a

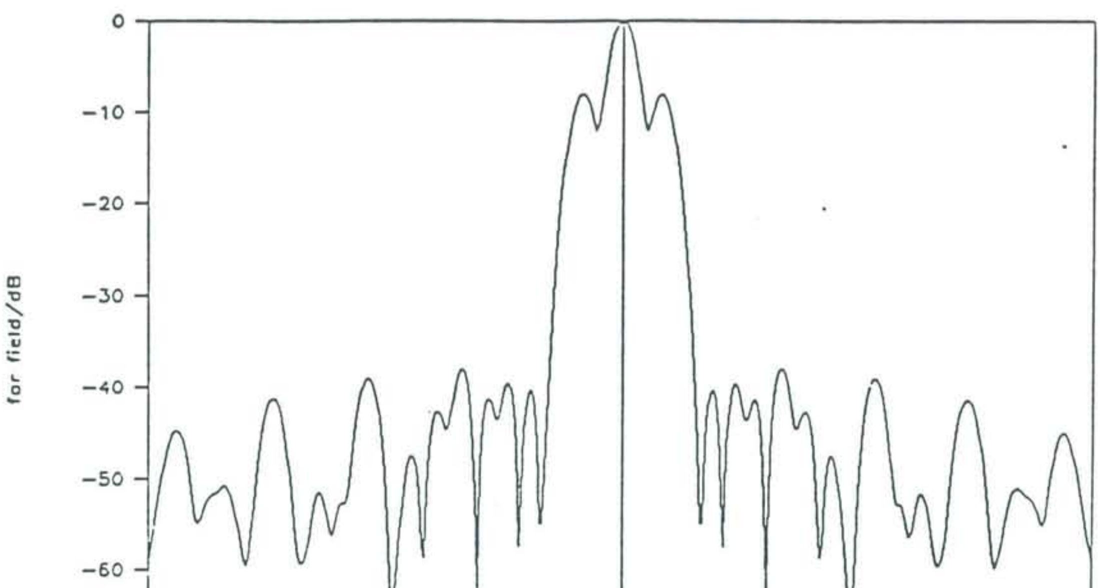

b

Figure 24

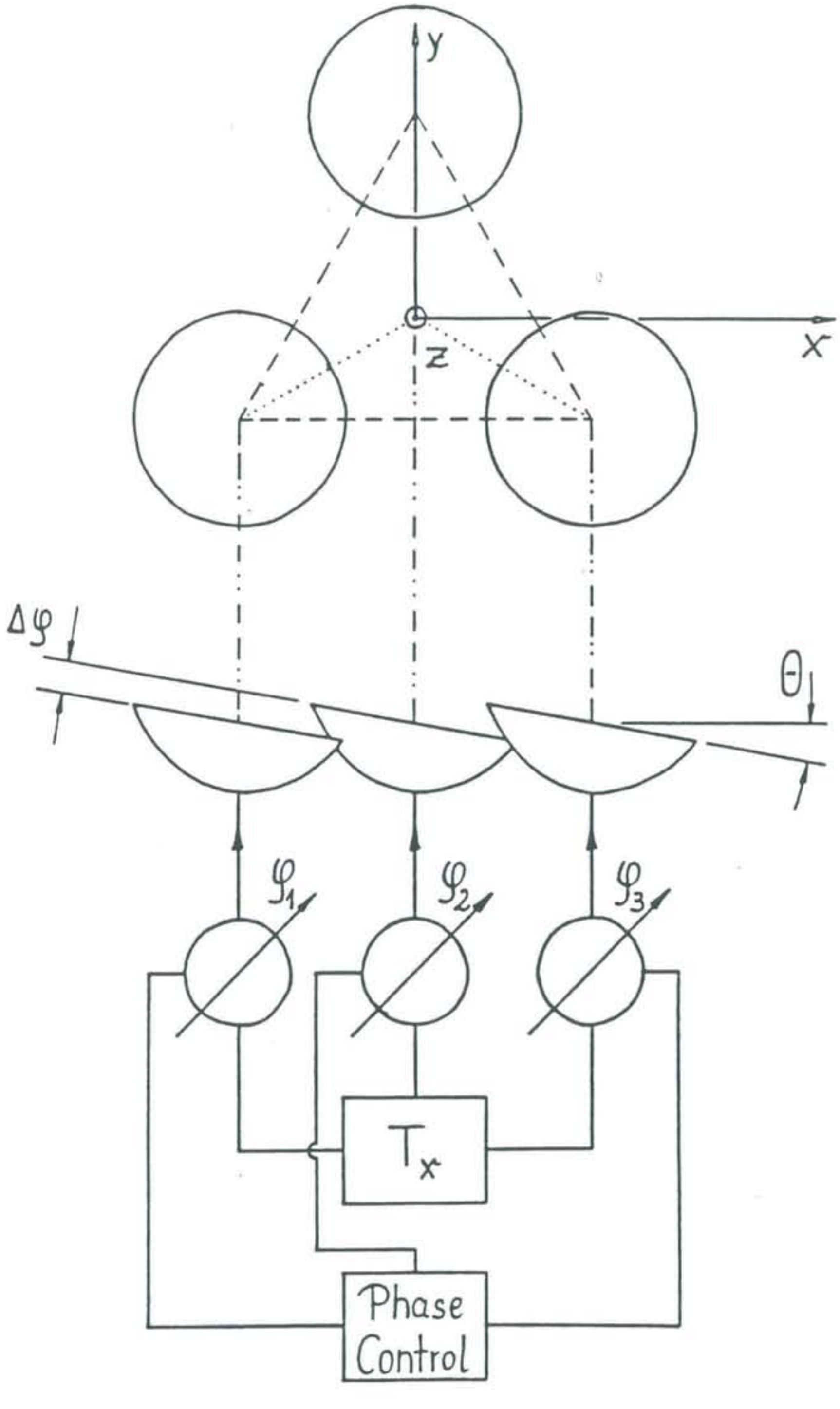

Figure 25

a) Principle

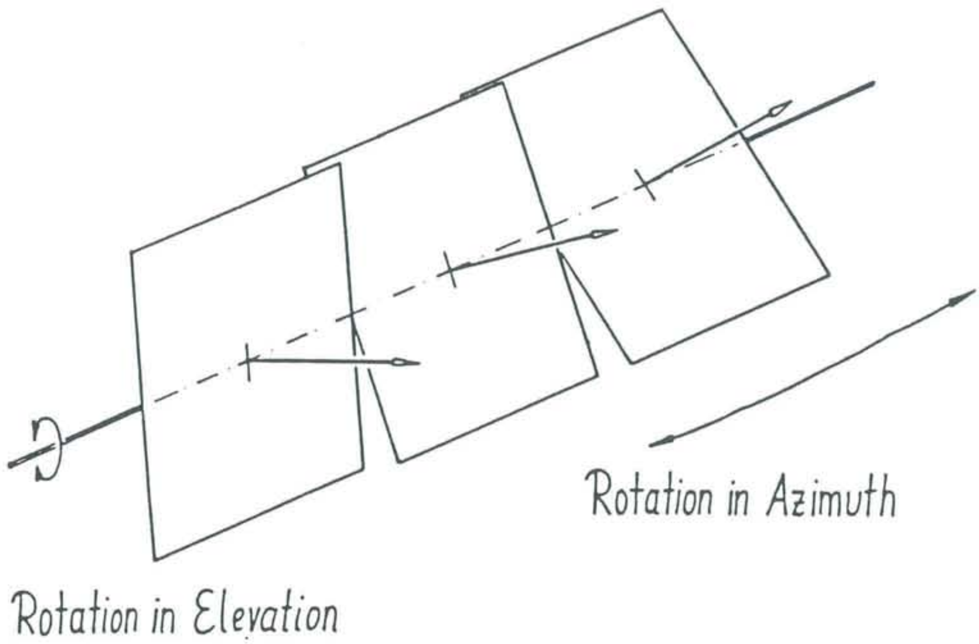

b) Achieveable Beam Configurations

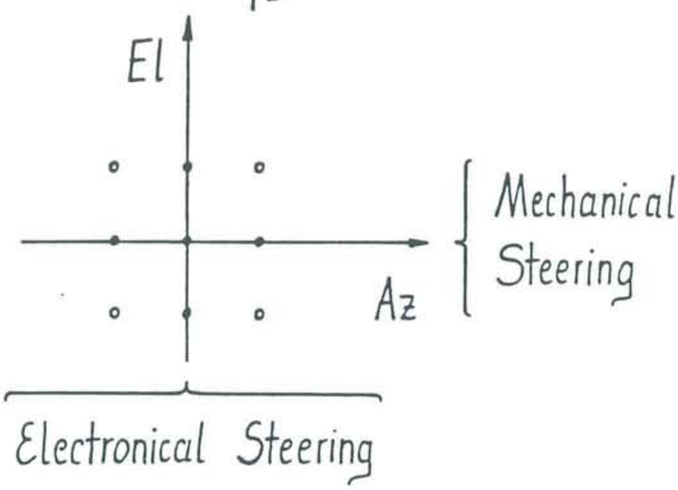

Figure 26

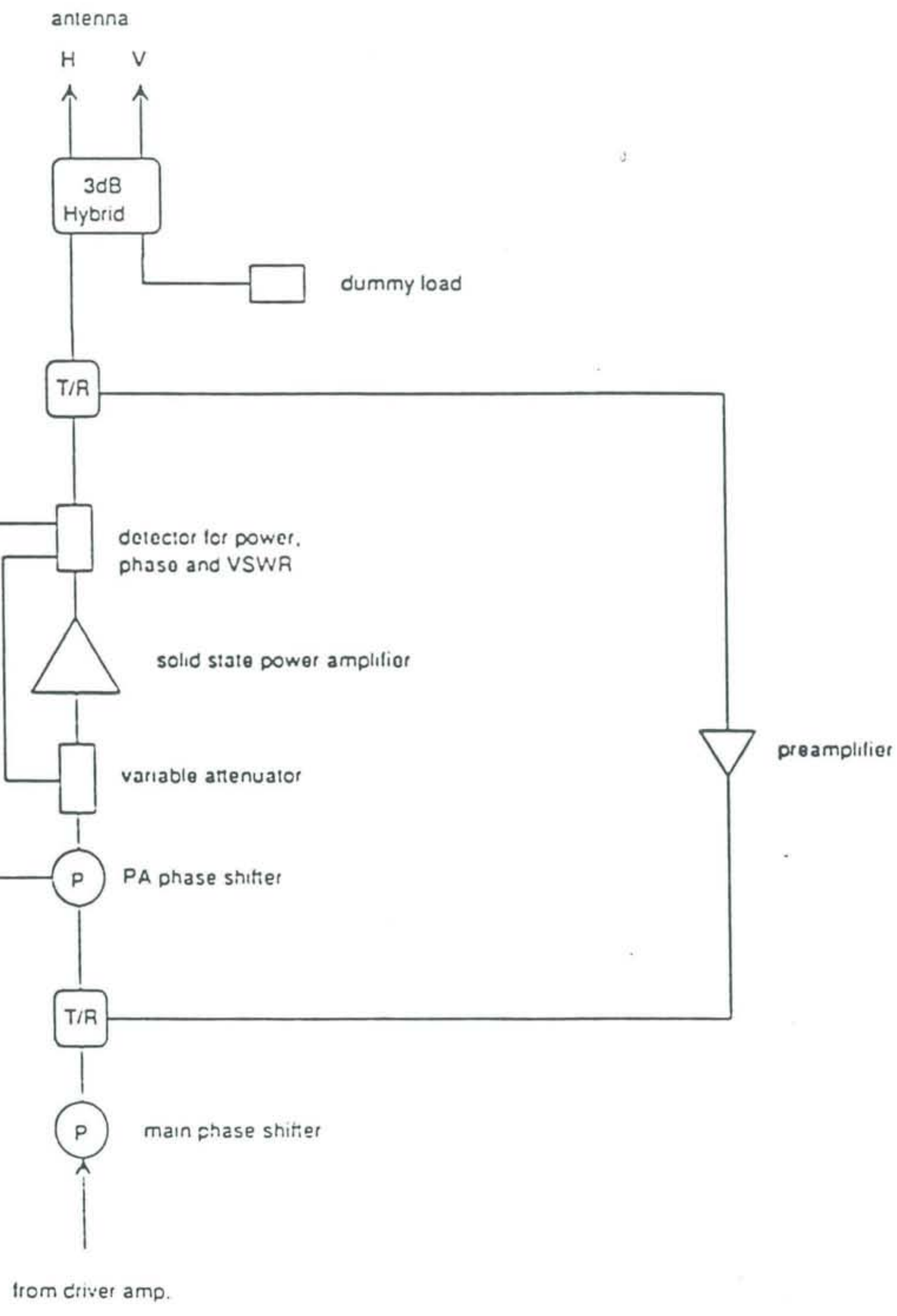
antenna
H
V
3dB
Hybrid
dummy load
T/R
detector for power,
phase and VSWR
solid state power amplifier
preamplifier
variable attenuator
P
PA phase shifter
T/R
P
main phase shifter
from driver amp.

Figure 27

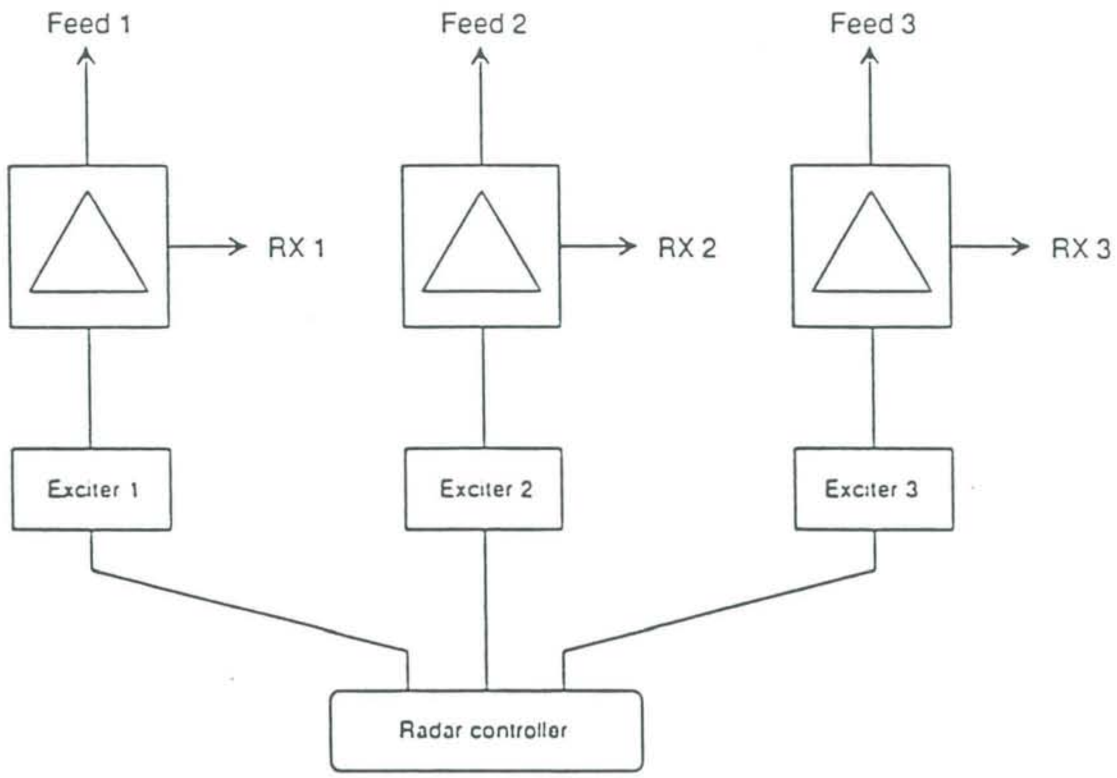
Feed 1
Feed 2
Feed 3
RX 1
RX 2
RX 3
Exciter 1
Exciter 2
Exciter 3
Radar controller

Figure 28

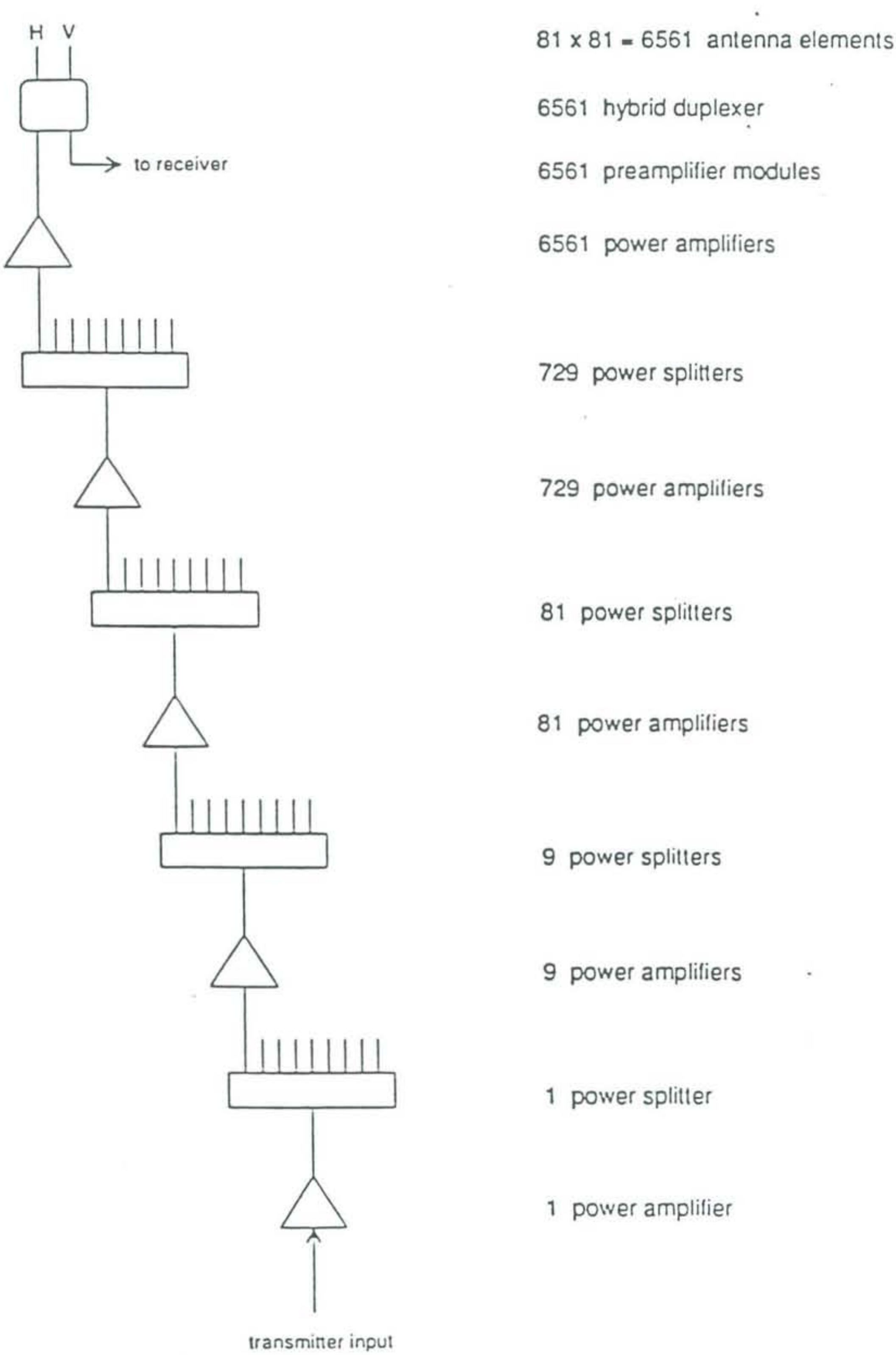
H V
to receiver
transmitter input
81 x 81 = 6561 antenna elements
6561 hybrid duplexer
6561 preamplifier modules
6561 power amplifiers
729 power splitters
729 power amplifiers
81 power splitters
81 power amplifiers
9 power splitters
9 power amplifiers
1 power splitter
1 power amplifier

Figure 29

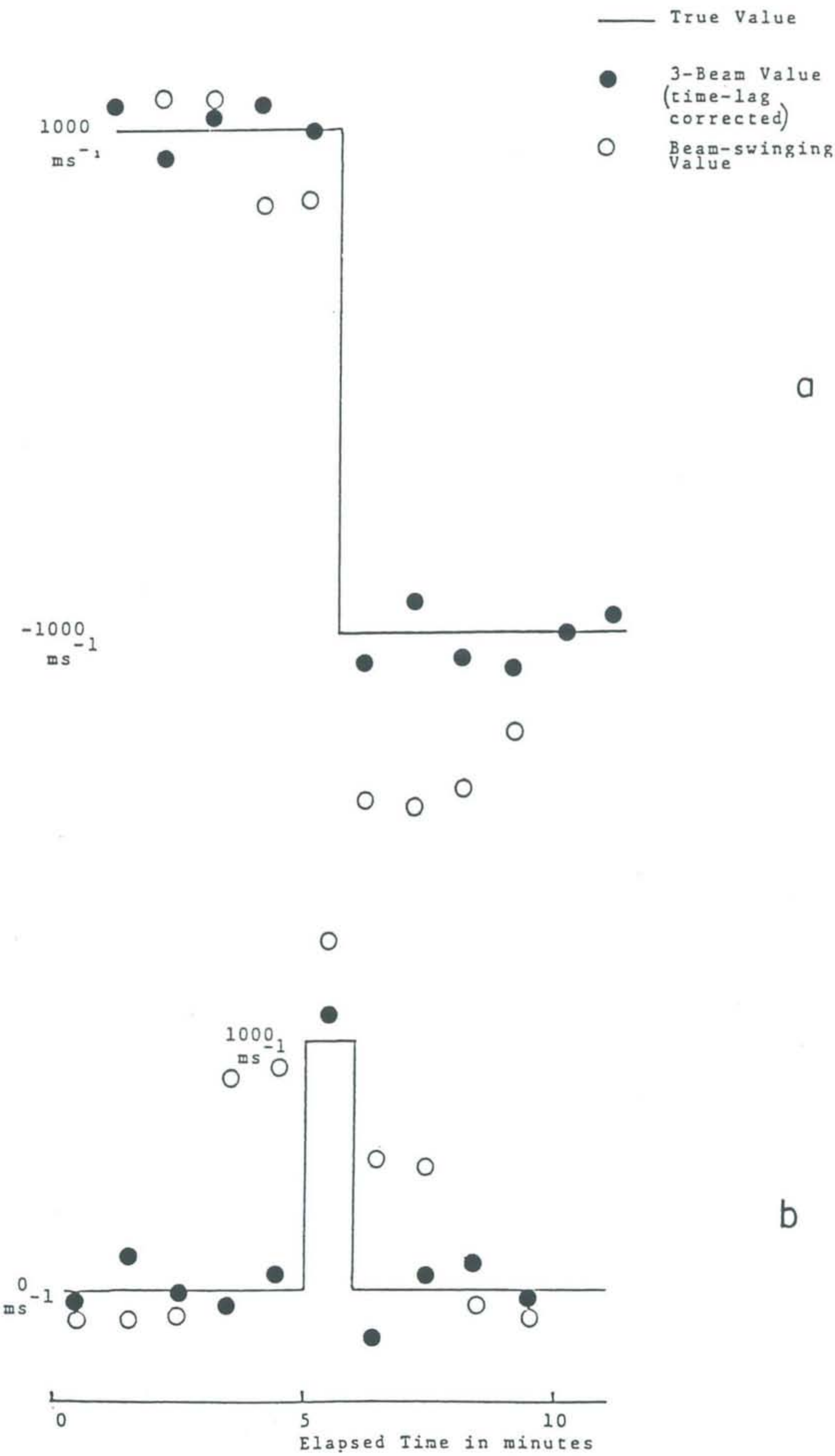
True Value
3-Beam Value (time-lag corrected)
Beam-swinging Value
1000 ms^{-1}
-1000 ms^{-1}
a
1000 ms^{-1}
0 ms^{-1}
b
0
5
10
Elapsed Time in minutes

Figure 30

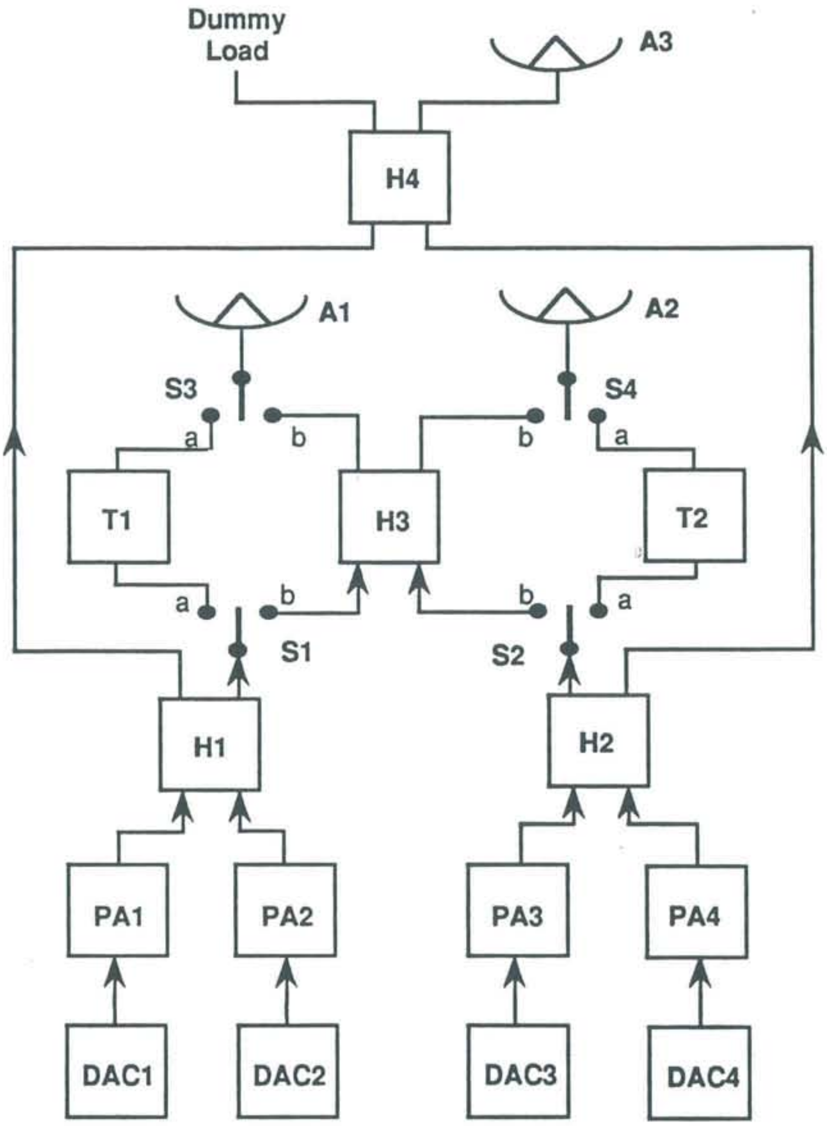

H Hybrid
A Antenna
PA RF Power Amp

DAC Digital to Analogue Converter
S Waveguide Switch
T Trombone - Mechanical Phase Shifter

Figure 31

Printed at the Rutherford Appleton Laboratory, Chilton, DIDCOT, Oxon., U.K.